The role of the UPRER in the acquisition of pluripotency during reprogramming

Milos Simic

The role of the UPR^{ER} in the acquisition of pluripotency during reprogramming

Doctoral work

Doctoral School Life Science Complexity ED 515

University Pierre and Marie Curie, Paris, France

Research conducted in the laboratory of Professor Andrew Dillin

UC Berkeley, USA

by

Milos Simic

Co-directed by

Professor Andrew Dillin

Siebel Distinguished Chair

HHMI - UC Berkeley

and Professor Olivier Bensaude

École Normale Supérieure, Paris

July, 2016

Table of Contents

Preface

This manuscript documents my doctoral work in Andrew Dillin's laboratory, UC Berkeley, USA, started in January 2013.

My doctoral experience was the occasion to show my ability to construct an innovative scientific project literally from the ground. Our laboratory's main focus is the study of aging mostly in C. *elegans* and mice as well as the study of cellular stresses. Even though the laboratory's expertise was not in stem cell biology, with Andrew Dillin's support, I decided to explore the role of stress pathways during cellular reprogramming. It was therefore very challenging to build all the protocols and techniques in cellular reprogramming by myself. But the outcome is very promising. For the first time we were able to bridge two fields and offered a new way to look at cellular reprogramming through the prism of protein quality control. The present manuscript will elaborate exclusively on this work.

Besides this exciting project, I had the chance to build another project to study the tissue-specific requirement of RPN-6, a subunit of the 19S proteasome, in C. *elegans*. Very stimulating results came from this project but we decided to focus on the role of the endoplasmic reticulum stress during cellular reprogramming. Therefore, no further mention of this project will follow.

The time I spent in the Dillin lab was also a great opportunity to establish collaborations and keep bridging fields. This also provided me with a platform to explore other model organisms such as C. *elegans* and techniques like genome-wide CRISPR-Cas9 screens. These collaborations are still ongoing and very promising. Some of this work already gave rise to publications in very high profile journals:

Kim, H., Rodrigues, A., Simic, M.S., Kohnz, A. R., Nomura, D. K., Durieux, J., Riera, C. E., Sanchez, M., Kapernick, E., Wolff, S. and Dillin, A. (2016). Lipid biosynthesis coordinates a Mitochondrial to Cytosolic Stress Response. **Cell** (in press).

Douglas, P.M.*, Baird, N.A.*, Simic, M.S., Uhlein, S., McCormick, M.A., Wolff, S.C., Kennedy, B.K., and Dillin, A. (2015). Heterotypic Signals from Neural HSF-1 Separate Thermotolerance from Longevity. **Cell Rep**. *12*, 1196–1204.

Baird, N.A.*, Douglas, P.M.*, Simic, M.S., Grant, A.R., Moresco, J.J., Wolff, S.C., Yates, J.R., Manning, G., and Dillin, A. (2014). HSF-1–mediated cytoskeletal integrity determines thermotolerance and life span. **Science** *346*, 360–363.

Vilchez, D.*, Simic, M.S.*, and Dillin, A. (2014). Proteostasis and aging of stem cells. **Trends Cell Biol.** *24*, 161–170.

* equal contribution

The published version of the articles can be found in the appendix section.

In order to facilitate your reading and draw your attention to the important genes/proteins that will be mentioned in the Result section, I underlined those genes/proteins in the Introduction section.

Abstract

Somatic cells can be reprogrammed into a pluripotent stem cells state and is achieved by the forced expression of 4 transcription factors: OCT4, SOX2, KLF4 and c-MYC. This process theoretically requires a global remodeling of the organelles and a drastic change in metabolism. Furthermore, reprogramming has an inherent property of stochastic variation that is limiting and largely unknown. We hypothesize that this variation is due, in part, by variable regulation of the protein homeostasis network. We therefore postulated that the early steps of reprogramming would result in the activation of a variety of stress pathways that regulate the protein homeostasis network, which might in turn impact the efficiency of reprogramming. We focused in particular on the endoplasmic reticulum unfolded protein response (UPR^{ER}). We find that the UPR^{ER} is activated during reprogramming and that its activation can increase the efficiency of this process. We find that stochastic activation of the UPR^{ER} can predict reprogramming efficiency. These results suggest that the low efficiency of cellular reprogramming is partly the result of the cell's inability to initiate a proper stress response to cope with the newly expressed load of proteins that will eventually change the fate of this cell.

Résumé

Les cellules somatiques peuvent être reprogrammées en cellules pluripotent en sur-exprimant 4 facteurs de transcriptions: OCT4, SOX2, KLF4 et c-MYC. Ce processus nécessite en théorie un remodelage des organelles et un changement drastique du métabolisme. De plus, la reprogrammation cellulaire possède une composante stochastique qui est peu comprise et conduit à une faible efficacité. Nous avons fait l'hypothèse que cette variabilité est en partie due aux variations de la régulation de l'homéostasie protéique. Nous nous attendons à ce que la première phase de reprogrammation active les voies de stress qui régulent l'homéostasie protéique, ce qui impacterait l'efficacité de reprogrammation. Notre attention s'est dirigée vers le rôle de la réponse aux protéines dépliées du réticulum endoplasmique. Nous avons découvert que cette voie est active pendant la reprogrammation cellulaire et que son activation peut augmenter l'efficacité de ce processus. Par ailleurs le niveau d'activation de cette voie peut prédire l'efficacité de reprogrammation. Ces résultats suggèrent que la faible efficacité de reprogrammation cellulaire est en partie due à l'incapacité des cellules à activer cette voie de stress afin de pouvoir correctement répondre à la nouvelle charge de protéines synthétisées qui changera l'état de cette cellule.

Acknowledgments

I would like to express my gratitude to everyone in Pr Andrew Dillin's laboratory for making me feel like part of a family.

I wish to express my deepest and sincere gratitude to my supervisor Andrew Dillin for his endless optimism, enthusiasm, support in my work and inspiration. Also, an enormous thanks to my other thesis co-director Olivier Bensaude for his invaluable advice and flexibility throughout my PhD.

I extend my gratitude to Dirk Hockemeyer and Xavier Darzacq for external tutorship and helpful discussions.

I would like to thank my reading committee and part of my jury, Valérie Lallemand-Mezger and Eric Chevet. I sincerely hope you will enjoy your summer reading.

I would like to extend my thanks to the rest of the jury, Jonathan Weitzman, Charles Durand, Han Li and Andrew Dillin for kindly accepting to be present at my thesis defense.

I thank my colleagues and friends at the lab, for providing a positive and stimulating work environment: Celine Riera, Carlos Daniel De Magalhaes Filho, Carsten Merkwirth, Jenni Durieux, Kristan Steffen, David Vilchez, Nate Baird, Pete Douglas, Ye Tian, Kristen Berendzen, Erik Kapernick, Thomas Heimbucher, Larry Joe, Sarah Uhlein Tronnes, Melissa Sanchez, Jonathan Halloran, Gilbert Garcia, Hope Henderson, Joseph Daniele, Ashley Frakes, Ryo Higuchi-Sanabria, Sabine Jordan, Hyun-Eui Kim, Erica Moehle, Vidhya Ramachandran, Robert Schinzel, Ophir Shalem, Brant Webster, Suzanne Wolff and Nan Xin.

Especially to Celine, Casi, Daniel and Jenni for their unselfish help.

I also wish to thank all members of the Hockemeyer and Tjian lab that helped me and for their friendship: Chiba, Franzi, George, Ryan, Tina, Tim, John Blair, John Boyle, Josh, Jaclyn, Lana, Kevin, Carla, Frank and Claudia.

A big thanks to the very special people outside the lab: Lana Bosanac, Maja Petkovic, Katlin Silm, Damien Jullié, David Fraser. Thank you for the comradeship and friendship.

A very particular thank to Anastasia Wolff for having been part of this journey even though we didn't finish it together.

Lastly, and most importantly, I would like to thank my family, my sister Milesa, my father Pribislav, and my aunt Radenka for their excessive love and support.

I dedicate this thesis to my beloved mother Ljiljana, my beloved uncle Borisav and my beloved friend Sophie Thomain, all gone too early!

Introduction

I. A brief history of cellular reprogramming

a) The reversibility of differentiated states

The notion of cell fate dates back to the late 19th century when August Weismann made the assumption that because germ cells mediate inheritance, there must be a deletion or inactivation of the unnecessary genetic codes in somatic cells. This is known as the Weismann barrier (Weismann et al., 1893). Later on, in the mid-20th century, Conrad Waddington used the image of a ball rolling downhill to describe embryonic development. The ball starts from the top of Waddington's mountain symbolizing the immature stem cells and rolls down in valleys representing the mature differentiated states (Waddington, 1957). In this model the ball is "trapped" in the valley with no possibility to come back or move to another valley because of gravity. Therefore, the cells are committed to one lineage that will result in a permanent cell state (Figure 1, p.13).

The first evidence that this theory was not accurate was discovered by Sir John Gurdon in 1962. He reported that cells could be reprogrammed to a different state using somatic cell nuclear transfer (SCNT) (Gurdon, 1962). Gurdon transferred the nucleus of the intestinal epithelium cells into an enucleated egg (Figure 1, p.13). This artificial chimera started to divide and generated an embryo identical to the donor of the somatic cell. This established that the somatic cell nucleus possesses all the genetic information that is present in the embryonic stem cells. Thus, a somatic nucleus can be reprogrammed to an embryonic state capable of generating an entire individual. Later during the 20th century, other groups expanded SCNT to mammals with the charismatic cloning of the sheep Dolly (Wilmut et al., 1997). Furthermore, mice were successfully derived by SCNT using B cells, which had undergone VDJ-recombination (the mechanism responsible for the high diversity of antibodies and T cell receptors found on B and T cells respectively)

(Hochedlinger and Jaenisch, 2002). Therefore, terminally differentiated cells were able to reprogram, breaking down the idea of irreversibility of the differentiation process.

The generation of heterokaryons, fusion of two different cell types that then contain two different nuclei, showed that it was possible to reprogram the gene expression profile of the cell (Figure 1, p.13). Genes that were usually silenced in one cell type could be reactivated by the fusion with another cell type that expresses them (Blau et al., 1983; Takagi et al., 1983). Very interestingly, this observation was expanded to the fusion of somatic cells such as fibroblast with pluripotent cells, cells that have the potential to produce any embryonic tissue. Pluripotency genes expressed predominantly by stem cells such as octamer-binding protein 3/4 (*OCT-3/4*; *OCT4*) were then expressed in fibroblasts opening the avenue to cell rejuvenation (Cowan et al., 2005; Tada et al., 2001). This discovery implied the existence of factors coming from the stem cell that are able to reprogram the somatic cell into a more "stem-like" cell state and more generally, that key factors could change the fate of a cell. The forced expression of key transcription factors known to mediate the cell identity was used to rewire the gene expression of different cell types and turn them into another. This process is known as transdifferentiation or direct cell conversion. For example, the forced expression of solely MYOD (myoblast determination protein), a muscle differentiation protein, in mouse fibroblasts is sufficient to turn the cells into myoblast-like (Davis et al., 1987). This finding was expanded to other cell type transdifferentiation.

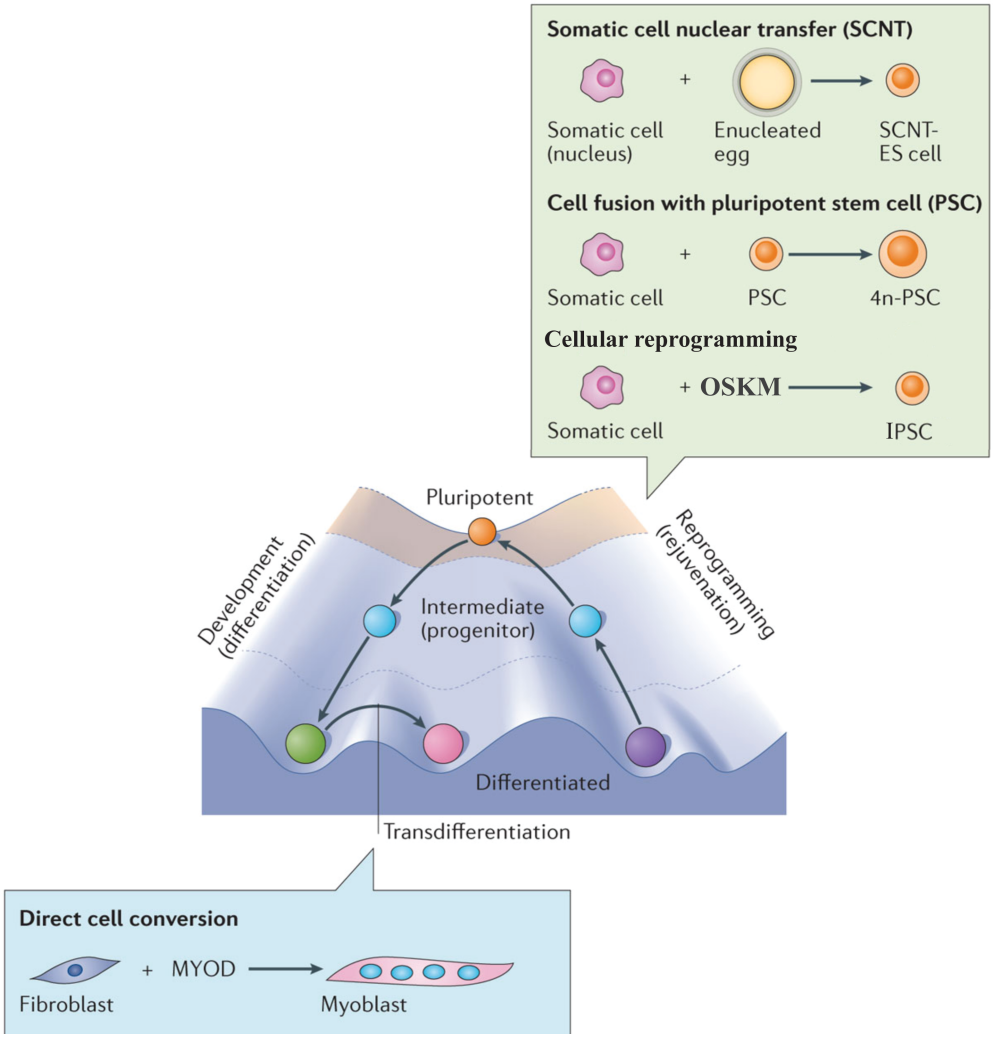

Figure 1: The plasticity of the cell fate. Cell fate acquisition was believed to be unidirectional, starting from an immature pluripotent to a mature differentiated state. Waddington described this process as a ball rolling from the top of the Waddington "mountain" to "valleys" where it will be "trapped". Somatic cell nuclear transfer and somatic cell fusion with pluripotent stem cell indicated that this hypothesis was wrong and established the first indication of cellular fate plasticity. The epigenetic memory of the somatic cell can be erased. It was later shown that ectopic expression of key transcription factors was able to convert a cell type to another. Overexpression of MYOD (myoblast determination protein) in fibroblast converted them into myoblasts. The most sticking evidence of cell fate plasticity came from the Yamanaka group showing that somatic cells were able to be reprogrammed into a pluripotent stem cells state called induced pluripotent stem cell (IPSC) by the ectopic expression of solely four factors: OCT4, SOX2, KLF4 and c-MYC (OSKM). PSC: pluripotent stem cell; ES: embryonic stem; SCNT: somatic cell nuclear transfer. This figure is adapted from (Takahashi and Yamanaka, 2016).

b) Induction of pluripotency

The idea that factors defining a particular cell state could be used to change the fate of other cell types gave rise to the discovery of induced pluripotent stem cells (IPSCs) by the group of Shinya Yamanaka (Takahashi and Yamanaka, 2006) (Figure 1, p.13).

i) Embryonic stem cells

ESCs are characterized by their ability to indefinitely self-renew and form all the embryonic tissues. This property is named pluripotency. It is noteworthy that totipotency defines cells that contribute to the formation of all the tissues from a developing organism such as extra-embryonic and placental tissues and obviously embryonic tissue. Only the zygote and the two first cleavage division cells possess this property.

The study of pluripotency was made easy by the derivation of ESCs lines form the inner cell mass of blastocyst first in mouse (Evans and Kaufman, 1981; Martin, 1981), and then in human (Thomson et al., 1998). Of interest, the culture conditions between mouse and human ESCs were distinct maybe due to species differences and stage of the inner cell mass cells from which they are derived from (Nichols and Smith, 2009).

ii) Identifying ES cell-associated transcripts (ECATs)

Several groups, including the Yamanaka group, developed tools to identify key factors required for pluripotency and infinite proliferation, key characteristics of ESCs. This was accomplished mainly by transcriptional profiling of mouse ES cells. These ES cell-specific genes were termed ES cell-associated transcripts (ECATs).

OCT4 and SOX2 (SRY box-containing factor 2) were among the first well-described core transcription factors of pluripotency networks. They regulate the expression of other pluripotency-associated genes (Tokuzawa et al., 2003; Tomioka et al., 2002).

By using the transcriptional profile of mouse ES cells, the Yamanaka group identified NANOG homeobox as an ECAT showing its crucial role in the maintenance of pluripotency (Mitsui et al., 2003). NANOG overexpression was able to overcome the absence of LIF (Leukemia inhibitory factor, an essential cytokine for mouse cell pluripotency used in serum-containing media (Smith et al., 1988)). LIF stimulates the STAT3 (signal transducer and activator of transcription 3) pathway preventing ES cell differentiation in culture (Matsuda, 1999; Niwa et al., 1998). By comparing the expression profile of NANOG overexpression in ES cells with and without LIF (Mitsui et al., 2003; Smith et al., 1988), the Yamanaka group showed that Krüppel-like factor 4 (KLF4) was a target downstream of the LIF-STAT3 signaling pathway.

KLF4 overexpression was able to sustain ES cells self-renewal in a LIF-independent manner indicating that KLF4 is a core component of the pluripotency network (Niwa et al., 2009). With numerous other studies, this helped dissect and establish the core pluripotency circuitry in ESCs (Figure 2, p.16).

Other molecules such as c-MYC (a proto-oncogene promoting cellular proliferation and survival) (Cartwright et al., 2005)), β-catenin (a WNT signaling pathway regulator) (Sato et al., 2004), TCL1 (T-cell leukemia/lymphoma protein 1, an activator of the PI3K pathway), and the dominant-negative form of GRB2 (growth factor receptor-bound protein 2) (Burdon et al., 1999a, 1999b; Cheng et al., 1998) were reported to be necessary for the maintenance and/or specific to ES cells. Based on these observations and others, the Yamanaka group established a list of 24 potential candidates for mediating cellular reprogramming (Figure 2, p.16).

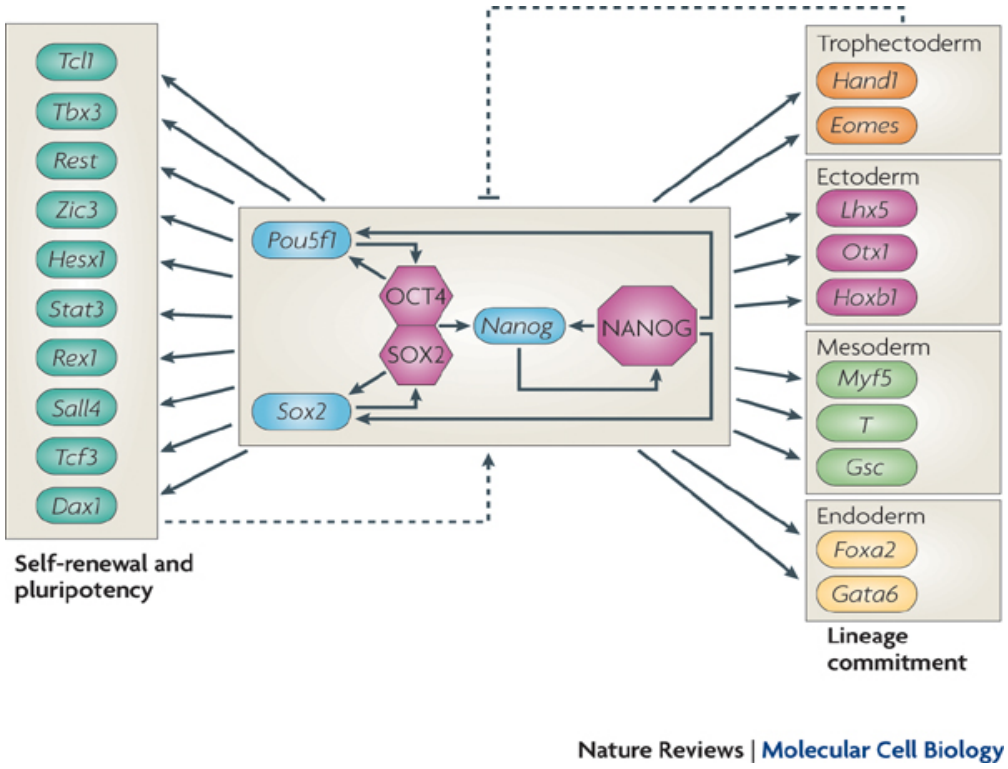

	Gene name	Expression	Function
1	Khdh3 (ECAT1)	pluripotent cells, germ cells	Putative RNA-interacting protein
2	Esg1 (ECAT2, Dppa5)	pluripotent cells	RNA-interacting protein
3	Fbxo15 (ECAT3)	pluripotent cells, germ cells	Target of Oct3/4 and Sox2
4	Nanog (ECAT4)	pluripotent cells, germ cells	Core transcription factor in pluripotent cells
5	ERas (ECAT5)	pluripotent cells	Activator of PI3K pathway
6	Dnmt3l (ECAT7)	pluripotent cells, germ cells	DNA methyltransferase family required for maternal genomic imprints
7	Tdrd12 (ECAT8)	pluripotent cells, germ cells	RNA-interacting protein required for germ cell development
8	Gdf3 (ECAT9)	pluripotent cells, early mesoderm	a member of TGFβ superfamily
9	Sox15	pluripotent cells	Sox family member has redundant function with Sox2
10	Dppa4 (ECAT15-1)	pluripotent cells, germ cells	DNA-interacting factor
11	Dppa2 (ECAT15-2)	pluripotent cells, germ cells	DNA-interacting factor plays important role in lung development
12	Fthl17 (ECAT20)	pluripotent cells	Ferritin, Heavy Polypeptide-Like protein
13	Sall4 (ECAT24)	pluripotent cells, germ cells	Transcription factor plays important role in pluripotency and embryogenesis
14	Oct3/4	pluripotent cells, germ cells	Core transcription factor in pluripotent cells
15	Sox2	pluripotent cells, germ cells, neural cells	Core transcription factor in pluripotent cells
16	Rex1 (Zfp42)	pluripotent cells, germ cells	Target of Oct3/4
17	Utf1	pluripotent cells, germ cells	Target of Oct3/4 and Sox2
18	Tcl1	pluripotent cells, germ cells	Activator of PI3K pathway
19	Dppa3 (Stella, PGC7)	pluripotent cells, germ cells	DNA-interacting molecule protects against DNA demethylation in early embryos
20	Klf4	widely expressed	Transcription factor plays important role in pluripotency
21	β-catenin (stabilized mutant)	widely expressed	Regulator of of cell adhesion and gene transcription as a target of Wnt pathway
22	c-Myc (stabilized mutant)	widely expressed	Transcription factor plays important role in pluripotency
23	Stat3 (dominant active)	widely expressed	Transcription factor plays important role in pluripotency
24	Grb2 (dominant negative)	widely expressed	Adaptor molecule of Ras/MAPK pathway

Figure 2: The stem cell core circuitry and potential reprogramming factors. A complex set of signaling controls embryonic stem cell (ESC) pluripotency and self-renewal. This circuitry is mostly base on mice data but seems to be conserved in humans. OCT4 (also known as POUF5F1), SOX2 and NANOG form a transcriptional module essential for ESC maintenance. Both SOX2 and NANOG (not shown) interact with OCT4 and positively regulate their three transcripts. These genes activate the expression of other pluripotency genes (left of the core circuitry) and at the same time repress lineage commitment genes (right of the core circuitry). The list of the 24 candidate genes for reprogramming selected by the Yamanaka group are enumerated in the table on the right. The core circuitry figure was adapted from (MacArthur et al., 2009) and the list of the 24 candidate genes from (Takahashi and Yamanaka, 2016).

iii) Looking for the reprogramming factors

Takahashi and colleagues (Takahashi and Yamanaka, 2006) tested the 24 candidates for their ability to transform mouse fibroblasts into embryonic stem cell-like cells. None of them on its own was able to support survival in their experimental design. Interestingly, the combination of the 24 factors gave rise to colonies resembling those of embryonic stem cells. By removing single factors of the 24-pool, they were able to narrow down the list to ten factors that were able to reprogram fibroblasts. Further removal of a particular combination of 4 factors showed to inhibit the formation of the colonies. Conversely, the expression of those 4 factors was able to give rise to colonies. Those factors referred as the Yamanaka factors consist of OCT4, SOX2, KLF4 and c-MYC, also know as OSKM.

The Yamanaka group using the same combination of transcription factors then expanded this discovery to human cells (Takahashi et al., 2007). Interestingly, almost at the same time, James Thomson's group at University of Wisconsin, Madison, generated human IPSCs using an alternative combination of transcription factors keeping OCT4 and SOX2 but differing by including NANOG and LIN28 (a cytoplasmic RNA-binding protein) (Yu et al., 2007) instead of KLF4 and c-MYC.

c) The power of IPSCs and their limits

i) Applications for regenerative medicine and disease research

ESCs are an infinite source of cells that could be used for regenerative medicine and a powerful tool to study the steps of development and differentiation. Yet, ethical concerns were raised due to the use of embryos and the likely immune rejection obstructed the potential use of ESCs.

The possibility to derive IPSCs lines from patient's cells removes these roadblocks. Autologous patient-specific stem cells can be derived avoiding the complications due to immune rejection. The derivation of these cells comes from the patient somatic tissue therefore escaping the use of embryos.

In order to use IPSCs for clinical applications, it was necessary to achieve reprogramming without changing the genome of the somatic cell by integrating the reprograming factors. Several techniques were developed such as Cre/Lox (Soldner et al., 2009) or piggyback (Kaji et al., 2009) system, non-integrating viruses (Fusaki et al., 2009), episomal vectors (Yu et al., 2009), and direct mRNA (Warren et al., 2010) or protein (Kim et al., 2009) delivery of the reprogramming factors.

Of great interest is the possibility to study diseases using patient-derived cells with all the genetic alterations. It is therefore possible to establish an *in vitro* system to investigate a particular disease and to potentially establish therapies (Robinton and Daley, 2012). Moreover, the combination with the newly developed genome editing strategies combined with IPSCs technologies open astonishing avenues for tackling those issues (Hockemeyer and Jaenisch, 2016).

ii) IPSCs quality and their resemblance to ESCs

IPSCs and ESCs share many similarities such as morphology, overall gene expression, telomeres and mitochondria biology (Suhr et al., 2010; Van Haute et al., 2013). Nevertheless, studies pointed out differences in the genome, epigenome, transcriptome and proteome raising concerns about their use for therapeutic applications (Gore et al., 2011; Hussein et al., 2011; Laurent et al., 2011). The observed genetic abnormalities could be the result of oncogenic stress induced by the reprogramming factors (González et al., 2013). Indeed, cells exposed to OSKM or OSK show higher levels of phosphorylated histone H2A.X (an early response to double strand breaks). Other studies failed to find genetic and epigenetic abnormalities that would distinguish IPSCs from ESCs (Bock et al., 2011; Cheng et al., 2012; Gore et al., 2011; Guenther et al., 2010; Newman and Cooper, 2010). Interestingly, these data showed that the extent of variations between IPSCs and ESCs were similar to those seen within different IPSCs and ECSs (Vitale et al., 2012).

Table 1, p.19 briefly summarizes the similarities between ESCs and IPSc and their potential for diverse applications.

Table 1: Comparison of embryonic stem cells and induced pluripotent stem cells. Both cells are pluripotent stem cells suitable for the study of stemness, development and differentiation. They differ in their potential to study disease specific models, their applicability for clinical applications and their origin.

	Embryonic stem cells	Induced pluripotent stem cells
Express stemness markers	YES	YES
Pluripotent	YES	YES
Study development and differentiation	YES	YES
Use for disease models	Some	YES, cells are patient-derived
Immune rejection for clinical applications	Very likely, cells are allogeneic	NO, cells are autologous patient-specific
Requires embryos or oocytes	YES	NO

d) Mechanisms of reprogramming: a two-step route

The exact way cellular reprogramming is achieved still remains unknown. The cells have to overcome a series of roadblocks such as apoptosis, cell-cycle arrest and senescence (Banito et al., 2009; Marión et al., 2009; Utikal et al., 2009), oxidative burst (Ji et al., 2014), and DNA damage (Ruiz et al., 2015) in order to successfully become IPSCs. It also includes the silencing of somatic cell genes, switch from an oxidative to a glycolytic metabolism (Panopoulos et al., 2012; Zhang et al., 2012) and requires a mesenchymal-to-epithelial transition (Li et al., 2010; Samavarchi-Tehrani et al., 2010). Population and single-cell based studies suggest a two-step process for cellular reprogramming. These results mainly rely on observations from mouse reprogramming, but seem to be conserved during human cell reprogramming (Figure 3, p.20).

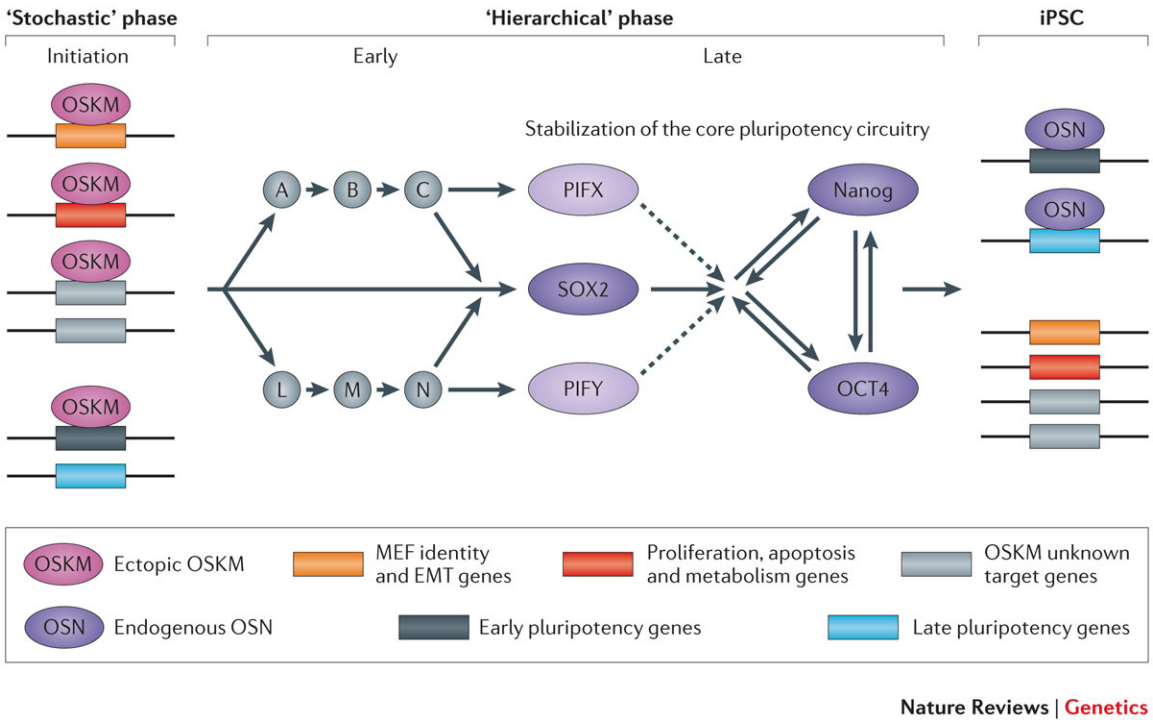

Figure 3: Mechanisms of reprogramming in two steps. During the first stochastic phase, OSKM (OCT4, SOX2, KLF4 and c-MYC) act as pioneer factors and bind many different regions of the genome that are not OSKM targets in embryonic stem cells. This generates a dynamic state of the chromatin. Among the early genes OSKM binds to are: identity genes of the somatic cell (*i.e.* mouse embryonic fibroblast: MEF genes) such as epithelial-to-mesenchymal transition identity genes (EMT) and mesenchymal-to-epithelial transition identity genes (MET) (orange box); genes involved in cellular proliferation, apoptosis and metabolism (red box); unknown target thought to facilitate the genomic fluidity (light grey); and distal regions of early pluripotency genes (dark grey). The light blue box represents the late pluripotency genes that are at this time refractory to be bound by OSKM. A second phase that is more hierarchical occurs. The first part of it is very speculative; in rare cells the early-activated pluripotency genes can start a more deterministic activation of core pluripotency genes such as *Sox2* through a direct or hierarchical fashion. *Sox2* is part of pluripotency initiating factors (PIFs) indispensable for the initiation of the core pluripotency circuitry. The endogenous pluripotency proteins OCT4, SOX2 and Nanog (OSN) bind their target genes (Boyer et al., 2005) and maintain the pluripotency of the induced pluripotent stem cells (IPSCs) in the absence of the exogenous targets. This figure was taken from (Buganim et al., 2013).

In the first step, OSKM bind to various loci not restricted to the ones they would usually bind to in ES cells (Soufi et al., 2012). For example, c-MYC binds to methylated H3K4 regions, marking open chromatin, which includes enhancers and promoters of the somatic genes leading to their silencing (Soufi et al., 2012; Sridharan et al., 2009). This first wave of gene activation is also characterized by the expression of genes implicated in cytoskeleton organization, metabolism, chromatin organization, cell cycle, mitochondria, DNA repair, RNA processing and proliferation (Hansson et al., 2012; Polo et al., 2012a; Zhang et al., 2012). At the same time, OSKM bind to promoters and enhancers of early

pluripotency-associated genes leading to their expression (Soufi et al., 2012). The nature of this early step is rather stochastic and inefficient (Buganim et al., 2012) due in particular to repressive methyl histone marks. These marks cover genes required for pluripotency induction and are responsible for closed chromatin conformations (Soufi et al., 2012).

In a second step, OSKM accesses loci of late pluripotency genes in a more hierarchical and predictable way (Buganim et al., 2012). The access to these late pluripotency gene loci can only occur after the first step. This enables the core pluripotency network to be stably activated.

e) Enhancing the efficiency of reprogramming

Cellular reprogramming is a very inefficient process, depending on the technique and the cell type used; it ranges from 0.001% to 0.1%. Additional factors and molecules were proposed to facilitate reprogramming and increase its efficiency. They are usually referred as "reprogramming enhancers".

i) Genes associated with pluripotency

The expression of other pluripotency-associated genes can increase and in some cases even replace one of the 4 reprogramming factors.

Together with OSKM, TBX3 (T-box transcription factor 3) in mouse and UTF1 (undifferentiated embryonic cell transcription factor 1) or SALL4 (Sal-like protein4) in human, can increase the reprogramming efficiency (Han et al., 2010; Tsubooka et al., 2009; Zhao et al., 2008). KLF4 can be replaced by ESRRβ (Oestrogen-related receptor β) in mouse and NANOG in humans (Feng et al., 2009; Picanço-Castro et al., 2010). Similarly, NR5A2 (nuclear receptor subfamily 5 group 2) and TCL1A can substitute OCT4 (Heng et al., 2010; Picanço-Castro et al., 2010). Enhancers of reprogramming or substitutes for OSKM can also be predicted by their role in the maintenance of ES cells pluripotency. Therefore, it is not surprising to find that ESRRβ is an enhancer. Indeed, it

is a direct target of NANOG that can rescue pluripotency in NANOG deficient ES cells (Festuccia et al., 2012).

ii) Genes involved in cell cycle-regulation

Infinite self-renewal is another characteristic of PSCs. c-MYC promotes cell proliferation. Cell proliferation is required to achieve cellular reprogramming. Tumor suppressor p53 inhibits proliferation and thus its inactivation increases cellular reprogramming probably by overcoming DNA damage and senescence (Banito et al., 2009; Hong et al., 2009; Kawamura et al., 2009; Li et al., 2009; Marión et al., 2009; Utikal et al., 2009). In line with this observation, CIP1, INK4A and ARF (all cell cycle-dependent kinase inhibitors) block cellular reprogramming (Banito et al., 2009; Li et al., 2009; Utikal et al., 2009). Expression of REM2 or cyclin D1 (two cell-cycle enhancers GTP-binding proteins) increases cellular reprogramming (Edel et al., 2010).

iii) Epigenetic modifiers

The passage from a differentiated to a pluripotent state requires a dramatic change in the gene expression profile implying a wide range of epigenetic changes. Therefore, by either promoting the expression of pluripotency genes or lowering the expression of somatic genes can increase the reprogramming efficiency. This altered gene expression profile is dependent on epigenetic marks and the roles they have on the transcriptional regulation of the genes. For example, WDR5 (WD repeat-containing protein) (Ang et al., 2011), DOT1L, SETDB1 and SUV39H1 (Onder et al., 2012) can positively or negatively affect the efficiency of reprogramming. Vitamin C, by enhancing the activity of JHDM1A and JHDM1B (histone demethylases), increases the efficiency of reprogramming (Wang et al., 2011).

II. Alternative routes for increasing the reprogramming efficiency and understanding its mechanism

a) Protein quality control as a necessity for ESCs maintenance

So far, in order to increase the efficiency of reprogramming, studies focused on mainly trying to improve the resemblance of cells to be reprogrammed to ESCs at a transcriptional level and by helping erase the epigenetic memory of the somatic cells in order to speed up the process and hopefully restore the expression of the core pluripotency genes network. This has been proven to be very efficient. We hypothesized that helping somatic cells obtain additional characteristics of ESCs could improve the efficiency of reprogramming. Because of their ability to indefinitely self-renew it is important for the ESCs to protect their protein homeostasis (proteostasis) over many cell divisions. This characteristic has to be shared with other stem cells such as adult stem cells.

In order to find key regulators of the reprogramming process we decided to study the features harbored by SCs to maintain their stemness through the prism of protein quality assurance. By doing that we hoped to find potential cellular pathways that we could modulate in somatic cells in order to increase the efficiency of reprogramming.

The following review is an effort to highlight characteristics of ESCs and also adult SCs that could be important for cellular reprogramming. The mechanisms in play in both ESCs and adult SCs to ensure their self-renewal and maintenance could be used to increase the efficiency of reprogramming. It underlines the need to maintain a healthy proteostasis in SCs in order to ensure their function during development and throughout the course of life. How SCs are able to maintain their function through aging and development are important characteristic of stemness.

This review summarizes how our laboratory relates protein quality control and stemness. We greatly encourage you to read it to have a broader view of our working hypothesis but it is not necessary for understanding the rest of the dissertation:

Vilchez, D.*, Simic, M.S.*, and Dillin, A. (2014). Proteostasis and aging of stem cells. **Trends Cell Biol.** *24*, 161–170.

* equal contributions

Appendix p. 118

While we were writing this review, we were excited to see the publication of studies that linked mechanisms ensuring the quality of proteostasis and the efficiency of reprogramming. Interestingly, two major pathways ensuring the protein quality control in the cells were also playing an important role during cellular reprogramming: autophagy (Wang et al., 2013; Wu et al., 2015) and the ubiquitin-proteasome system (UPS) (Buckley et al., 2012a; Qin et al., 2014). Inhibition of the proteasome activity by either drug treatment with MG132 or genetically by knocking down PSDM14 (a deubiquinating enzyme), decreased significantly the efficiency of reprogramming (Buckley et al., 2012a). Conversely, the knockdown of FBXW7 (F E3 box ligase) increased the reprogramming efficiency (Buckley et al., 2012). Recently, in a genome-wide RNAi screen, Qin and colleagues (Qin et al., 2014) also identified the UPS as a potent barrier for reprogramming.

Even though controversial results have been published, it appears that autophagy also plays an important role in reprogramming. Autophagy is transiently induced during the early stages of reprogramming (Wang et al., 2013; Wu et al., 2015). Whether it plays a positive or negative role is up to debate. Wang and colleagues (Wang et al., 2013) reported that knockdown of ATG5, a key player in the autophagosome formation, resulted in an impaired reprogramming. Wu and colleagues (Wu et al., 2015) reported the opposite; they knocked-down additional player in autophagy such as BECN1 and VSP34 and observed a higher efficiency of reprogramming suggesting a negative role of autophagy during reprogramming.

Based on these observations, we reasoned that not only the quality of the proteostasis has to be high in ESCs but also the path towards the acquisition of pluripotency during reprogramming has to enable the renewal and ensure the quality of the proteaome. This would explain why autophagy is transiently activated during reprogramming (Wang et al., 2013; Wu et al., 2015). Mechanisms important for the maintenance of pluripotency are intrinsically important during the loss of pluripotency that happens during development and differentiation. Because reprogramming seems to be to some extent the reversal of development and differentiation we hypothesized that cellular pathways ensuring the quality of the proteome during normal development and differentiation should also be required for reprogramming.

b) Insights from developmental biology

In order to narrow down which pathways could be the most important for cellular reprogramming, we turned to development. Indeed, reprogramming can be comprehended as a reversal of development. Using a mouse secondary reprogramming system, Cacchiarelli and colleagues (Cacchiarelli et al., 2015) observed distinct waves of gene network activation corresponding to developmental genes characteristic of early embryonic patterning genes and followed by a pre-implantation gene signature, such as miR371, DPPA3 (developmental pluripotency-associated 3) and DNMT3L (DNA methyltransferase 3-like). This being the case, we hypothesized that key cellular processes required during normal development and differentiation could be potential candidates to study reprogramming and increases its efficiency. Besides the obvious epigenetic remodeling that is required to change cell fate, we propose that the maintenance of the cell proteostasis should be of great benefit to reprogram efficiently and successfully.

c) The role of the UPR^{ER} during development and differentiation

Cellular reprogramming by its nature requires a wide morphological change of the somatic cell. Remodeling of organelles such as mitochondria has been shown to take place during reprogramming (Wang et al., 2013; Wu et al., 2015). To our knowledge, no data have been published regarding the remodeling of the ER. This was surprising because the ER homeostasis can be disrupted during tissue development, cell differentiation, senescence (Pluquet et al., 2015), by altered redox status (Merksamer et al., 2008), DNA damage (Fornace et al., 1988) or during an increase of protein synthesis (Kozutsumi et al., 1988). All these changes also happen during cellular reprogramming.

Interestingly, evidence suggests that the ER stress and UPR effectors are required during development. Indeed, the homozygous deletion of either *Hspa5* (Luo et al., 2006), *Grp94* (Wanderling et al., 2007), *Grp58* (Garbi et al., 2006), *Ire1a* (Iwawaki et al., 2009), *Xbp1* (Reimold et al., 2000), *Calreticulin* (Mesaeli et al., 1999), or deletion of both *Atf6a* and *Atf6b* (Yamamoto et al., 2007) leads to embryonic lethality in mice. This is particularly interesting if reprogramming has reversal features of development; it would not be surprising that the ER stress and UPR modulators would be beneficial for reprogramming. To further support this idea, several components of the endoplasmic reticulum unfolded protein response (UPR^{ER}) have been shown to have an important role during differentiation. IRE1 increases lymphopoiesis of B cells (Zhang et al., 2005), XBP1 induces osteogenic and plasma differentiations (Iwakoshi et al., 2003), and CHOP plays an important role in the differentiation of B cells, erythrocytes, osteocytes and chondrocytes (Cui et al., 2000; Pereira et al., 2004; Skalet et al., 2005; Yang et al., 2005). The UPR^{ER}, as a stress-coordinated pathway, is important in the regulation of differentiation of the mouse intestinal epithelial stem cell (Heijmans et al., 2013).

III. The importance of the ER and UPR^{ER}

a) The integrative role of the ER

The ER is the main organelle responsible for the synthesis, maturation and post-translational modification of secreted and membrane proteins. It is involved in the synthesis of 1/3 of the cell proteome, the biogenesis of membranes structures and metabolic process such as ion storage (Kleizen and Braakman, 2004). Fatty acid desaturation and other lipogenic reactions such as those involved in ceramides, sterols, triacylglycerols and most phospholipids synthesis, occur on the cytosolic face of the ER membrane. The ER houses enzymes involved in fatty acid oxidation and gluconeogenesis. Its membrane forms the nuclear envelope and contributes to the biogenesis of autophagic membranes, peroxisomes and lipid droplets. The transfer of various molecules, lipids and calcium are facilitated by its numerous contacts with other membranes structures of the cell (Rutkowski and Hegde, 2010).

Hence, the ER integrates these various aspects of cellular and organismal homeostasis into a unique molecular response: the unfolded protein response (UPR^{ER}). The UPR^{ER} is an important pathway as shown by its conservation among various species from yeast to mammals (Ruberti and Brandizzi, 2014). This integration has to take into account the nature of the perturbation, intensity and duration in order to properly maintain homeostasis.

b) The molecular mechanism of the UPR^{ER}

Kozutsumi and colleagues (Kozutsumi et al., 1988), and later Dorner and colleagues (Dorner et al., 1990) observed that the impairment of ER protein folding in consequence to toxin exposure can lead to the induction of ER chaperones. This set the path to look for signaling mechanisms from the ER to the nucleus and eventually uncover this more general pathway that is the UPR^{ER}.

Upon ER stress, three main responses take place (Ron and Walter, 2007). First, a transient adaptation occurs by lowering protein synthesis and translocation in the ER. Second, UPR^{ER} targets are transcriptionally activated in order to increase the capacity to handle the unfolded proteins, in particular chaperones. Lastly, if the ER isn't able to restore its homeostasis, cell death is triggered as a response to protect the organism.

Yeast has a simple UPR^{ER}, a single arm compared to vertebrates. Ire1p (the ER-resident transmembrane kinase) upon ER stress activates Hac1p, a transcription factor responsible for the activation of numerous genes (Sidrauski et al., 1998).

In vertebrates, the UPR^{ER} involves three ER-resident transmembrane proteins: IRE1 (inositol-requiring protein-1), PERK (protein kinase RNA (PRK)-like ER kinase) and ATF6 (activating transcription factor 6). Upon acute stress, these three branches reduce the import of proteins into the ER by specific mechanisms.

These three ER-resident transmembrane proteins have a luminal portion able to sense protein-folding environment in the ER, and a cytoplasmic portion transducing the state of the ER to the rest of the cell via transcriptional and translational means. Figure 4, p.29, summarizes the mechanism of the UPR^{ER}; a more detailed description of the three pathways involved follows.

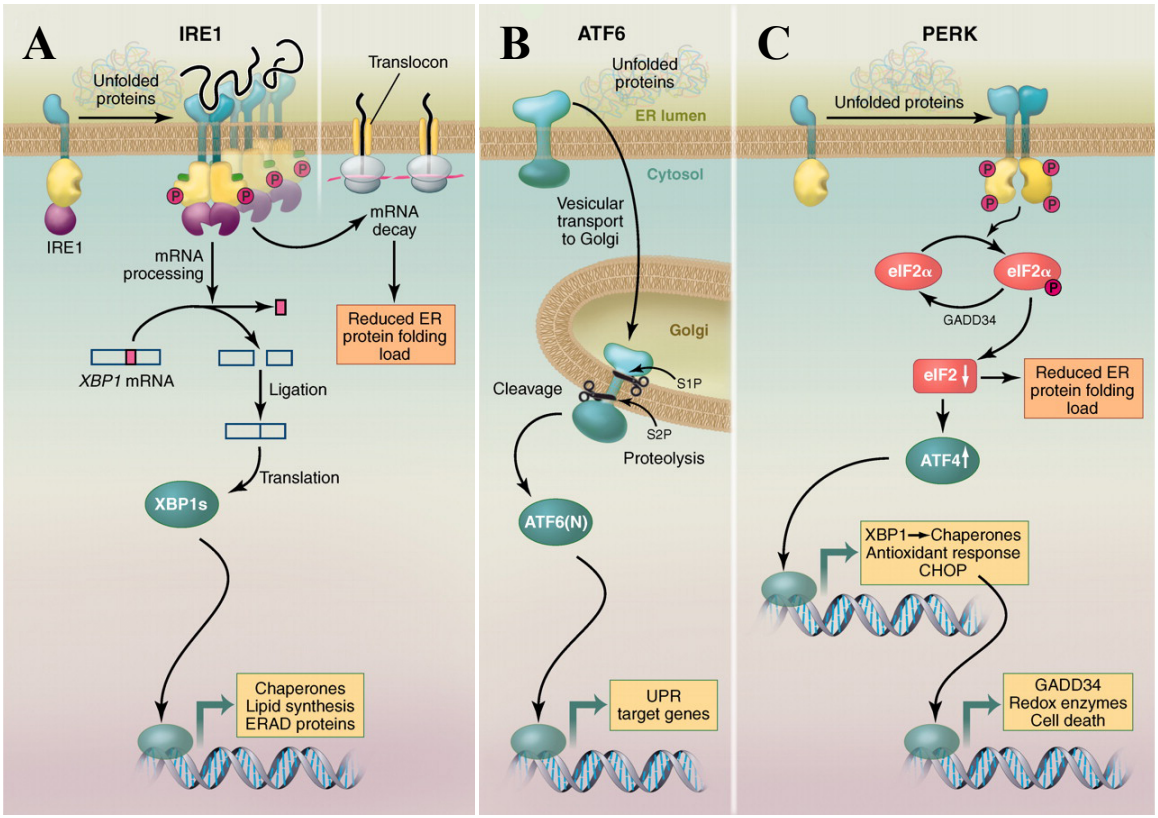

Figure 4: The molecular mechanisms of the UPR^{ER}. A: In stressed cells, IRE1 oligomerizes and trans-autophosphorylates, which unmasks its dormant endoribonucleolytic activity. Active IRE1 excises a small RNA fragment in *XBP1* mRNA. This spliced version encodes a potent transcription factor, XBP1s, which activates a variety of genes including chaperones. This helps to deal with the unfolded proteins. In parallel, active IRE1 degrades specific mRNAs, which results in a reduced protein load on the ER. B: Upon stress, ATF6 is delivered to the Golgi apparatus where it is cleaved by SP1 and SP2. The cytosolic portion of ATF6 is then imported into the nucleus where it activates UPR target genes. C: Similarly to IRE1, PERK oligomerizes and is activated by trans-autophosphorylation during stress. Subsequent phosphorylation of eIF2α at Ser51 leads to a global decrease of translation. Through a particular mechanism, ATF4 translation is increased. ATF4 activates CHOP and GADD34. The later is important to dephosphorylate eIF2α and stop the activation of the PERK pathway. The figure was adapted from Walter and Ron (Walter and Ron, 2011).

i) IRE1 pathway

IRE1 (inositol-requiring protein-1) was discovered in yeast screen aiming at identifying blockers of the UPR^{ER} activation. IRE1 is type 1 ER-resident transmembrane protein. Its cytoplasmic domain contains a kinase domain (Cox et al., 1993; Morl et al., 1993). During stress, IRE1 oligomerizes and trans-autophosphorylates the juxtaposed cytoplasmic kinase domain (Figure 4A, p.29). Interestingly, IRE1 is its own and only substrate unlike classic cascade of kinase activation (Shamu and Walter, 1996). This

results in the activation of its endoribonucleolytic activity (Sidrauski and Walter, 1997). IRE1 cuts twice the only precursor mRNA *Hac1* in yeast (Cox and Walter, 1996; Mori et al., 1996) and *XBP1*, x-box binding protein 1, in metazoans (Calfon et al., 2002; Yoshida et al., 2001). A spliced version is then generated after the ligation of the 5' and 3' mRNA ends that encodes an activator of UPR^{ER} target genes. Interestingly, in metazoans, both the precursor and the spliced forms are translated (Calfon et al., 2002). The spliced form of XBP1 is more stable and is a more potent activator of UPR target genes while the precursor encodes a protein that represses UPR target genes (Calfon et al., 2002; Yoshida et al., 2001). Among those genes are HSPA5 (also known as BIP or GRP78) and $p58^{IPK}$ (Lee et al., 2003).

Levels of *XBP1* mRNA will continue to rise even when the ER stress decreases and IRE1 is inactivated (Yoshida et al., 2006). This potentially serves to terminate the activation of the UPR^{ER} since the precursor *XBP1* mRNA encodes for a repressor of the UPR^{ER} target genes that could compete with the spliced form for binding sites.

In parallel, IRE1 is able to cleave diverse mRNA at the ER membrane, therefore reducing the load of proteins in the ER by a mechanism called RIDD (regulated IRE1-dependent decay) (Hollien and Weissman, 2006).

ii) ATF6 pathway

Haze and colleagues (Haze et al., 1999) searched for proteins able to bind UPR-activated promoters and found ATF6 (activating transcription factor 6). Synthesized as an inactive precursor, ATF6 is tethered to the ER membrane and has a stress-sensing portion in the lumen. Upon ER stress, ATF6 is shuffled from the ER to the Golgi where two Golgi-resident proteases will cleave it (Figure 4B, p.29). The first is S1P (site 1 protease) and the second S2P (site 2 protease), which cleave ATF6 in an intramembrane region releasing its cytosolic DNA-binding domain that can in turn go to the nucleus and activate target genes (Haze et al., 1999). This binding domain is a basic leucine zipper (bZIP) domain; it binds to ER stress response element in the promoter of genes such as

HSPA5, CHOP, XBP1, GRP94 (glucose-regulated protein 94, an HSP90 chaperone family member) (Yoshida et al., 2000).

iii) PERK pathway

PERK (protein kinase RNA (PKR)-like ER kinase) is another ER-localized type I transmembrane protein. It has a stress-sensing luminal domain and a cytoplasmic portion that contains a protein kinase domain. Upon stress, PERK is able to trans-autophosphorylate after oligomerization (Figure 4C, p.29). PERK phosphorylates the α-subunit of eIF2α (eukaryotic initiation factor-2) at Ser51. This inhibits the pentameric guanine nucleotide exchange factor eIF2B and prevents the recycling of eIF2α to its active GTP-bound form. Less active eIF2α are available which results in less translation initiation, reducing the load of proteins in the ER (Harding et al., 1999). Parallel to its role in reducing the global translation, phosphorylation of eIF2α at Ser51 leads to the transcriptional activation of genes involved in the UPR^{ER} (Harding et al., 2003; Lu et al., 2004). In mammalians, phosphorylated eIF2α results in the translation of ATF4, a transcription factor responsible for the activation of a wide variety of UPR^{ER} genes. The 5'-untransltated region of ATF4 (uORF1, upstream open reading frame 1) facilitates the scanning and reinitiation of ribosomes at downstream coding regions. Under unstressed conditions, ribosomes scan downstream of uORF1 and reinitiate at the next coding region: uORF2, an inhibitory element, which inhibits ATF4 translation. Under stress, levels of the active GTP-bound eIF2α form decrease and results in a delayed reinititation of the ribosomes at the uORF2. This allows the ribosomes to scan through uORF2 and to reinitiate at the coding region of ATF4 (Vattem and Wek, 2004). Two key target genes of the PERK pathway are CHOP (transcription factor C/EBP homologous protein) and GADD34 (growth arrest and DNA damage-induced 34). CHOP is induced by ATF4 and controls the expression of genes involved in apoptosis (Marciniak et al., 2004). Therefore, the PERK signaling pathway can be very protective under low activation and initiate apoptosis when the stress is prolonged and stronger. CHOP induces the expression of GADD34 which restores the protein translation by dephosphorylating

eIF2α (Gorman et al., 2012). In order to fine tune the activity of CHOP and prevent the premature activation of apoptosis, it has been observed that $p58^{IPK}$ (protein 58 inhibitor protein kinase) binds and inhibits the PERK kinase domain, which stalls its activity (Yan et al., 2002).

It is noteworthy that other signaling pathways such as amino-acid deprivation or double-stranded RNA accumulation lead to the phosphorylation of eIF2α and the activation of common target genes with the UPR^{ER}. For this reason, the signaling pathway downstream of the eIF2α phosphorylation was called integrated stress response (ISR) (Harding et al., 2003). ATF4, in mammalian cells, accounts for about half of the PERK-dependent UPR genes induction, suggesting the existence of other effectors downstream of phosphorylated eIF2α (Harding et al., 2003).

c) Stress recognition

The exact mechanism of how these three transmembrane proteins sense stress and misfolded proteins is still unclear. A titration type hypothesis was proposed to explain the activation of the UPR^{ER}. Under normal conditions, the ATP-dependent ER chaperone HSPA5 maintains these sensors in an inactive state by binding to their luminal domain. HSPA5 is a member of the HSP70 family of heat-shock proteins; it is the most abundant protein in the ER lumen. Under conditions of stress, HSPA5 binds to nascent peptides and unfolded proteins and promotes proper folding in an ATP-dependent manner preventing protein aggregation. Thus, when excessive amounts of misfolded proteins occur, HSPA5 is titrated away from the three stress-sensing transmembrane proteins. Consistent with this idea, HSPA5 overexpression attenuates PERK and IRE1 activities and limits the UPR^{ER} (Okamura et al., 2000).

A direct binding of the unfolded protein to one of these stress-sensors has also been proposed based on crystal structures studies. The yeast IRE1 luminal domain has a major histocompatibility complex-like domain architecture compatible with peptide binding (Credle et al., 2005).

d) The ER shape and its contribution to the ER function

The ER is comprised of different domains that expand throughout the entire cell. The nuclear envelope is a particular part of the ER composed of two flat and large membrane bilayers (the outer and inner nuclear membranes) punctually connected by nuclear pores (Hetzer et al., 2005). Branching out of the outer nuclear membrane, the peripheral ER is a wide network of tubules and cisternae structures through the entire cytoplasm to the plasma membrane. Importantly, the perinuclear space and the peripheral ER lumen are continuous. Tubules are characterized by their high membrane curvature while cisternae are regions of piled parallel flat bilayer membranes (Friedman and Voeltz, 2011). Key proteins shape the ER and are associated to either tubules or cisternae structures. Reticulon proteins, such as Reticulon 4 also called Nogo, are responsible for the tubules high curvature and are required for their formation (Shibata et al., 2008). CLIMP-63 is responsible for the proper intraluminal spacing of the cisternae (Shibata et al., 2010).

The shape of the ER is highly correlated to its function. Indeed, muscle cell ER is enriched in tubules devoid of ribosomes. This could help to quickly control calcium levels during contractions. Whereas secretory cells, which require abundant secretion of proteins, have abundant cisternae densely covered with ribosomes (Friedman and Voeltz, 2011). Interestingly, the shape of the ER can be modulated in response to UPR^{ER} activation in order to alleviate the stress (Schuck et al., 2009).

IV. Working hypothesis

During normal development and differentiation, cells can dramatically change their morphology and remodel their organelles such as the ER. The UPR^{ER} plays a crucial role during those events. We reasoned that because cellular reprogramming can be comprehended as a reversal of reprogramming, the UPR^{ER} should have an essential function in this process. The ER homeostasis is disrupted under conditions of senescence (Pluquet et al., 2015), by altered redox status (Merksamer et al., 2008), DNA damage (Fornace et al., 1988) or during an increase of protein synthesis (Kozutsumi et al., 1988). These events happen during cellular reprogramming. We therefore hypothesized that the UPR^{ER} should be activated and play an active role during reprogramming.

Genes responsible for pluripotency and self-renewal, two of the key characteristics of ESCs, greatly improve the reprogramming efficiency. Because SCs can indefinitely divide, they must maintain an extremely "healthy" proteostasis, another key characteristic of SCs. We therefore hypothesized that cellular pathways insuring this task could enhance cellular reprogramming. We postulated that the proteotoxic-protective role of the UPR^{ER} could be beneficial for cellular reprogramming.

The following chapter summarizes our main findings regarding the contribution of the UPR^{ER} during cellular reprogramming.

Results

This part summarizes the main results achieved during my doctoral work to study the role of the UPR^{ER} during cellular reprogramming. At the time of the writing, this work is almost ready to be submitted, we decided to present our results in a paper manuscript format. Due to formatting requirements for the manuscript, the discussion section of the manuscript is very condensed and doesn't go into details. Therefore, an extended discussion section of the results follows. To avoid multiple identical citations, all the references are summarized in one section at the end of the dissertation.

The activation of the UPR^{ER} is an essential step in the acquisition of pluripotency during reprogramming

Milos S. Simic[1, 2, 3], Robert T. Schinzel[1, 2, 3], Erica Moehle[1, 2, 3], Jonathan J. Halloran[1, 2, 3], Kartoosh Heydari[3], Melissa Sanchez[1, 2, 3], Dirk Hockemeyer[3] and Andrew Dillin[1, 2, 3, 4]

[1] Howard Hughes Medical Institute University of California, Berkeley, CA 94720 USA

[2] California Institute for Regenerative Medicine, Berkeley, CA 94720 USA

[3] University of California, Berkeley, CA 94720 USA

[4]correspondence to: dillin@berkeley.edu

ABSTRACT

Somatic cells can be reprogrammed into a pluripotent stem cells state and is achieved by the forced expression of 4 transcription factors: OCT4, SOX2, KLF4 and c-MYC (Takahashi and Yamanaka, 2006). This process theoretically requires a global remodeling of the organelles and a drastic change in metabolism (Folmes et al., 2011). Furthermore, reprogramming has an inherent property of stochastic variation that is limiting and largely unknown. We hypothesize that this variation is due, in part, by variable regulation of the proteostasis network. We therefore postulated that the early steps of reprogramming would result in the activation of a variety of stress pathways that regulate the proteostasis network, which might in turn impact the efficiency of reprogramming. We focused in particular on the endoplasmic reticulum unfolded protein response (UPR^{ER}). We find that the UPR^{ER} is activated during reprogramming and that its activation can increase the efficiency of this process. We find that stochastic activation of the UPR^{ER} can predict reprogramming efficiency. These results suggest that the low efficiency of cellular reprogramming is partly the result of the cell's inability to initiate a proper stress response to cope with the newly expressed load of proteins that will eventually change the fate of this cell.

Introduction

Cellular reprogramming of somatic cells into induced pluripotent stem cells (IPSCs) through the forced expression of a set of factors (OCT4, SOX2, KLF4 and c-MYC for example) (Takahashi and Yamanaka, 2006) highlights the remarkable plasticity found within cells and provides an incredible potential for regenerative medicine applications (Polo et al., 2012). However, the quality and the high variability in efficiencies are problematic (González et al., 2011). Evidence of DNA damage and genomic instability in IPSCs raises concerns for their use in patients (Ruiz et al., 2015). It is therefore important to better understand the mechanisms underlying reprogramming to improve this method (Vierbuchen and Wernig, 2012). The early phases of reprogramming is hypothesized to be stochastic and responsible for its low efficiency (Takahashi and Yamanaka, 2016). What drives this early stochastic variation is unknown and it remains the major hurdle in the reprogramming process.

The endoplasmic reticulum (ER) is the site where secreted and membrane-bound proteins are synthesized and represents 1/3 of the proteome. The ER machinery integrates various signals such as growth, differentiation and inflammation. When ER homeostasis is disrupted by increased protein synthesis, cell differentiation, tissue development, senescence, DNA damage and many other stressors, a complex signaling process is activated: the unfolded protein response (UPR^{ER}) (Walter and Ron, 2011). The UPR^{ER} is composed of three branches. They operate in parallel and use distinctive signal transduction mechanism. Each branch senses the protein folding state in the ER lumen using three transmembrane proteins: ATF6 (activating transcription factor 6), PERK (double-stranded RNA-activated protein kinase (PRK)-like ER kinase) and IRE1 (inositol requiring enzyme 1) (Walter and Ron, 2011). IRE1 converges on the x-box binding protein 1 transcription factor, XBP1, causing its splicing to create the *XBP1s* mRNA that can be translated and incorporated into the nucleus to regulate hundreds of genes required for ER protein folding and morphology.

Cellular reprogramming causes a dramatic change in cell morphology and imposes the remodeling of many organelles such as mitochondria (Wang et al., 2013). We therefore hypothesized that cellular reprogramming would restructure the ER and could potentially activate the UPR^{ER}.

Results

The UPR^{ER} is activated during reprogramming

Organelles such as mitochondria, ER and Golgi are less abundant and less mature in embryonic stem cells (ESCs) compared to their differentiated counterparts (Sathananthan et al., 2002). Therefore, cellular reprogramming involves a wide remodeling of these organelles and a dramatic change in gene expression (Koche et al., 2011; Mikkelsen et al., 2008). Synthesis of new proteins and proteins characteristic of the somatic state coexist for a brief time (Koche et al., 2011; Mikkelsen et al., 2008) possibly creating an imbalance in protein homeostasis. Thus, we hypothesized that cellular reprogramming could activate particular stress pathways regulating protein homeostasis. We focused

upon the UPR^{ER}, which integrates intra- and extra-cellular signals for its role in cell differentiation and development.

During ER stress, the transcription of central regulators of the UPR^{ER} stress response are increased as well as their downstream targets. We analyzed the mRNA levels of the major transcription factors representing the three braches involved in the UPR^{ER}: ATF6, ATF4 and XBP1s (Walter and Ron, 2011), during reprogramming of human somatic cells. All the three factors showed significantly higher levels than the control at day 6 after reprogramming suggesting an activation of the UPR^{ER} (Figure 1A, pp.54-55). We analyzed the canonical downstream transcriptional targets of the UPR^{ER}, such as HSPA5 and GRP94 (Walter and Ron, 2011) and found that both had higher levels than cells not undergoing reprogramming (Figure 1A, pp.54-55). The fold induction was similar to what would be observed by the overexpression of XBP1s, the active form of XBP1 that activates downstream targets of the UPR^{ER} (Walter and Ron, 2011) (supplementary Figure 1A, pp.62-63). To corroborate the RNA levels, we analyzed HSPA5 protein levels and found that it too was increased (Figure 1B, pp.54-55). To further characterize the activation of the UPR^{ER} we analyzed the phosphorylated state of IRE1 and PERK and found that both were highly phosphorylated during the reprogramming process (Figure 1B, pp.54-55 and supplementary Figure 1C, pp.62-63). During the reprogramming process, the 4 reprogramming factors are delivered by viral infection, to rule out the possibility that the UPR^{ER} is induced by the use of a viral delivery system, we used an episomal delivery by electroporation of the reprogramming factors and observed UPR^{ER} activation (supplementary Figure 1B, pp.62-63).

In yeast, ER stress induces a change in the ER morphology to allow supplementary handling of misfolded proteins (Schuck et al., 2009). By electron microscopy analysis, the ER appears largely tubular and lacking sheet structures during reprogramming (Figure 1C, pp.54-55), strikingly resembling cells treated with the ER stressor, tunicamycin (supplementary Figure 1D, pp.62-63). When we analyzed Reticulon 4 (a marker of tubular ER) and CLIMP-63 (a marker of cisternae) (Friedman and Voeltz, 2011) levels during reprogramming, we found that Reticulon 4 was increased and

CLIMP-63 was decreased, consistent with the EM analysis revealing tubular ER structures and few sheet structures (supplementary Figure 1C, pp.62-63).

Tubular ER morphology is associated with impaired secretory capacity of the ER. We tested the secretion capacity of cells undergoing reprogramming by following the secretion of the exogenously expressed humanized *Gaussia* luciferase protein (Gluc) (Badr et al., 2007). We collected the supernatant of cells expressing the reprogramming factors and observed a reduction in secreted Gluc as measured by luciferase activity. The reduced Gluc was not due to reduced expression of during the reprogramming process (Figure 1D, pp.54-55). On the contrary, Gluc is unable to be secreted and stays in the ER.

Because basal levels of ER stress are observed during the early phase of reprogramming, we reasoned that this could be protective against an additional ER stress such as the addition of tunicamycin. We established dose-survival curve to calculate the EC50 and found that cells undergoing reprogramming were more protected than control cells (Figure 1E, pp.54-55). Taken together, ER stress and morphology are dramatically altered during the reprogramming process.

Activation of the UPR^{ER} increases the efficiency of cellular reprogramming

To better understand the role of the UPR^{ER} during reprogramming and test if it could be a limiting factor for successful reprogramming, we followed induction of the endogenous HSPA5 fused to eGFP. Using transcription activator-like effector nuclease (TALENs) genome editing, we placed the eGFP encoding sequence into the 3' end of one allele of the *HSPA5* locus in H9 ESCs. Successful targeting was confirmed by southern blotting (supplementary Figure 2A, pp.64-65). The HSPA5-GFP cell line was then differentiated into fibroblast-like cells to use for cellular reprogramming using an embryoid mediated differentiation protocol (Ruiz et al., 2012). HSPA5-GFP fibroblast cells responded faithfully to ER stress caused by tunicamycin, showing robust induction under the stress condition. Likewise, after removal of the tunicamycin, GFP levels dropped from these cell lines (supplementary Figure 2B,C, pp.64-65).

During the process of reprogramming the use of cell surface markers allows an accurate assessment of the reprogramming efficiency. Previous studies showed that the fibroblast surface marker CD13 is downregulated during successful reprogramming while the pluripotency markers such as SSEA-4 and TRA-1-60 are upregulated (Chan et al., 2009). Interestingly, SSEA-4 appears earlier than TRA-1-60, the latter serving as a marker of more mature IPSCs (Chan et al., 2009). Therefore, the simultaneous presence of both SSEA-4 and TRA-1-60 is an indication of cells further along in the reprogramming process (Figure 2A, I, pp.56-57), while cells only positive for SSEA-4 and lacking TRA-1-60 would be less far progressed (Figure 2A, II, pp.56-57). Finally, cells with none of these markers are the furthest from achieving the reprogrammed state (Figure 2A, III, pp.56-57). Based on the distinction of the different reprogramming states using these makers, we analyzed the levels of HSPA5-GFP at different time points of reprogramming (Figure 2B, pp.56-57). Consistently we observed higher levels of HSPA5-GFP in the cells that had progressed the furthest in the reprogramming process (SSEA-4 and TRA-1-60 positive, I).

To validate the GFP reporter, we sorted the three populations (I, II, and III) at day 7 of reprogramming and assessed their UPR^{ER} levels by mRNA levels. As expected, we found higher levels of induction in the SSEA-4+/TRA-1-60+ cells (Figure 2C, pp.56-57). Additionally, we confirmed the reactivation of the endogenous stemness genes in the SSEA-4+/TRA-1-60+ population (supplementary Figure 3, pp.66-67).

Because of the correlation between increased HSPA5 levels and progression towards the reprogrammed state, we asked what role, if any, did the UPR^{ER} play in the reprogramming process. To address this question, we modulated the UPR^{ER} during reprogramming either pharmacologically or genetically. Pharmacologically, we either activated the UPR^{ER} using APY29, a drug that activates the RNAse activity of IRE1 (Hetz et al., 2013) , or inactivated the UPR^{ER} using GSK2656157, a compound that inhibits both PERK and eIF2α phosphorylation (Atkins et al., 2013) (supplementary Figure 4A, pp.68-69). In all cases cell proliferation rates were unaffected (supplementary Figure 4B, pp.68-69). Strikingly, activation of the UPR^{ER} with APY29

increased the percentage of cells expressing the SSEA-4 and TRA-1-60 while limiting the UPR^{ER} with GSK2656157 decreased this population (Figure 2D, pp.56-57).

Intrigued by the pharmacological manipulation of the UPR^{ER} upon reprogramming, we investigated whether overexpression of XBP1s could increase the reprogramming efficiency in keratinocytes. Consistent with the previous results, XBP1s increased the reprogramming efficiency and this activity was dependent upon the transcriptional activity of XBP1s since overexpression of a mutant version of XBP1s that lacked its DNA binding domain was unable to promote reprogramming (Figure 2E, pp.56-57). We confirmed that the increase in reprogramming efficiency was not the result of a higher proliferation rate due to XBP1s overexpression (supplementary Figure 5A, pp.70-71) and also followed cells to full IPSCs formation verifying the expression of stemness genes (supplementary Figure 5B, pp.70-71). We were able to expand these observations by reprogramming fibroblast using an episomal method (supplementary Figure 6, pp.72-73).

Taken together, UPR^{ER} activation is necessary and sufficient to promote reprogramming of fibroblast-like cells. On the basis of these results we concluded that activation of the UPR^{ER} increases reprogramming efficiency.

Activation of the UPR^{ER} must be transient during reprogramming

Interestingly, we observed qualitatively that the success of IPSCs clonal expansion was lower when cells overexpressed XBP1s driven by the EF1α promoter with retroviral reprogramming. On the contrary, in the episomal reprogramming method, IPSCs clonal derivation was very similar between the GFP control and XBP1s overexpression driven by a CMV promoter. EF1α promoter is notoriously used in embryonic stem cells because it is rarely silenced contrary to CMV (Xia et al., 2007). This led us to postulate that high levels of XBP1s in IPSCs would be detrimental and that the UPR^{ER} is required transiently during reprogramming. Consistent with this observation, EF1α driving *XBP1s* IPSC successfully derived clones showed silencing to levels similar to EF1α driving *emGFP* derived clones while the *XBP1s-DBD* (coding for the transcriptionally inactive XBP1s) IPSC derived clones failed to do so (supplementary Figure 7A, pp.74-75). Remarkably, overexpression of XBP1s using the EF1α promoter in H9 ESCs prevented their proper

spreading (supplementary Figure 7B, pp.74-75). Notably, basal levels of UPR^{ER} activity are low in embryonic stem cells compared to their differentiated counterparts as shown by transcriptome analysis from a published data set (Lowry et al., 2008; Soufi et al., 2012) (supplementary Table 1, p.80), the HSPA5-GFP levels (supplementary Figure 7C, pp.74-75) and western blot of XBP1s and ATF6 (supplementary Figure 7D, pp.74-75). Therefore, activation of the UPR^{ER} must be transient during reprogramming.

HSPA5-GFP levels predict the efficiency of reprogramming

Because reprogramming efficiency could be increased by the activation of the UPR^{ER}, we postulated that the levels of HSPA5-GFP might predict the efficiency of reprogramming in populations of cells undergoing the process of reprogramming. Therefore, we hypothesized that variations in the levels of HSPA5 could be a driving factor for successful reprogramming. During the early phase of reprogramming using our HSPA5-GFP reporter we observed a Gaussian distribution of GFP fluorescence amongst the cell population (Figure 3A, pp.58-59). We subdivided the GFP positive population into 3 equal subpopulations according to their levels of HSPA5-GFP expression (low, medium and high) at day 8 of reprogramming. The percentage of SSEA-4+/TRA-1-60+ cells was the highest in cells with the higher levels of HSPA5-GFP and lowest in the cells with the lower levels of HSPA5-GFP expression (Figure 3A, pp.58-59). We expanded this observation to multiple time points during reprogramming and observed the same result: higher HSPA5-GFP correlated with increased SSEA-4/TRA-1-60+ cells (Figure 3B, pp.58-59). This finding suggests that levels of HSPA-5 could serve as a good predictor of reprogramming efficiency.

To test this idea, we sorted cells at day 7 of reprogramming based on their levels of HSPA5-GFP into two populations: high and low levels. Cells were plated onto MEFs and we assessed IPS colony formation. After 10 days in culture, cells were stained for TRA-1-60. As postulated, cells with higher levels of HSPA5-GFP at day 7 gave rise to more IPS colonies (Figure 3C, pp.58-59). Taken together, HSPA5-GFP levels appear to be predictive of IPSC formation during the reprogramming process.

Cellular internal complexity predicts the efficiency of reprogramming

During FACS analysis of the high HSPA5-GFP fibroblast-like cells we noticed that the Side SCatter (SSC) and Forward Scatter (FSC) parameters of these cells were distinct from low HSPA5-GFP cell populations under normal growth conditions (Figure 4A, pp.60-61). SSC reflects the internal cellular complexity and membrane texture while FSC measures the size of the cells (Figure 4A, pp.60-61), suggesting that high HSP5-GFP cells might have more complex internal granularity and possibly be larger. Under normal conditions, the top 33% HSPA5-GFP fibroblast-like cells had high internal cellular complexity and size; conversely the lowest 33% HSPA5-GFP cells had a lower internal cellular complexity and size. Therefore, there appears to be a gradient that positively correlates the levels of HSPA5-GFP with SSC and FSC. To exclude the possibility that those are two distinct populations resulting from a heterogeneous differentiation, we sorted these two populations. Seven days later the HSP5-GFP medians were similar (Figure 4B, pp.60-61). In addition, when the UPR^{ER} was ectopically induced, by expression of XBP1s, the SSC and FSC parameters were increased (Figure 4C, pp.60-61). Interestingly, the addition of tunicamycin to naïve cells also changed the SSC and FSC measurements to match those found with ectopic XBP1s expression. Addition of tunicamycin to the XBP1s cells did not further change the SSC and FSC (Figure 4C, pp.60-61 and supplementary Figure 8A, pp.76-77). Lastly, knockdown of XBP1 decreased the population of cells with high SSC and FSC values (supplementary Figure 8B and C, pp.76-77).

Intrigued by the correlation of increased HSPA5-GFP expression, ER stress, SSC/FSC increases, we hypothesized that SSC and FSC might predict the efficiency of reprogramming, much like increased HSPA5-GFP did. On day 8 of reprogramming we gated cells with high and low SSC/FSC. Interestingly, cells with higher SSC and FSC had a higher percentage of SSEA-4+/TRA-1-60+ cells than their counterparts (Figure 4D, pp.60-61).

Because these results were obtained from fibroblast-like cells derived from ESCs, we further tested the predictive reprogramming efficiency of high SSC/FSC values of

primary human dermal fibroblasts (HDFs). We found that much like the fibroblast-like derived ESCs, HDFs with high SSC and FSC values produced a greater proportion of SSEA-4+/TRA-1-60+ cells (Figure 4E, pp.60-61).

We tested the high SSC/FSC and low SSC/FSC populations for their ability to form IPSCs. Surprisingly, cells exhibiting high SSC and FSC at day 7 of reprogramming gave rise to less IPSCs than cells with lower ones (Figure 4F, pp.60-61). This unexpected result will be discussed further down.

Taken together, a strong correlation between the cellular internal complexity and the efficiency to reprogram exist that might be linked to ER stress.

Discussion

Cellular reprogramming is a poorly understood process with really low efficiency. Most of the current knowledge on reprogramming relies on the Yamanaka factors which ensure pluripotency and cell proliferation, and therefore contribute to the identity of ESCs (Takahashi and Yamanaka, 2006). The extremely low efficiency of reprogramming can be enhanced by the addition of supplementary factors such as other pluripotency-associated genes, cell cycle-regulating genes and epigenetic modifiers (Takahashi and Yamanaka, 2016). However, the lack of other reprogramming enhancers remains a critical issue to advance IPS research. Here we demonstrate that an early ER stress is an essential step for a cell's ability to reprogram. Accordingly, the dramatic morphological changes and organelles remodeling that occur during reprogramming require the activation of potent cellular pathways such as the UPR^{ER}. Our work not only documents this early stress for the first time but also provides strategies to increase the reprogramming efficiency by modulating the UPR^{ER}.

During their discovery of IPSCs, the Yamanaka group hypothesized that the potential reprogramming factors should contribute to the identity of ESCs (Takahashi and Yamanaka, 2006). The identification of these ES-cell specific genes was based on their transcriptional profile (Mitsui et al., 2003). It is therefore surprising that XBP1s can robustly increase the reprogramming efficiency. Indeed, *XBP1* is not a pluripotent gene

and its levels are low in ESCs. Moreover, the UPR^{ER} is less active than in differentiated counterparts. We propose an alternative and novel approach in increasing the reprogramming efficiency based on the theory establishing reprogramming as a process which reverses cellular development (Cacchiarelli et al., 2015). Thus, utilizing genes required for normal development and differentiation could help reprogram better by enabling a successful transition between the two cell states. In line with this theory, XBP1s, among other UPR^{ER} effectors, is required during development and differentiation and therefore expected to regulate reprogramming. Indeed, the homozygous deletion of either *Hspa5* (Luo et al., 2006), *Grp94* (Wanderling et al., 2007), *Grp58* (Garbi et al., 2006), *Ire1a* (Iwawaki et al., 2009), *Xbp1* (Reimold et al., 2000), *Calreticulin* (Mesaeli et al., 1999), or deletion of both *Atf6a* and *Atf6b* (Yamamoto et al., 2007) leads to embryonic lethality in mice. IRE1 increases lymphopoiesis of B cells (Zhang et al., 2005), XBP1 induces osteogenic and plasma differentiations (Iwakoshi et al., 2003), and CHOP plays an important role in the differentiation of B cells, erythrocytes, osteocytes and chondrocytes (Cui et al., 2000; Pereira et al., 2004; Skalet et al., 2005; Yang et al., 2005).

The mechanism through which the activation of the UPR^{ER} increases reprogramming efficiency remains to be elucidated. The UPR^{ER} activation leads to a global reduction of protein synthesis (Harding et al., 1999) and the degradation of mRNA associated to the ER membrane (Hollien and Weissman, 2006). A possibility is that the somatic ER associated proteome is cleared from a substantial part of its somatic signature giving room to the new proteome to be set. Therefore, the activation of the UPR^{ER} must be transient, which is suggested by our results. It is also tempting to speculate that the UPR^{ER} activation may lower levels of secreted factors that could inhibit cellular reprogramming. A more comprehensive analysis of the secretome would be interesting to pursue. The ectopic activation of the UPR^{ER} could provide a buffer and a bigger reservoir for the cell to explore different states and consequently reach pluripotency without inducing apoptosis along the way.

We also reported that the number of IPS colonies could be enriched based on the levels of fluorescently tagged endogenous *HSPA5* gene, which integrates the global state of the

UPR^{ER}. We propose that technologies that enable tracking UPR^{ER} activity such as the HSPA5-GFP reporter line or live staining will be great tools to increase the number of IPS colonies.

Interestingly, we found a positive correlation between SSC and FSC parameters and HSPA5-GFP levels. Consistent with that, cells with high SSC/FSC values had more SSEA-4+/TRA-1-60+ cells. Very surprisingly, we found that cells with low SSC/FSC sorted at day 7 of reprogramming gave rise to more IPSCs than cells with high SSC/FSC values. We should indeed expect to find more fully reprogrammed cells in the low SSC/FSC population since ESCs exhibit low SSC/FSC compared to derived fibroblast-like cells (supplementary Figure 9A, pp.78-79). While the positive correlation between SSC and FSC parameters and HSPA5-GFP levels holds for a homogenous population such as fibroblast-like cells or ESCs (Figure 4A, pp.60-61 and supplementary Figure 9B, pp.78-79), we think that the correlation is not fully applicable on a population that is going through reprogramming. Our hypothesis is that during the course of reprogramming, cells going through intense remodeling will activate the UPR^{ER}, the ones that exhibit higher levels of HSPA5-GFP are the most likely to fully reprogram, they also have a higher percentage of cells that are SSEA-4+/TRA-1-60+. Successful cells change their morphology to resemble an ESCs and acquire low SSC/FSC values, while still under reprogramming stress and keeping their HSPA5-GFP levels high. The correlation between high HSP5-GFP levels and high FSC/SSC values, true on the population level, is lost for these few cells. This happens for a very small subset of cells while most of the other cells still remain with high SSC/FSC values, high HSPA5-GFP and are SSEA-4+/TRA-1-60+.

We predict that studying the pathways required to transit from one cell state to another can identify potent facilitators of reprogramming such as effectors ensuring protein quality control. Previous work in our lab (Vilchez et al., 2012) and others (Buckley et al., 2012) has already linked protein quality control through the ubiquitin-proteasome system with stem cell maintenance and differentiation. We showed that high levels of proteasome activity are required for hESCs maintenance (Vilchez et al., 2012). Furthermore, knockdown of the ubiquitin E3 ligase FBXW7 increased the

reprogramming efficiency. Conversely, knockdown of the deubiquinating enzyme PSMD14 failed to reprogram and generate IPSCs from mouse embryonic fibroblasts (Buckley et al., 2012). The role of other regulatory elements of protein quality control such as the mitochondrial unfolded protein response (UPR^{mt}), and molecular chaperones involved in the heat shock response remain largely unexplored in the regulation of stem cell differentiation or reprogramming. How these processes are involved in reprogramming, as well as their potential cross-play with the UPR^{ER} will need to be explored. We believe that our observations can be expended to transdifferentiation paradigms, an extremely promising field for regenerative therapies.

Material and methods

Cell culture. Human dermal fibroblasts (Lonza CC-2511 and CC-2509), HEK293FT (ThermoFisher, R70007), BJ human fibroblasts (ATCC, CRL-2522), fibroblast-like cells and irradiated CF-1 mouse embryonic fibroblasts (GlobalStem) were grown in DMEM, 10% FBS, 1x Pen/Strep, 1x glutamax and 1X non-essential amino acids (NEAA) (all from Invitrogen).

The hESC line H9 (WA09, WiCell Research Institute) and the other hIPS generated lines were cultured with mTeSR1 media (Stem Cell Technologies) on Geltrex (Invitrogen). Human keratinocytes (Lonza 192907) were cultured with KGM-Gold media (Lonza).

Plasmids. A list of the plasmids and the cloning strategy can be found in supplementary Table 2, pp.81-82.

Viral production. Lentiviral and moloney-based retroviral pMX-derived vectors were co-transfected with their respective packaging vectors in 293FT cells using JetPrime transfection reagent to generate viral particles as previously described (Ruiz et al., 2012). The viral supernatant was filtered through a 0.45 uM filter.

iPSC generation. Primary cells were spinfected with the viral supernatant containing the reprogramming factors and other factors during 1hour at 1000g in presence of 5ug/mL of polybrene (Millipore) twice, 24 hours apart. The regular media was replaced after each round. Selection was started the next day of the last transfection, 48 hours later cells were dissociated with TrypLE (Invotrogen) and plated on top of irradiated MEFs in their regular media. The next day cells were switched to IPS media containing DMEM/F12, 20% knockout serum replacement, 1X Pen/Strep, 1X glutamax, 1X NEAA, 10ng/mL bFGF (all from Invitrogen), and 55 uM β-mercaptoethanol (Sigma). To evaluate reprogramming efficiency, the same number of infected cells was plated, after 2-3 weeks cells were fixed with 4% PFA and stained for TRA-1-60 as previously described (Onder et al., 2012) and scored. Briefly, fixed cells were blocked for 1 hour at room temperature in 1xPBS, 3% FBS, 0.3% Triton X-100, then incubated with biotin-anti-Tra-1-60 (eBioscience13-8863-82, 1:250) over night at 4C and the next day streptavidin horseradish peroxidase (Biolegend 405210, 1:500) for 2 hours at room temperature. Staining was developed with the sigmaFast DAB kit (D0426). Alternatively, an alkaline phosphatase (AP) staining was performed for episomal reprogramming experiments as instructed by the Millipore detection kit (SCR004). Briefly, cells were fixed in 4% PFA for less than a minute to avoid losing the AP activity. Cells were rinsed with TBS-T and covered with Fast Red Violet Solution/water/Naphthol (2:1:1) for 20 min followed by a wash with PBS. AP positive colonies were then counted.

For time course studies, imaging and flow cytometry, cells were plated on geltrex coated plates instead of MEFs.

Where indicated, after plating on geltrex, cells were incubated with APY29 (Chem Scene, CS-2552) or GSK 2656157 (Chem Scene, CS-3262) for 3 days.

Alternatively, cells were also reprogrammed using an episomal electroporation system (Okita et al., 2011). Briefly, cells were first selected with the appropriate factor. 500,000 cells were then electroporated with the episomal constructs using the nucleofector kit (Lonza, VPD-1001). Cells were plated and kept in their original media. After 6 days, cells were dissociated and plated on freshly plated MEFs. Cells were switched to IPS media the next day.

Derivation of fibroblast-like cells. Stem cells were differentiated into fibroblast-like cells using an embryoid body (EB)-mediated protocol. Stem cells grown on Geltrex were detached using dispase, resuspended in DMEM/F12, 20% FBS, 1x glutamax, 1x NEAA, 1x Pen/Strep and 55 μM β-mercaptoethanol and grown on low adhesion plates for 4 days with media change. EBs were plated on gelatin-coated plates and cultured with the same media. When EBs spread and cells appeared fibroblast looking, the culture was dissociated using TrypLE and replated using a regular fibroblast media. This was serially done until the whole population became uniform.

RNA isolation and real-time PCR. Cells were collected in Trizol®. A classic chloroform extraction followed by a 70% ethanol precipitation was performed. The mixture was then processed through column using the RNeasy quiagen kit as described by the manufacturer. Quantitect reverse transcription kit (Quiagen) was used to synthesize complementary DNA. Real-time PCR was performed using Sybr select mix (Life Technologies). *GAPDH* expression was used to normalize gene expression values. Primer sequences can be found in the supplementary Table 3, p.83.

Western blot analysis. Cells were washed with PBS and RIPA buffer was added to the plates on ice. Cells were scraped, collected and stored at -20C. The RIPA buffer was always supplemented with Roche cOmplete mini, and phosSTOP when needed. 20 μg of protein was loaded per lane and actin or tubulin was used as a loading control in pre-cast 4-12% Bis-Tris NuPage gels (Invitrogen). Proteins were blotted on nitrocellulose membranes using the NuPage reagents according to the manufacturer instructions. Membranes were prepared for imaging using Odyssey® CLx Imaging System-LI-COR Biosciences with the appropriate reagents. Briefly, membranes were incubated in the proprietary blocking buffer for 1 hour at room temperature. Overnight primary antibody incubation at 4C was done using the blocking buffer and 0.1% Tween-20. Membranes were washed in TBS-T then incubated with secondary antibody for 1 hour at room temperature. Membranes were then washed in TBS-T with a final wash in TBS. For the list of antibodies and concentrations refer to supplementary Table 4, pp.84-85.

Fluorescent immunostaining. Cells on slides were fixed with 4% PFA for 15min and washed with PBS. 2% donkey-serum blocking buffer in PBS was used for 1 hour at room

temperature. Primary antibody incubation was done overnight. After PBS washes, secondary antibody was added for 1 hour at room temperature. After PBS washes, slides were mounted with mounting media containing DAPI. For the list of antibodies and concentrations refer to supplementary Table 4, pp.84-85.

Flow cytometry. For cell analysis, cells were dissociated with TrypLE and pelleted. 100 µL of a fluorescent-conjugated antibodies cocktail (5 µL of SSEA-4 330408, 5 µL of TRA-1-60 330610 Biolegend) in staining media (1xPBS, 2% FBS) was used to resuspend the pellet and incubated 30min on ice. Cells were then resuspended in excess of staining media, span down and resuspended in staining media, filtered through a cell strainer and kept on ice. Cells were analyzed using the BD Bioscience LSR Fortessa. The analysis was done using the FlowJo software.

For cell sorting, a similar procedure was followed. Cells were eventually resupsended in their media supplemented with rock inhibitor and sorted accordingly using the BD Bioscience Influx Sorter. Cells were then transferred to appropriate dishes for culture and kept on rock inhibitor during the next 24 hours.

ER secretion assay. Transduced cells with Gluc-CFP were incubated 24 hours with fresh media and the supernatant was collected for analysis. An equal volume of Gluc Glow buffer (nanolight) was added to the supernatant in a 96-well plate format. The luminescence was measured by a TECAN plate reader and integrated over 50 ms.

Cell health/survival assay. Cells were plated on 96-well plates and treated with the appropriate condition. After the desired incubation time, cell titer glow buffer (Promega) was added to the wells (1:5 volume) and incubated for 12min on a shaker. The luminescence was measured with the TECAN plate reader and integrated over 1s.

Electron microscopy. Cells were fixed with 2% glutaraldehyde in 0.1 M phosphate buffer for 5 min. Samples were rinsed with 0.1M sodium cacodylate Buffer (3x5 min) followed by the addition of 1% osmium tet, 1.5% ferrocyanide in 0.1M cacodylate buffer (5min). After washing with water (3x5min), 2% uranyl acetate was added for 5min followed by a water rinse. A dehydration series of ethanol was then completed: 35%, 50% 75%, 100%, 100% (5 min each). A 1:1 ethanol/resin (3x10min) incubation followed

by 100% resin (3x10min) was done. The samples were cured over 48hrs, sectioned at 50nm with a microtome using a Diatome. Sections were placed on a coated copper mesh grid. They were then stained with uranyl acetate for 5 min, and then stained with lead citrate for 5 min before imaging.

Genome editing and southern blot. Transcription activator-like effector nuclease (TALENs) technology was used to create a fusion HSPA5-GFP by insertion of eGFP at the 3' end of the HSPA5 locus. We followed the protocol described in (Hockemeyer et al., 2011). TALENs were cloned to bind ACAGCAGAAAAAGATGA and ATTACAGCACTAGCA sequences and generate a double-stranded break around the STOP codon. The donor plasmid OCT4-eGFP-PGK-Puro, published in (Hockemeyer et al., 2011), was adapted to target HSPA5 by changing the homology arms. H9 cells were electroporated and clonal expansion after puromycin selection was done. Successful targeting was confirmed by southern blot using the GFP probe published in (Hockemeyer et al., 2011).

Statistical analysis. The software Prism was used to perform the statistical tests. The corresponding statistical tests and the number of biological repeats, denoted as n, are indicated in the figure legends. For drug dose response assays, a log(drug) vs normalized response with viable slope model was used to determine the EC50.

Acknowledgements

Funding was provided by HHMI and CIRM grants.
We thank Dr B. Tannous who generously provided the Gluc-CFP, the Tjian lab for the episomal reprogramming vectors, Dr A. Panopoulos and Dr S. Ruiz for the pMX reprogramming vectors and the reprogramming protocols.

Figures and their Legends

Figure 1: The UPR^{ER} is activated during reprogramming. **A**: Relative mRNA levels of the three UPR^{ER} branches effectors relative to *GAPDH* determined by qRT-PCR (n=3). D3 GFP control was set to 1. **B**: Time course reprogramming western blot analysis of HSPA5, P-IRE1 and IRE1. **C**: Electron microscopy of day 3 reprogramming fibroblasts and GFP control, scale bar = 0.2 µm. Pseudo-colors blue and red mark respectively the nucleus and the ER. **D**: Secretion capability of the ER measured by luciferase activity secreted in the media (n=12) and western blot analysis of the *Gaussia* luciferase. **E**: Sensitivity to tunicamycin treatment determined by EC50 measurement at day 4 of reprogramming of fibroblast-like cells (n=3). * indicates statistical difference (p-value<0.05) using an unpaired two-tailed t-test, n.s. indicates statistical non significance. Error bars indicate the standard deviation.

Figure 1

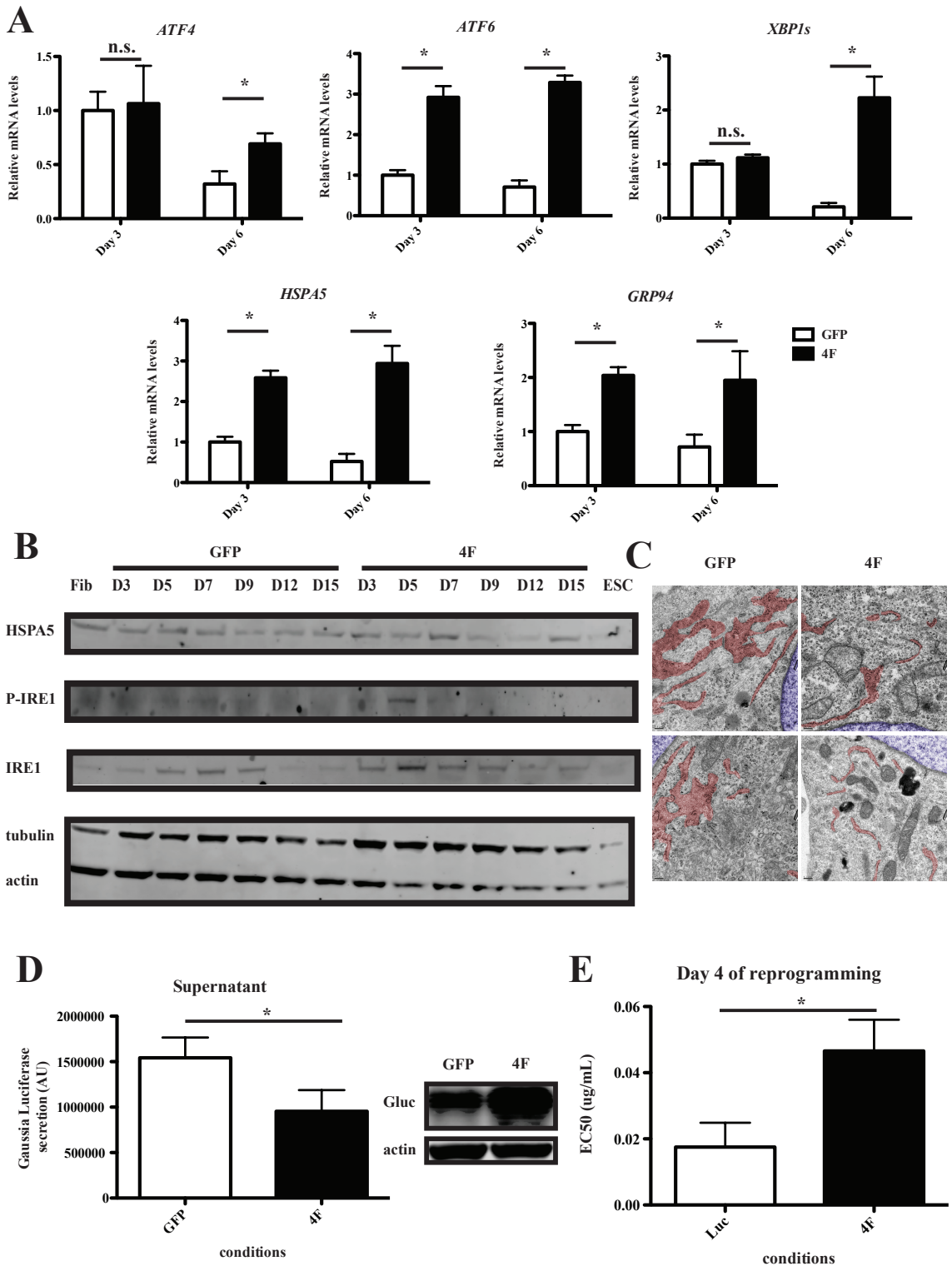
A
ATF4
ATF6
XBP1s
HSPA5
GRP94
Relative mRNA levels
n.s.
*
Day 3
Day 6
GFP
4F
B
GFP
4F
Fib D3 D5 D7 D9 D12 D15 D3 D5 D7 D9 D12 D15 ESC
HSPA5
P-IRE1
IRE1
tubulin
actin
C
GFP
4F
D
Supernatant
Gaussia Luciferase secretion (AU)
2000000
1500000
1000000
500000
0
GFP
4F
conditions
Gluc
actin
E
Day 4 of reprogramming
EC50 (ug/mL)
0.06
0.04
0.02
0.00
Luc
4F
conditions

Figure 2: The reprogramming efficiency is improved upon UPR^{ER} activation. A: Flow cytometry analysis of fibroblast-like HSPA5-GFP cells at day 8 of reprogramming stained with SSEA-4 and TRA-1-60 surface markers. I,II,III represent the different cell states of reprogramming. **B**: Median HSPA5-GFP of the different cell states (I,II,III) during reprogramming (n=3). **C**: Relative mRNA levels of the UPR^{ER} effectors relative to *GAPDH* determined by qRT-PCR (n=3). Values for SSEA-4-/TRA-1-60- were set to 1. **D**: Percentage of SSEA-4+/TRA-1-60+ cells at day 14 of reporgramming after drug treatment with APY29, an inducer of the UPR^{ER}, and GSK2656157, an inhibitor of the UPR^{ER} from day 2 to day 5 of reprogramming (n=3). **E**: Relative reprogramming efficiency of keratinocytes measured by colony TRA-1-60 staining after 3 weeks in culture upon overexpression of emGFP, XBP1s and XBP1s-DBD (missing its DNA binding domain) with the EF1α promoter, shown are two biological replicates done in duplicate. Conditions with different letter denote a statistical significant difference between them (p-value<0.05, Tukey's multiple comparison test). Error bars indicate the standard deviation.

Figure 2

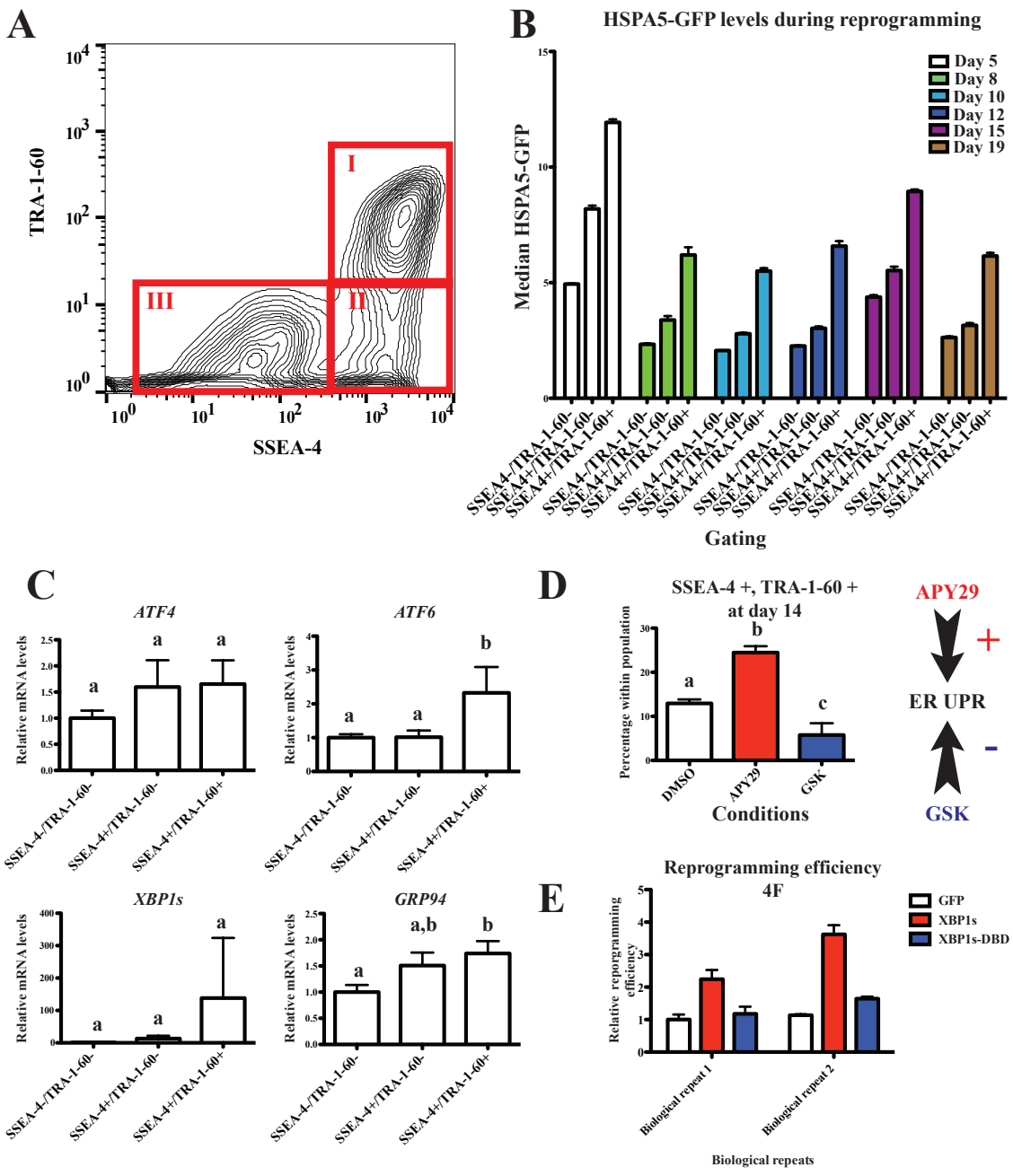
A
TRA-1-60
SSEA-4
I
II
III
B
HSPA5-GFP levels during reprogramming
Median HSPA5-GFP
Day 5
Day 8
Day 10
Day 12
Day 15
Day 19
Gating
C
ATF4
ATF6
XBP1s
GRP94
Relative mRNA levels
SSEA-4-/TRA-1-60-
SSEA-4+/TRA-1-60-
SSEA-4+/TRA-1-60+
D
SSEA-4 +, TRA-1-60 + at day 14
Percentage within population
DMSO
APY29
GSK
Conditions
APY29
ER UPR
GSK
E
Reprogramming efficiency
4F
Relative reporgramming efficiency
GFP
XBP1s
XBP1s-DBD
Biological repeat 1
Biological repeat 2
Biological repeats

Figure 3: HSPA5-GFP levels increase the reprogramming efficiency. **A**: Histogram of fibroblast-like HSPA5-GFP at day 8 of reprogramming. 1,2,3 subdivide the population into 3 equal parts. Each of them is represented in the right panel by their SSEA-4 and TRA-1-60 staining. The percentage of double positive cells within each of these populations is shown. **B**: Percentage of SSEA-4+/TRA-1-60+ cells within each population 1,2,3 during reprogramming (n=3). **C**: Upper panel shows relative reprogramming efficiency of fibroblast-like HSPA5-GFP sorted at day 7 of reprogramming based on their GFP levels and assessed by TRA-1-60 colony staining (n=2). Lower panel shows a representative picture of the staining. * indicates statistical difference (p-value<0.05) using an unpaired two-tailed t-test. Error bars indicate the standard deviation.

Figure 3

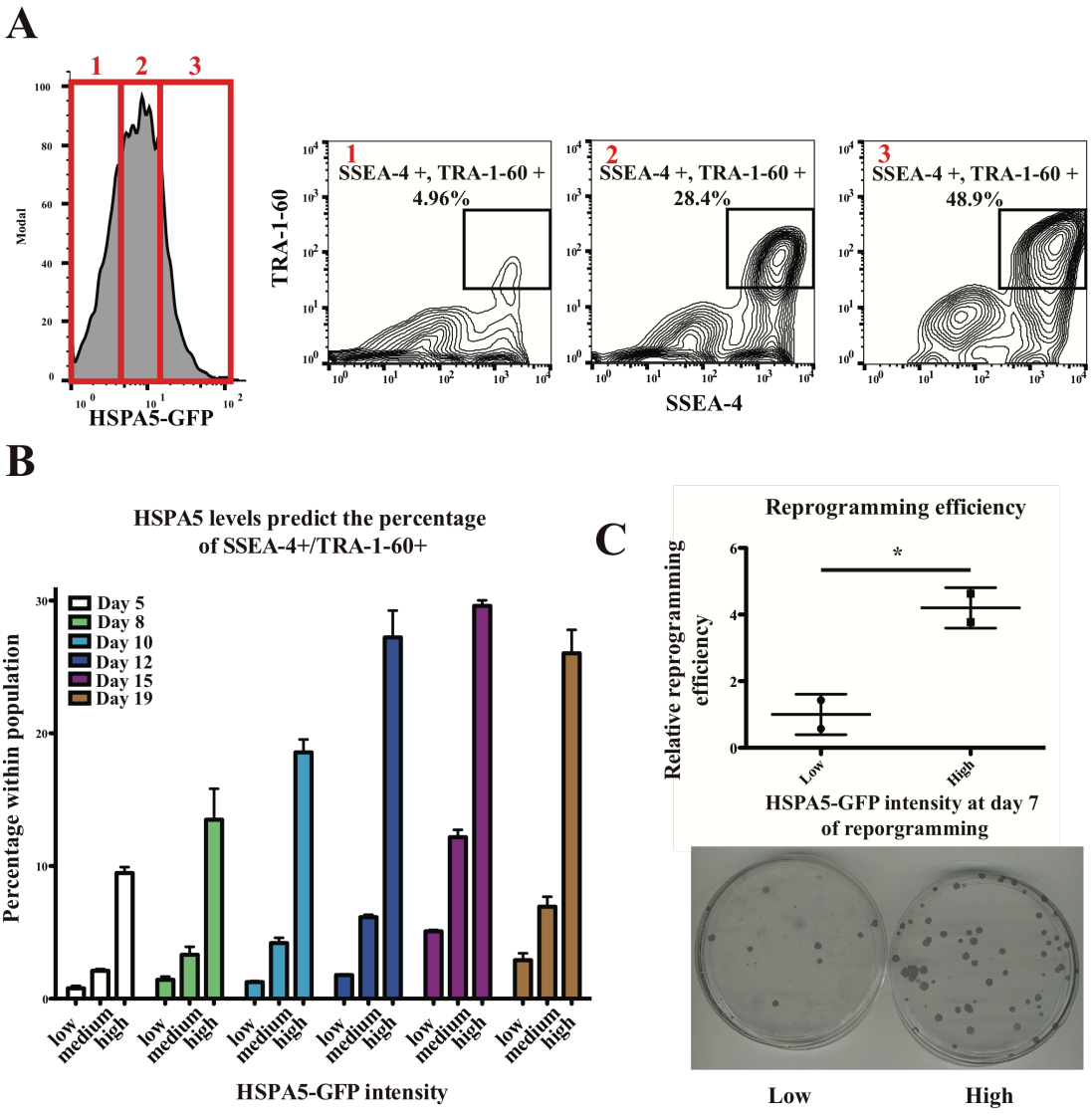
A
1
2
3
Modal
HSPA5-GFP
TRA-1-60
SSEA-4
1
SSEA-4 +, TRA-1-60 +
4.96%
2
SSEA-4 +, TRA-1-60 +
28.4%
3
SSEA-4 +, TRA-1-60 +
48.9%
B
HSPA5 levels predict the percentage
of SSEA-4+/TRA-1-60+
Day 5
Day 8
Day 10
Day 12
Day 15
Day 19
Percentage within population
low
medium
high
HSPA5-GFP intensity
C
Reprogramming efficiency
Relative reprogramming
efficiency
*
Low
High
HSPA5-GFP intensity at day 7
of reporgramming
Low
High

Figure 4: SSC and FSC parameters predict the reprogramming efficiency. A: Left panel explains the meaning of the Side Scatter and Forward Scatter parameters on the cellular levels. Right panel represents the distribution of the top high (red) and low (blue) 1/3 HSPA5-GFP regarding their SSC and FSC values. **B**: Median HSPA5-GFP values after sorting fibroblast-like HSPA5-GFP on day 0 and after 7 days in culture (n=3). **C**: Top, respectively bottom, panel show the median Side SCatter, respectively Forward SCatter, after overexpression of luciferase (LUC), XBP1s and XBP1s-DBD with and without 1µg/mL tunicamycin treatment for 24 hours. **D**: SSEA-4 and TRA-1-60 parameters are shown based on the SSC and FSC selected population. Shown is the percentage within these populations at day 8 of reprogramming of the double positive cells (n=3). **E**: Upper panel shows the percentage of SSEA-4+/TRA-1-60+ neonatal fibroblasts at day 10 of reprogramming within the population. Bottom panel shows the relative reprogramming efficiency of sorted neonatal fibroblasts cells at day 10 based on their FSC/SSC values (n=3). **F**: Relative reprogramming efficiency of sorted fibroblast-like HSPA5-GFP cells at day 7 based on their FSC/SSC values (n=3). Conditions with different letter denote a statistical significant difference between them (p-value<0.05, Tukey's multiple comparison test). * indicates statistical difference (p-value<0.05) using an unpaired two-tailed t-test, n.s. indicates statistical non significance, only statistical comparisons of importance were performed. Error bars indicate the standard deviation.

Figure 4

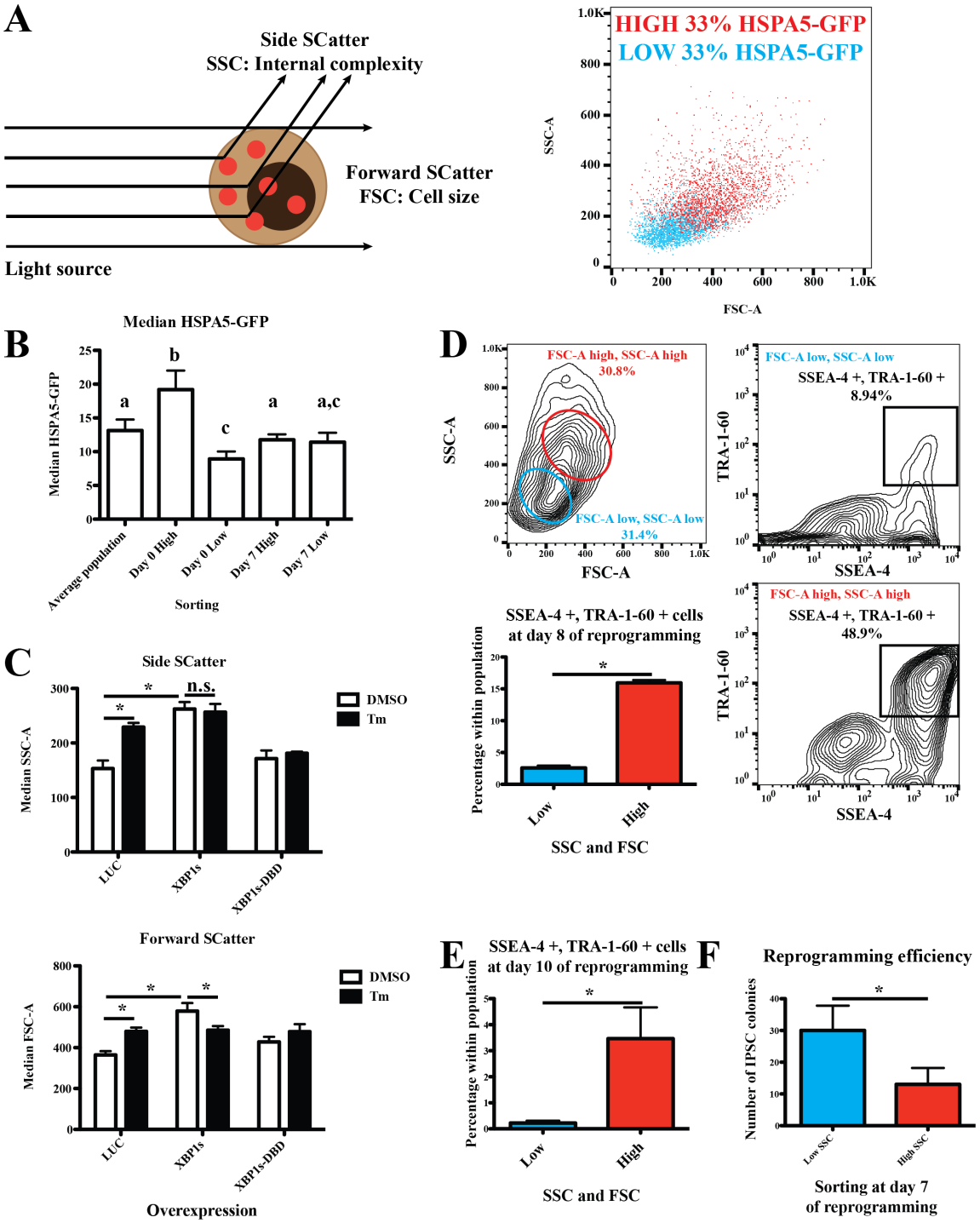
A
Side SCatter
SSC: Internal complexity
Forward SCatter
FSC: Cell size
Light source
HIGH 33% HSPA5-GFP
LOW 33% HSPA5-GFP
SSC-A
FSC-A
B
Median HSPA5-GFP
Median HSPA5-GFP
a
b
c
a
a,c
Average population
Day 0 High
Day 0 Low
Day 7 High
Day 7 Low
Sorting
C
Side SCatter
Median SSC-A
n.s.
DMSO
Tm
LUC
XBP1s
XBP1s-DBD
Forward SCatter
Median FSC-A
Overexpression
D
FSC-A high, SSC-A high
30.8%
FSC-A low, SSC-A low
31.4%
SSC-A
FSC-A
FSC-A low, SSC-A low
SSEA-4 +, TRA-1-60 +
8.94%
TRA-1-60
SSEA-4
SSEA-4 +, TRA-1-60 + cells
at day 8 of reprogramming
Percentage within population
Low
High
SSC and FSC
FSC-A high, SSC-A high
SSEA-4 +, TRA-1-60 +
48.9%
E
SSEA-4 +, TRA-1-60 + cells
at day 10 of reprogramming
Percentage within population
Low
High
SSC and FSC
F
Reprogramming efficiency
Number of IPSC colonies
Low SSC
High SSC
Sorting at day 7
of reprogramming

Supplementary Figure 1: The reprogramming factors activate the UPR^{ER} during reprogramming similarly to XBP1s overexpression or tunicamycin treatment. A: mRNA levels of *XBP1*s, *HSPA5* and *GRP94* upon overexpression of XBP1s (n=3). GFP control was set to 1. **B**: mRNA levels of *ATF4*, *ATF6, XBP1*, *HSPA5* and *GRP94* during episomal reprogramming with electroporation (n=3). GFP control was set to 1. **C**: Time course reprogramming western blot analysis of PERK, P-PERK, CLIMP-63, Reticulon 4 (isoform Nogo B) and loading controls. **D**: Electron microscopy of fibroblasts treated with tunicamycin, an ER stress inducer, scale bar = 0.2 μm. Pseudo-colors blue and red mark respectively the nucleus and the ER. * indicates statistical difference (p-value<0.05) using an unpaired two-tailed t-test, n.s. indicates statistical non significance. Error bars indicate the standard deviation.

Supplementary Figure 1

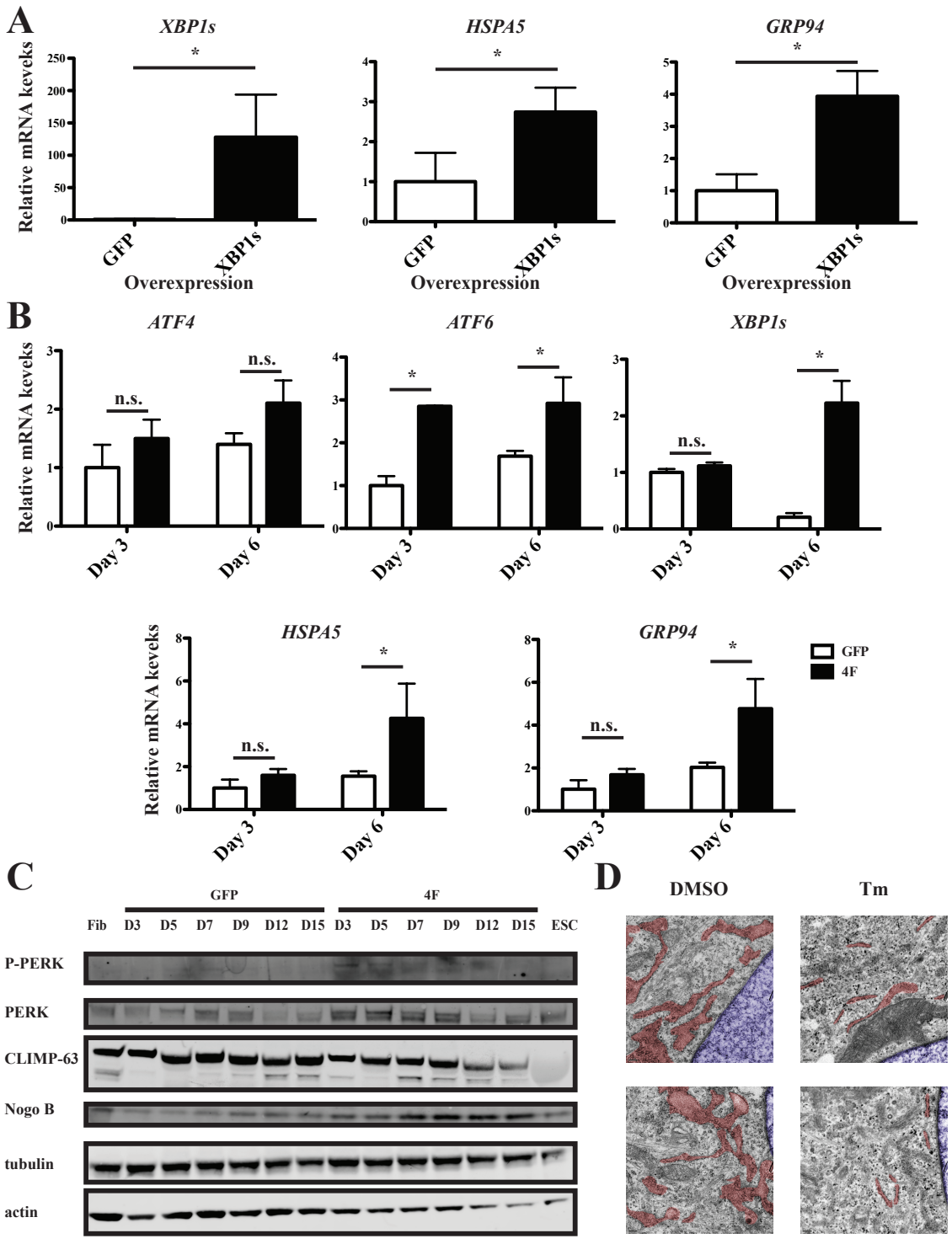

Supplementary Figure 2: Characterization of the fibroblast-like HSPA5-GFP line. **A**: Schematic of the genome editing strategy and southern blot using a GFP probe. The red arrow shows the expected size of the targeted allele while the black arrows show two off-target integrations. **B**: Schematic of the fibroblast-like cells differentiation protocol (left panel) and median HSPA5-GFP levels analyzed by FACS upon 1ug/mL tunicamycin treatment during 24h (right panel). **C**: Western blot of HSPA5, GFP and actin showing the dynamical induction of the reporter line after the addition and removal of 1ug/mL tunicamycin. The same band was targeted by both GFP and HSPA5 antibodies using dual channel imaging with the Odyssey® CLx Imaging System confirming the correct targeting. Only a single intense GFP band was observed suggesting the off-targets integrations are not translated. * indicates statistical difference (p-value<0.05) using an unpaired two-tailed t-test. Error bars indicate the standard deviation.

Supplementary Figure 2

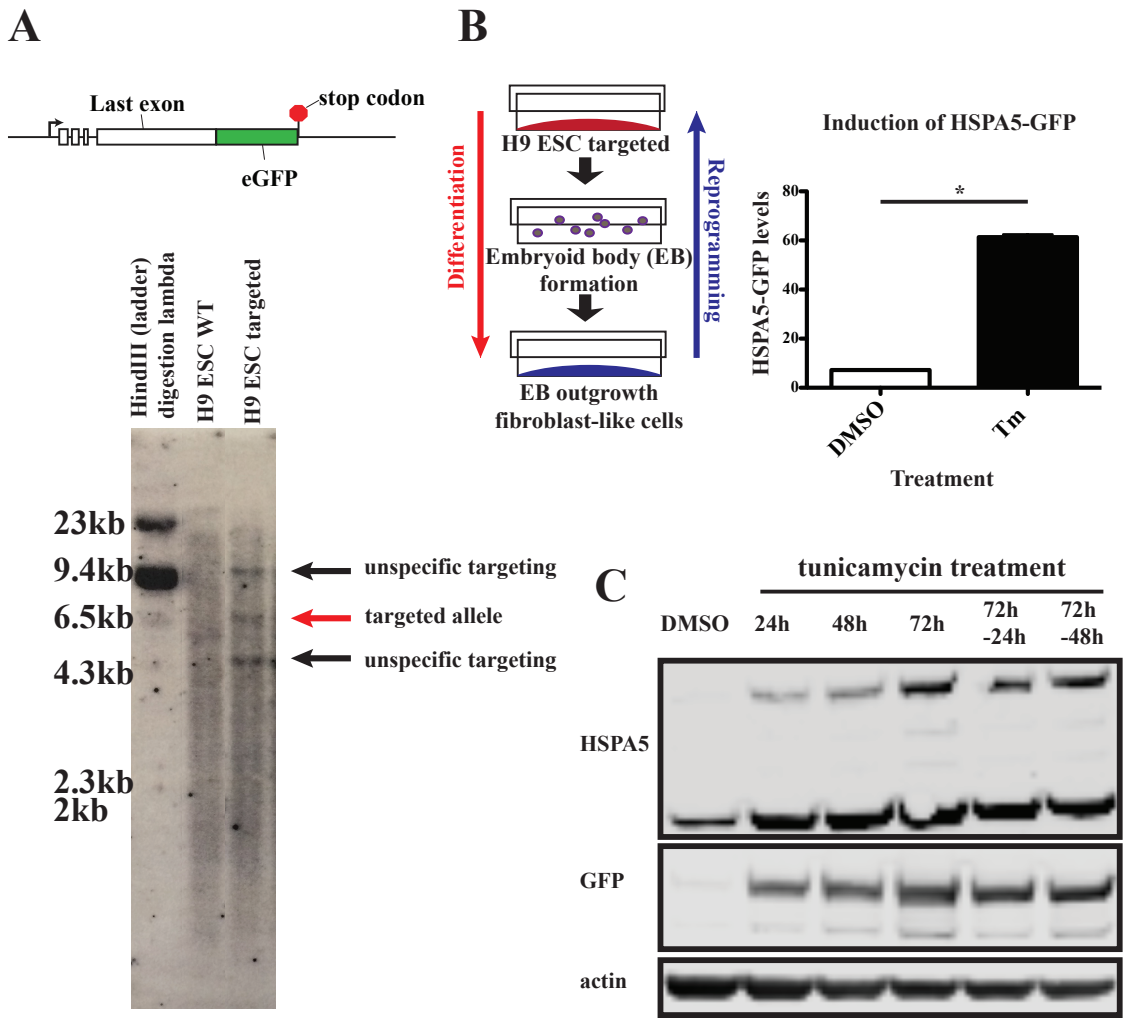

Supplementary Figure 3: Reactivation of the endogenous pluripotent genes during the different cellular reprogramming stages. Relative endogenous mRNA levels of pluripotent genes in the differentially reprogrammed populations relative to *GAPDH* determined by qRT-PCR (n=3). Values for SSEA-4-/TRA-1-60- were set to 1. Conditions with different letter denote a statistical significant difference between them (p-value<0.05, Tukey's multiple comparison test). Error bars indicate the standard deviation.

Supplementary Figure 3

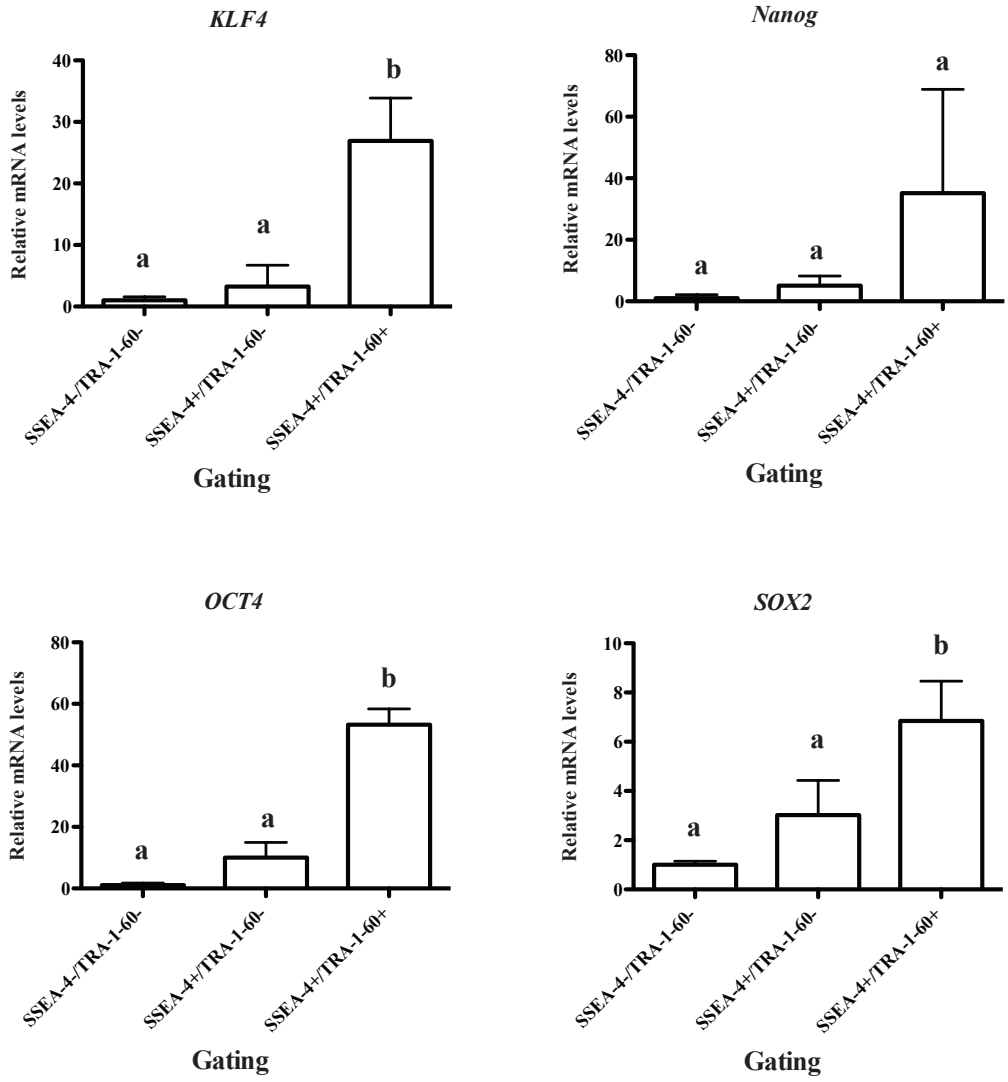

Supplementary Figure 4: Concentration optimization of APY29 and GSK2656157 to modulate the UPR^{ER} without affecting growth. A: Median HSPA-GFP levels with and without 1ug/mL tunicamycin treatment during 48 hours pretreated during 24 hours with different concentration APY29 and GSK2656157. The drugs were kept during the entire experiment (n=4). **B**: Growth tested by cell-titer glow assay with different concentrations of APY29 and GSK2656157 treated during 3 days (n=8). The red rectangle corresponds to the concentration used for the experiment in Figure 2D, pp.56-57. Error bars indicate the standard deviation.

Supplementary Figure 4

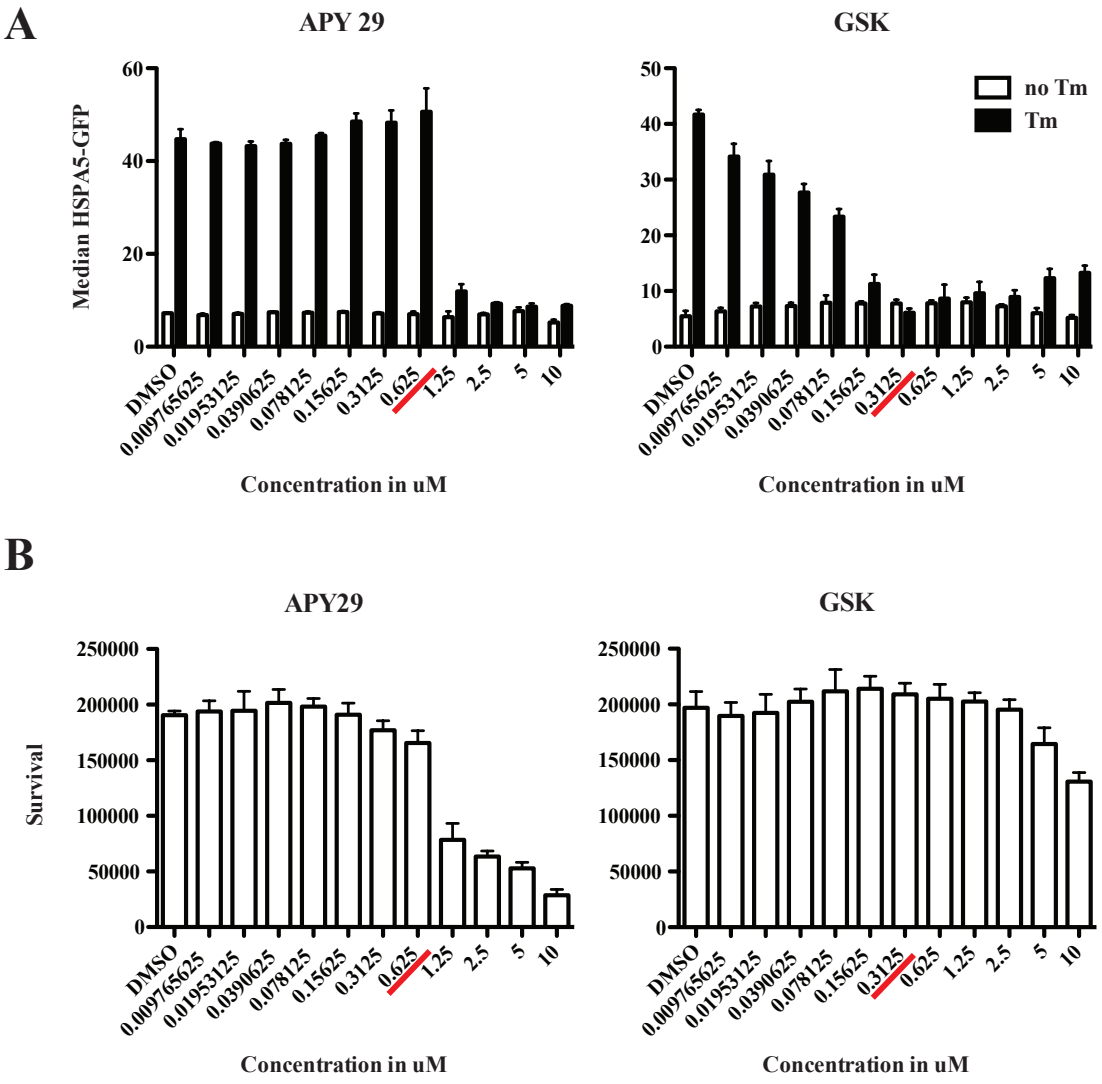

Supplementary Figure 5: XBP1s doesn't increase the replication rate of the cells during reprogramming and derived IPSCs express stemness markers. A: Growth tested by cell-titer glow assay on keratinocytes upon expression of the 4 reprogramming factors and the overexpression of emGFP, XBP1s and XBP1s-DBD with the EF1α promoter at 3 days of reprogramming (n=3). **B**: Relative endogenous mRNA levels of pluripotent genes in the derived IPSC lines relative to *GAPDH* determined by qRT-PCR (n=3). Values for H9 ESCs were set to 1.

Supplementary Figure 5

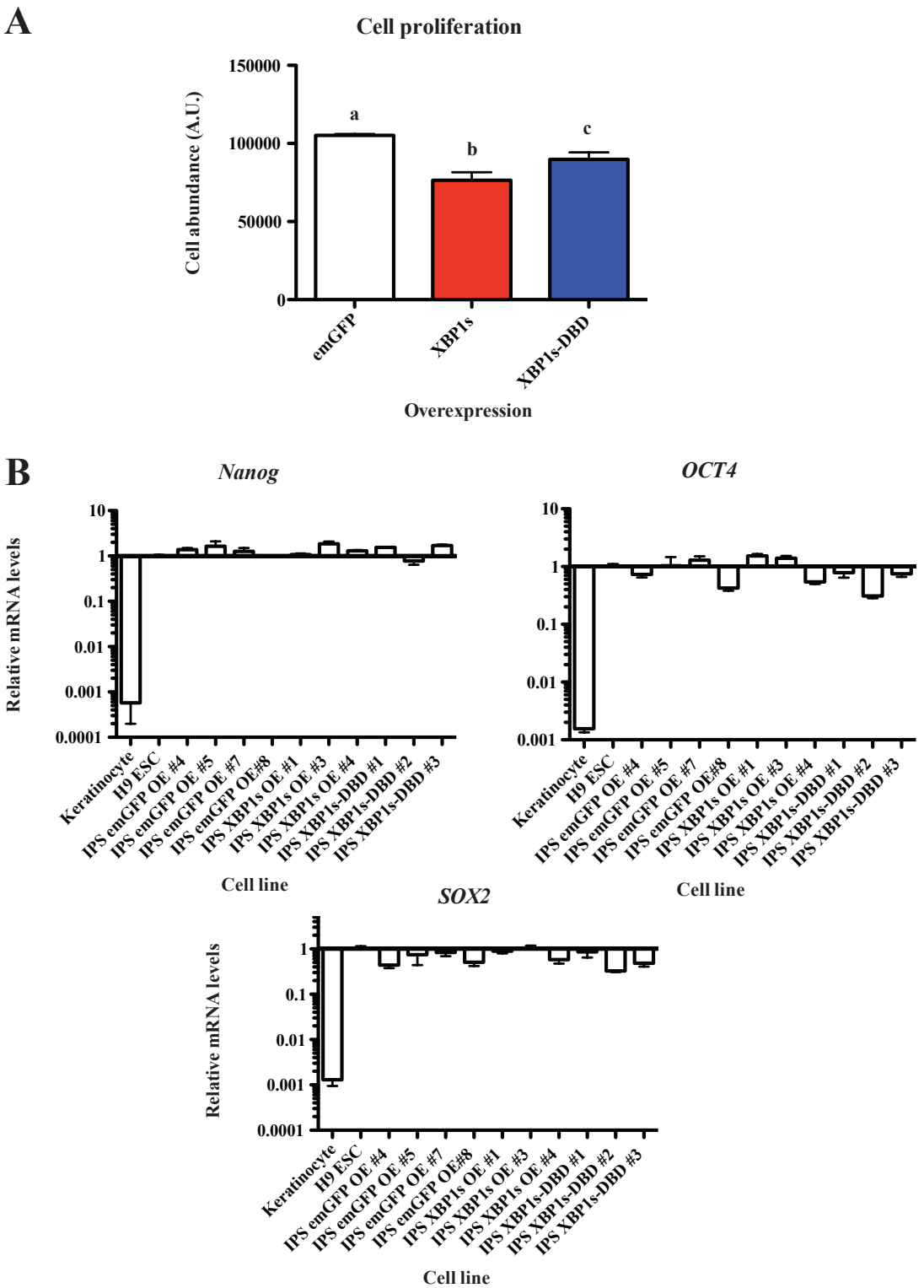

Supplementary Figure 6: Episomal reprogramming of fibroblasts by XBP1s overexpression. A: reprogramming efficiency scored by alkaline phosphatase staining. Biological repeat 1 has 2 technical replicates, biological repeat 2 has 3 technical repeats for eGFP but only 1 for XBP1s (very few cells survived suggesting a problem during the experiment). CMV promoter was used to overexpress the transgenes. **B**: Relative mRNA levels of three stemness markers (*Nanog*, *SOX2* and *OCT4*) and a fibroblast marker (*COL1A1*) relative to *GAPDH* determined by qRT-PCR (n=3). H9 line was used as ESC control and IPS C1 OSKM line (Ruiz et al., 2012) was used as IPS control. Values for H9 ESCs were set to 1 for stemness genes while human dermal fibroblast (HDF) values were set to 1 for fibroblast marker *COL1A1*. **C**: Relative mRNA levels of *XBP1s* relative to *GAPDH* determined by qRT-PCR (n=3). **D**: Fluorescent immunostaining of stemness markers Nanog (transcription factor expected localize in the nucleus), TRA-1-60 and SSEA-4 (both cell surface proteins) with DAPI. A secondary only control was done and showed no background (data not shown). No scale bar is provided.

Supplementary Figure 6

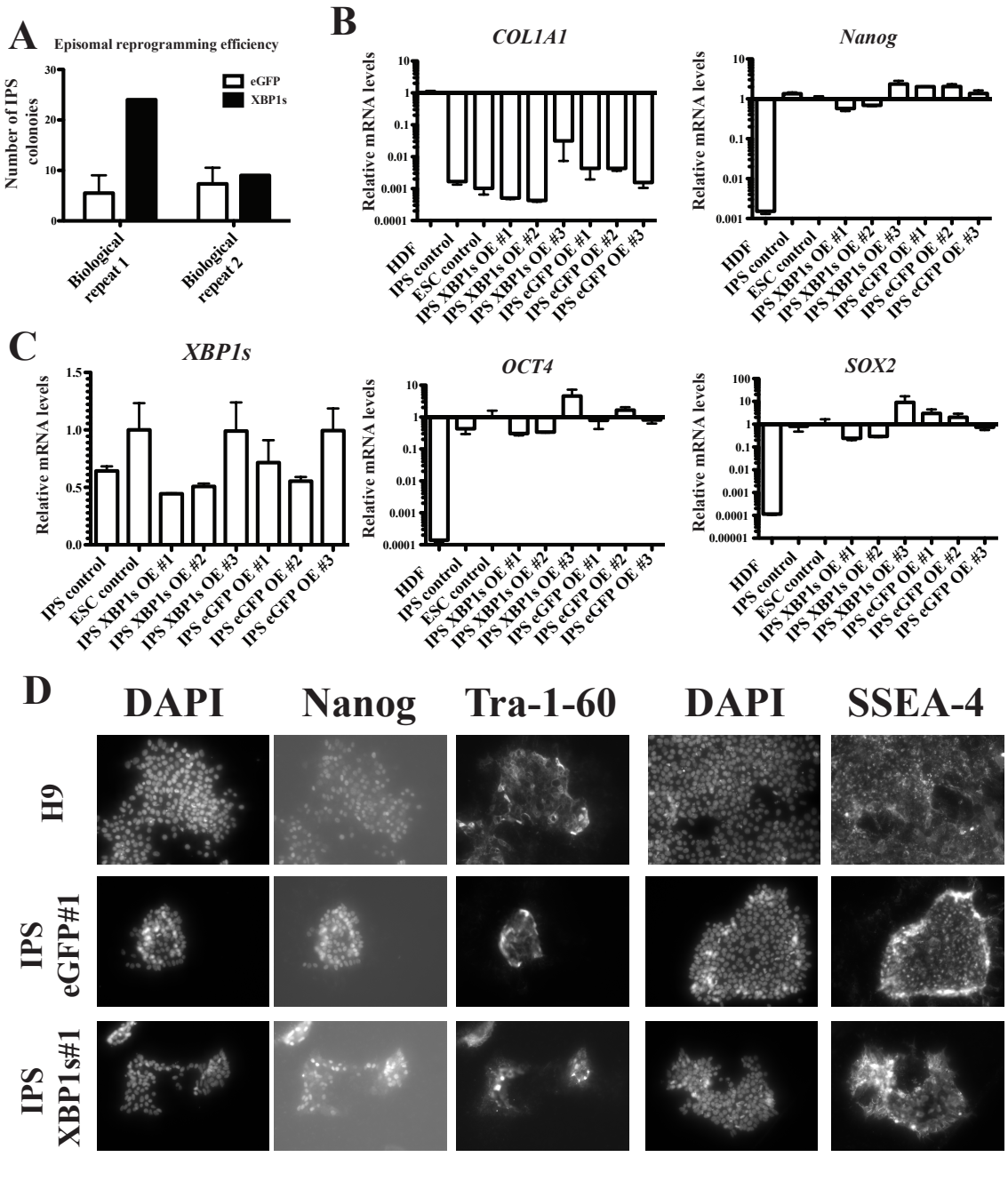

Supplementary Figure 7: Transient activation of the UPR^{ER} is necessary during reprogramming. A: Relative mRNA levels of *XBP1s* relative to *GAPDH* determined by qRT-PCR in IPSC colonies derived from either *emGFP*, *XBP1s* or *XBP1s-DBD* driven by EF1α promoter (n=3). **B**: Morphology of H9 ESC colonies overexpressing *emGFP*, *XBP1s* or *XBP1s-DBD* driven by EF1α promoter after selection. Scale bar for 10x is 20μm, and 10μm for 20X. **C**: Flow cytometry analysis of HSPA5-GFP in ESC HSPA5-GFP and the differentiated fibroblast-like cells. **D**: Western blot analysis of ATF6 and XBP1 in pluripotent stem cells and fibroblasts. Equal amounts of protein were loaded.

Supplementary Figure 7

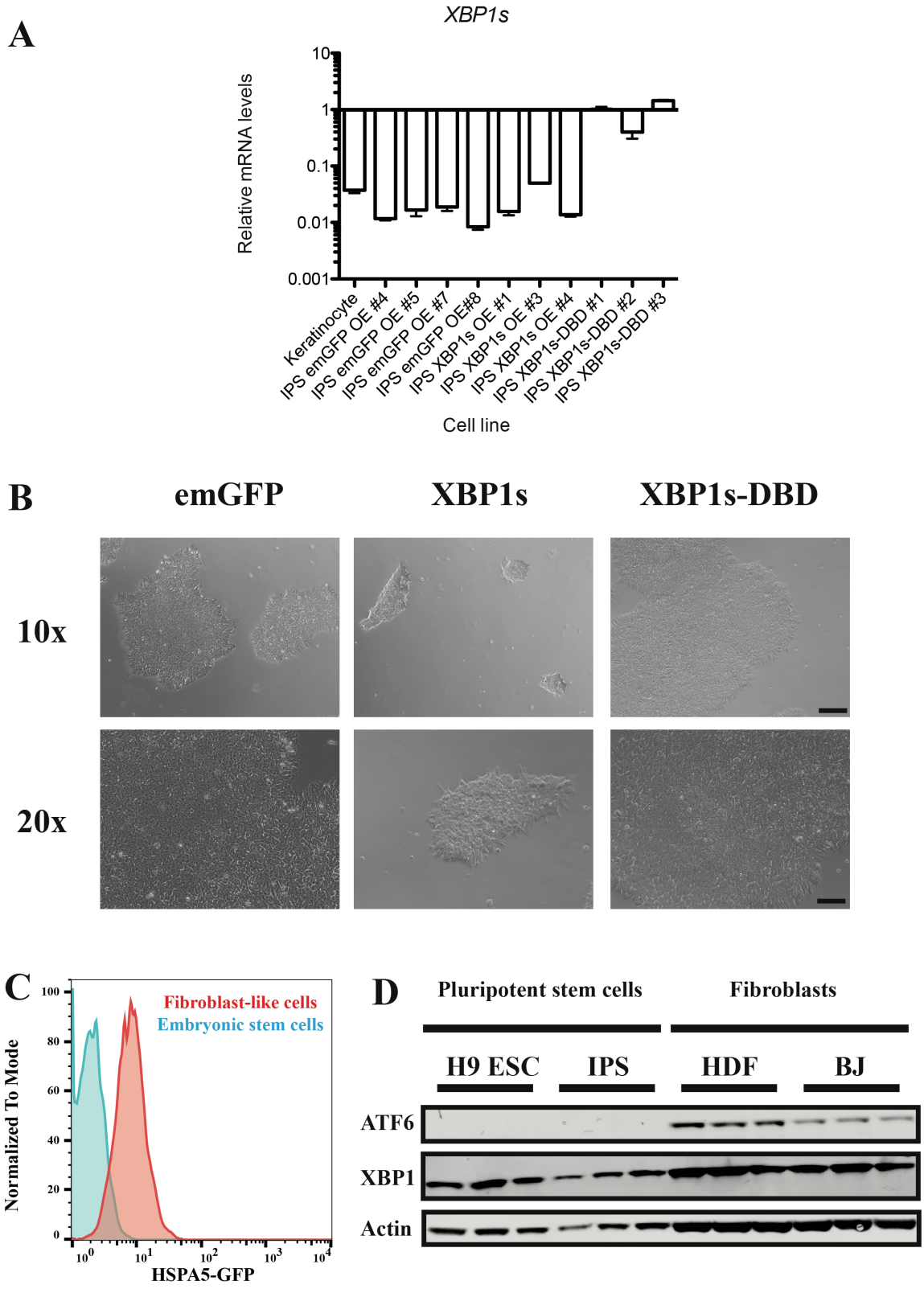

Supplementary Figure 8: Correlation of the SSC and FSC parameters upon modulation of XBP1 levels. A: Median HSPA5-GFP upon expression of LUC, XBP1s and XBP1s-DBD with and without 1ug/mL tunicamycin treatment for 48 hours (n=3). **B**: Left, respectively middle, panel shows the Side Scatter, respectively Forward Scatter, values upon knockdown of XBP1 with different hairpin constructs with and without 1ug/mL tunicamycin treatment for 48 hours (n=3). Left panel shows the median HSPA5-GFP upon knockdown of XBP1 with different hairpin constructs with and without 1ug/mL tunicamycin treatment for 48 hours (n=3). **C**: Efficiency of XBP1s knockdowns by shRNAs measured by median HSPA5-GFP with and without 1ug/mL tunicamycin treatment for 48 hours (n=3).

Supplemetary Figure 8

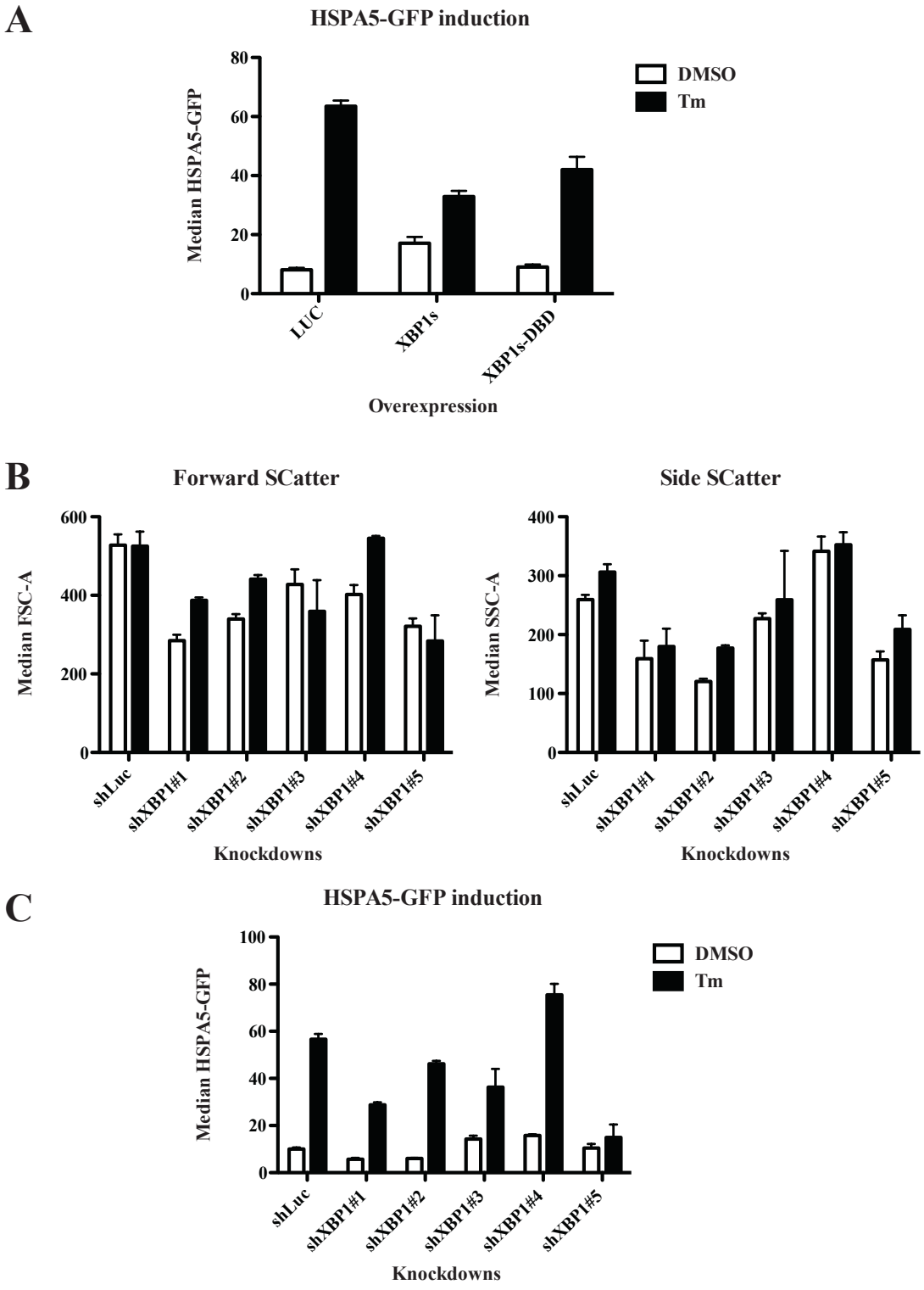

Supplementary Figure 9: FSC and SSC values are lower in ESCs compared to their differentiated fibroblast-like cell counterparts and positively correlate with HSPA5-GFP levels. A: Flow cytometry density plot analysis of FSC and SSC of HSPA5-GFP ESCs and differentiated fibroblast-like cell counterparts. **B**: Flow cytometry density plot analysis of FSC and SSC in according to HSPA5-GFP levels in ESCS.

Supplementary Figure 9

A

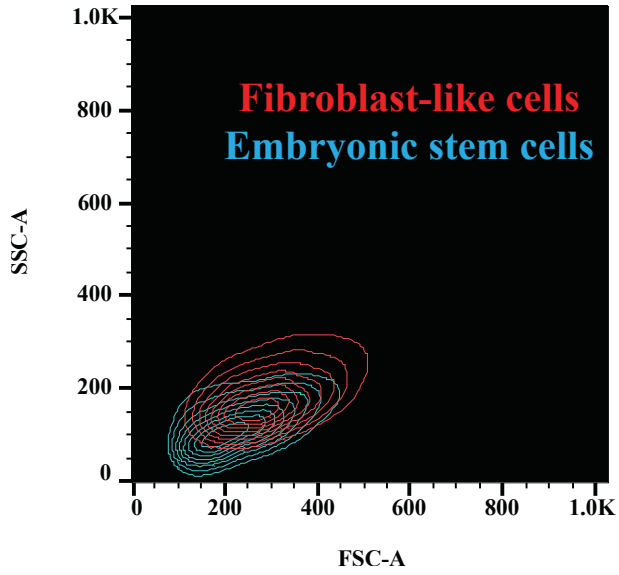

B

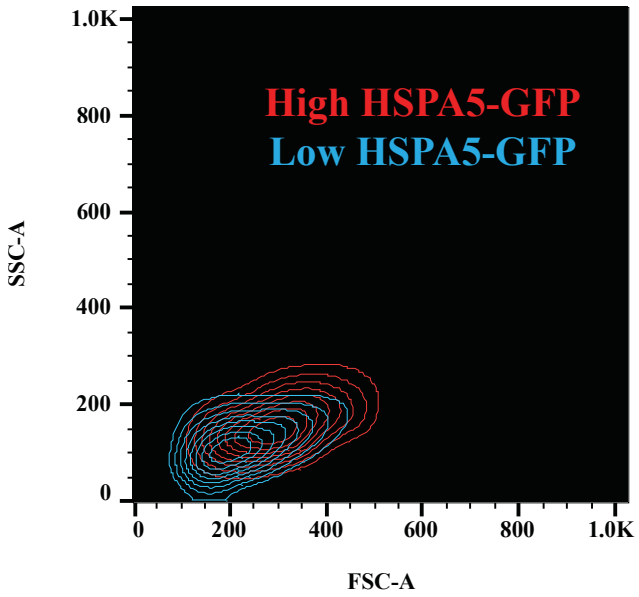

Supplementary Table 1: Transcriptome analysis of ER UPR genes in fibroblasts, IPSCs and ESCs. The data analysis of Lowry and colleague data set (Lowry et al., 2008) was done by Soufi and colleague (Soufi et al., 2012). We picked seven UPR^{ER} related genes of interest and summarized their results. As control, we picked *Nanog* a stemness marker and *COL1A1* a fibroblast marker.

RefSeq annotation			Gene expression log2 (GCRMA Intensities)		
Transcript ID	**Gene name**	**Category**	**BJ fibroblasts**	**iPS**	**ES**
NM_007348	*ATF6*	UPR effector	8.7025125	8.090600833	7.826710833
NM_182810	*ATF4*		13.4154	13.2858	12.74163333
NM_005080	*XBP1*		8.555195	8.339443333	8.249261667
NM_005347	*HSPA5*		11.02015167	10.60684667	10.482925
NM_003299	*HSP90B1/GRP94*		11.143225	11.47603333	11.61726667
NM_014330	*PPP1R15A/GADD34*		9.644111667	8.035643333	7.938243333
NM_004083	*DDIT3/CHOP*		11.4228	8.592626667	8.161856667
NM_024865	*NANOG*	Stemness marker	5.443613333	12.3643	12.88126667
NM_000088	*COL1A1*	Fibroblast marker	12.27041533	9.244766	10.051136

Supplementary Table 2: List of plasmids and cloning strategies. The restriction site is in green. The Kozak sequence is in red.

Name	Description	Addgene reference/vector name	Cloning strategy or targeting sequence	Gift from
pMX-Oct4	Retroviral OCT4	17217		Dr A. Panopoulos
pMX-Sox2	Retroviral SOX2	17217		Dr A. Panopoulos
pMX-Klf-4	Retroviral KLF4	17217		Dr A. Panopoulos
pMX-c-Myc	Retroviral cMYC	17217		Dr A. Panopoulos
pMX-GFP	Retroviral GFP	NA		Dr A. Panopoulos
pCMV-VSV-G	Retroviral packaging vector	8454		Dr A. Panopoulos
MSCV-gag/pol	Retroviral packaging vector	14887		Dr A. Panopoulos
CMV-eGFP	Lentiviral CMV eGFP	in CD510-B1 purchased from Systembio	Conventional restriction enzyme cloning XbaI NheI: F eGFP AAAtctagaGCCACCATGgtgagcaagggcgagg; R emGFP ttaGCTAGCCTActtgtacagctcgtccatgcc	
CMV-XBP1s	Lentiviral CMV XBP1s	in CD510-B1 purchased from Systembio	Conventional restriction enzyme cloning NotI BamHI: F XBP1 NotI aaaGCGGCCGCGCCACCATGgtggtggtggcagc; R XBP1 BamHI CTTGGATCCTTAgacactaatcagctggggaaag	XBP1s cDNA was a gift from Proteostasis Therapeutics
pPAX2	Lentiviral packaging vector			Pr R. Tjian
pMD2.G	Lentiviral packaging vector			Pr R. Tjian
pHAGE-EF1α-emGFP-IRES-Puro	Lentiviral EF1α emGFP			Pr R. Tjian

EF1α XBP1s	Lentiviral EF1a XBP1s	in pHAGE-EF1α-emGFP-IRES-Puro	Conventional restriction enzyme cloning NheI NotI: F XBP1s AAAGCTAGCGCCACCATGgtggtggtggcagc; R XBP1s CTTGCGGCCGCTTAgacactaatcagctggggaaag	
EF1α XBP1s-DBD	Lentiviral EF1a XBP1s-DBD	in pHAGE-EF1α-emGFP-IRES-Puro	A 2-step PCR was performed. Two fragments of XBP1s were generated with ATGGTGGTGGTGGCAGCC/ACTCATTCGAGC CTTCGCCTTCTCCTCGGGGC and CCGAGGAGAAGGCGAAGGCTCGAATGAGT GAGC/TTAGACACTAATCAGCTGGGG. After gel extraction, the two purified fragments were combined and PCRed with the same primers as for EF1a XBP1s contruct.	
Gluc-CFP	Lentiviral *Gaussia* luciferase			Dr B. Tannous
pCXLE-h Oct3/4-shP53	Episomal reprogramming vectors	27077		Pr R. Tjian
pCXLE-h SK	Episomal reprogramming vectors	27078		Pr R. Tjian
pCXLE-h UL	Episomal reprogramming vectors	27080		Pr R. Tjian
pLKO.1	pLKO.1 lentiviral shRNA empty for cloning		Cloning was done following this protocol: https://www.addgene.org/tools/protocols/plko/	Pr R. Tjian
shLuc	Targeting *Renilla* Luciferase	in pLKO.1	CGCTGAGTACTTCGAAATGTC	
shXBP1_1	Targeting XBP1	in pLKO.1	GCTGGAAGCCATTAATGAACT	
shXBP1_2	Targeting XBP1	in pLKO.1	GCTGGAAGCCATTAATGAA	
shXBP1_3	Targeting XBP1	in pLKO.1	CGGTATTGACTCTTCAGATT	
shXBP1_4	Targeting XBP1	in pLKO.1	GAGACATATTACTGGAAGTAAG	
shXBP1_5	Targeting XBP1	in pLKO.1	TTGTTCAGATCTCATAGATGAC	

Supplementary Table 3: List of primers.

House keeping gene	Forward	Reverse	Reference
GAPDH	TGTTGCCATCAATGACCCCTT	CTCCACGACGTACTCAGCG	(Maherali et al., 2008)
Stemness genes			
Endo OCT4	TGTACTCCTCGGTCCCTTTC	TCCAGGTTTTCTTTCCCTAGC	(Maherali et al., 2008)
Endo SOX2	GCTAGTCTCCAAGCGACGAA	GCAAGAAGCCTCTCCTTGAA	(Maherali et al., 2008)
Endo Nanog	CAGTCTGGACACTGGCTGAA	CTCGCTGATTAGGCTCCAAC	(Maherali et al., 2008)
Differentiated gene			
COL1A1	AAGAGGAAGGCCAAGTCGAG	CACACGTCTCGGTCATGGTA	(Vilchez et al., 2012)
Stress genes			
HSPA5	AAGACAAGGGTACAGGGAAC	CTTTCCAGCCATTCAATCTTTTC	(Jeanne et al., 2012)
ATF4	GTTTGGGGGCTGAAGAAAG	ACCCATGAGGTTTGAAGTGC	(Kuwabara et al., 2015)
ATF6	TTGGCATTTATAATACTGAACTATGGA	TTTGATTTGCAGGGCTCAC	(Benosman et al., 2013)
GRP94	CTGGAAATGAGGAACTAACAGTCA	TCTTCTCTGGTCATTCCTACACC	(Jagannathan et al., 2014)
CHOP	TTGCCTTTCTCCTTCGGGAC	GCTCTGGGAGGTGCTTGTGA	(Jeanne et al., 2012)
XBP1s	CGGAAGCCAAGGGGAATGAA	CTGCACCTGCTGCGGACT	F: (Ming et al., 2015); R: (Boden et al., 2008)
Control gene			
eGFP	AAGCTGACCCTGAAGTTCATCTGC	CTTGTAGTTGCCGTCGTCCTTGAA	(Adler-Wailes et al., 2015)

Supplementary Table 4. List of antibodies used for western blot and immunofluorescence

	Provider	catalog number	Concentration
WESTERN BLOT			
Primary antibodies			
ATF6	ThermoFisher	MA5-16172	1/500
XBP1	Abcam	ab37152	1/500
IRE1	Cell Signaling Technology	3294S	1/200
IRE1 Phospho	Abcam	ab81936	1/200
PERK	Cell Signaling Technology	5683S	1/200
PERK Phospho	Santa Cruz Biotechnology	sc-32577	1/200
HSPA5	Sigma-Aldrich	HPA038846	1/500
CLIMP-63	Enzo Life Sciences	ALX-804-604-C100	1/500
Nogo A+B (Reticulon 4)	Abcam	ab47085	1/500
GFP	Roche	11814460001	1/1,000
tubulin	Sigma-Aldrich	T6074-200UL	1/1,000
actin	Abcam	ab3280	1/1,000
actin	Cell Signaling Technology	4970S	1/1,000
Secondary antibodies LiCor			
IRDye® 680CW Donkey anti-Rabbit IgG (H + L)	LiCor	926-68073	1/5,000
IRDye® 680CW Donkey anti-Mouse IgG (H + L)	LiCor	926-68072	1/5,000

IRDye® 800CW Donkey anti-Mouse IgG (H + L)	LiCor	926-32212	1/5,000
IRDye® 800CW Donkey anti-Rabbit IgG (H + L)	LiCor	926-32213	1/5,000
IMMUNOFLURESCENCE			
Primary antibodies			
Nanog	Abcam	ab21624	1/500
TRA-1-60	Abcam	ab16288	1/500
SSEA-4	Abcam	ab16287	1/500
Secondary antibodies			
Alexa Fluor® 488 Donkey Anti-Rabbit IgG (H+L)	Life Technologies	A-21206	1/500
Alexa Fluor® 555 Donkey Anti-Mouse IgG (H+L)	Life Technologies	A-31570	1/500

Discussion

Our research shows that the UPR^{ER} is transiently activated during reprogramming. This is in line with the expectations, as this process results in dramatic morphological changes and organellar remodeling. Our work not only documents an early stress that upregulates the UPR^{ER} but also provides strategies to increase the reprogramming efficiency by modulating the UPR^{ER}.

I. Main results

a. Possible roles of single reprogramming factors in inducing the UPR^{ER} during cellular reprogramming

The UPR^{ER} is activated during cellular reprogramming. Whether the induction is the result of the cellular reprogramming process itself or due to the direct action of a single reprogramming factor is unclear. Soufi and colleagues (Soufi et al., 2012) performed a chromatin immunoprecipitation sequencing (ChiP-seq) to map the early protein-DNA interactions of OCT4, SOX2, KLF4, and c-MYC with the human genome using a doxycycline-inducible system. The authors used a 48 hr dox induction point on the basis that OSKM expression was maximal at that time and that most of the transcriptional changes are not happening yet. Therefore, only the primary effects of the reprogramming factors are studied. Based on their genome-wide ChiP-seq data we picked seven UPR^{ER} related genes of interest and summarized their results in Table 2, p.83.

Table 2: Occupancy of OCT4, SOX2, KLF4, c-MYC at 48h of reprogramming. These data were adapted from Soufi and colleagues (Soufi et al., 2012). TSS: transcription start site; MACS: Model-based analysis of ChIP-seq; FDR: false discovery rate.

RefSeq annotation		Chromatin occupancy within 20 kb upstream TSS and gene body (peaks called with MACS at 0.005 FDR)			
transcript ID	**gene name**	**c-MYC**	**KLF4**	**OCT4**	**SOX2**
NM_007348	*ATF6*	bound	bound	bound	bound
NM_182810	*ATF4*	not bound	not bound	not bound	not bound
NM_005080	*XBP1*	bound	bound	not bound	not bound
NM_005347	*HSPA5*	bound	not bound	not bound	not bound
NM_003299	*HSP90B1/GRP94*	not bound	not bound	not bound	not bound
NM_004083	*DDIT3/CHOP*	bound	not bound	not bound	not bound
NM_014330	*PPP1R15A/GADD34*	bound	bound	not bound	not bound

Strikingly, all the genes involved in the UPR^{ER} were bound by one or multiple reprogramming factors with the exception of *ATF4* and *GRP94*. This suggests that activation of the UPR^{ER}, at least of some of its components, could potentially be the result of the overexpression of any single reprogramming factor independently; therefore questioning the idea that the process of cellular reprogramming triggers the activation of the UPR^{ER}. We think that while it is possible that each reprogramming factor can bind the DNA at UPR^{ER} promoter genes and induce their expression at a low level, it is more likely that the wide remodeling and transcriptional changes occurring during reprogramming induce an excessive load on the ER and result in a potent activation of the UPR^{ER}. Key points should be raised regarding the study in order to draw the proper conclusions. The possible cooperation between the different factors is not addressed by this experiment. Indeed, transcriptional activation of certain target genes involves OCT4 and SOX2 to co-bind on their promoters. There is a sequential binding step that is required in order to induce the expression of these target genes (Chen et al., 2014).

Additionally, the physical presence of a transcription factor on a promoter does not necessitate transcriptional activity. Also, in a context where high overexpression of the reprogramming factors is observed, the specificity of binding must be questioned.

Though the direct contribution of the reprogramming factors directly binding the UPR^{ER} promoters resulting in the induction of the UPR^{ER} cannot be excluded, we believe that it only plays a minor role. The major cellular and organellar remodeling that occurs during reprogramming appears to have a more potent responsibility as detailed further below.

b. The temporal requirement of the UPR^{ER}

Our data suggest a temporal requirement of the UPR^{ER} during cellular reprogramming. This observation comes from the fact that embryonic stem cells have lower UPR^{ER} activity than some of their differentiated counterparts (supplementary Table 1, p.80 and supplementary Figure 6, pp.72-73). As observed either by transcriptome analysis, protein levels or HSPA5-GFP levels, UPR^{ER} effectors are lower in hESCs compared to the derived fibroblast-like cells or normal fibroblasts. The fact that UPR^{ER} activation was beneficial for cellular reprogramming (Figure 2, pp.56-57) was surprising and lead us to hypothesize that perhaps transient UPR^{ER} activation is needed during a specific time during reprogramming, after which UPR^{ER} activity levels are decreased to a low basal state.

Our data are consistent with this hypothesis. The time course experiments in Figure 1B, pp.54-55 and supplementary Figure 1C, pp.62-63 show a transient activation of the PERK and IRE1 branches of the UPR^{ER} during the early phase of cellular reprogramming. Activation of the UPR^{ER} by pharmacological means using APY-29, an activator of the IRE1 ribonuclease activity (Hetz et al., 2013), increased the percentage of the SSEA-4+/TRA-1-60+ cells in the population during reprogramming. This effect was achieved by only exposing the cells to the drug during 3 days at the beginning of the reprogramming process. Therefore, a short and transient ectopic induction of the UPR^{ER} was sufficient to increase the efficiency of reprogramming. Conversely, inhibiting the

UPR^{ER} with the drug GSK2656157, a compound that inhibits both PERK and eIF2α phosphorylation (Atkins et al., 2013), for 3 days during the beginning of cellular reprogramming decreased the percentage of the SSEA-4+/TRA-1-60+ population. It would be interesting to vary the exposure time to the drugs and/or change the time window during which the drugs are applied during cellular reprogramming to further support our statement.

An indirect validation that the induction of the UPR^{ER} was required transiently came from our experiments that use the EF1α promoter to drive *XBP1s*. We initially decided to choose the EF1α promoter because the overexpression is mild preventing initiation of cell death while maintaining the UPR^{ER} activated and because the promoter is not completely silenced in ESCs (Xia et al., 2007). Therefore, the expression of the transgenes will be sustained during most of the reprogramming process. We assumed this would be beneficial for reprogramming. We observed that despite substantially increasing the reprogramming efficiency, IPSCs clones derived from the EF1α promoter driving *XBP1s* cells had poor survival. The picked colonies would round up and not spread evenly leading to the formation of an embryoid body (EB)-like structure. A major difference observed at the time of picking was that the entire colony would detach preventing us from effectively being able to dissociate it. The extracellular matrix was stickier when the colonies came from XBP1s overexpression cells. Considering the role of the ER for secretion and the synthesis of transmembrane proteins we speculated that *XBP1s* was not completely silenced and could be responsible for this phenotype. It is established that the EF1α promoter is not silenced in ESCs while others like CMV are (Xia et al., 2007). We observed a similar "rounding up" phenotype when we overexpressed XBP1s in ESCs with the EF1α promoter. In line with these observations, all the IPSCs lines successfully derived from XBP1s overexpression showed silencing of the transgene while silencing of the transcriptional inactive *XBP1s-DBD* was not required for successful derivation. Additionally, when we derived IPSCs using an episomal reprogramming protocol together with the CMV promoter driving either *GFP* or *XBP1s*, we did not observe any differences in deriving IPSCs between the two conditions. As anticipated, the expression of *XBP1s* was similar between the derived lines and the controls suggesting a proper silencing of the transgene promoter.

To confirm the transient role of the UPR^{ER}, it would be important to use an inducible system to express *XBP1s*. This would also allow testing the time window of the UPR^{ER} activation requirement during cellular reprogramming.

c. Reconciling the granularity and shape with IPSCs formation prediction

We also reported that the number of IPS colonies could be enriched by FACS sorting based on the fluorescently tagged endogenous *HSPA5* gene. High levels of HSPA5-GFP correlated with a higher efficiency of reprogramming. High levels of HSPA5-GFP are an indicator of cells remodeling their ER, and by extension, those going through reprogramming. The high HSPA5-GFP population had a higher percentage of SSEA-4+/TRA-1-60+ cells, suggestive of being more advanced toward full pluripotency and gave rise to more IPSC colonies. It would be interesting to extend this finding to other genes involved in the UPR^{ER}. The utility of this method is limited by the fact that it involves the creation of a reporter line. Other methods such as live staining that could report the status of the UPR^{ER} would be perhaps more versatile tools to increase the number of IPS colonies.

Remarkably, we found a correlation between the basal levels of HSPA5-GFP and the Side SCatter (SSC) and Forward Scatter (FSC) parameters in fibroblast-like cells (Figure 4A, pp.60-61). SSC reflects the internal cellular complexity and membrane texture while FSC is an indicator of the cell size. Indeed, high levels of HSPA5-GFP correlated with higher SSC/FSC values. Even more exciting, during cellular reprogramming, cells exhibiting high SSC/FSC values showed a higher population of SSEA-4+/TRA-1-60+ like high HSPA5-GFP cells which we know to be more efficiently reprogrammed (Figure 3C, pp.58-59). It was therefore tempting to hypothesize that high SSC/FSC would be predictive of higher number of IPSC colonies. Very surprisingly, the opposite was true (Figure 4F, pp.60-61). This observation raises interesting questions regarding our results. While it is true that potential IPSCs have to stain positive for SSEA-4 and TRA-1-60, the reciprocal is not true. Indeed, all SSEA-4+/TRA-1-60+ cells are not going to give rise to

completely reprogrammed cells (Kahler et al., 2013). Approximately 3.6% of the SSEA-4+/TRA-1-60+ cells gave rise to IPSC colonies in the Kahler and colleagues study starting with human fibroblasts. It is important to consider that the actual IPSCs are merely a small fraction of cells, diluted in a larger population that can exhibit some characteristics that would mislead us. In the previous study, this means that 96.4% of the cells are blocked in an intermediate state of reprogramming. From our results, high SSC/FSC values have more SSEA-4+/TRA-1-60+ cells. Importantly, this does not imply low SSC/FSC have none. We would, in fact, expect to find more mature IPSCs among the low SSC/FSC population because ESCs have low SSC/FSC when compared to their differentiated counterparts such as fibroblast-like cells (supplementary Figure 8, pp.76-77). It is noteworthy that the correlation between high HSPA5-GFP and high SSC/FSC was established under unstressed conditions in fibroblast-like cells and ESCs (Figure 4A, pp.60-61 and supplementary Figure 8B, pp.76-77). During the process of reprogramming, the cell state dramatically changes and does not resemble a fibroblast anymore. We believe that the correlation between the cell SSC/FSC parameters and HSPA5-GFP levels is lost for the fully reprogrammed cells, because diluted in a larger population, while still valid for most of the cells in a transient state of reprogramming. Cells with low SSC/FSC (that include fully reprogrammed cells) can exhibit high HSPA5-GFP levels, which would explain why high HSPA5-GFP correlates better with more IPSC formation. Our hypothesis is that during the course of reprogramming, cells going through intense remodeling will activate the UPR^{ER}, the ones that exhibit higher levels of HSPA5-GFP are the most likely to fully reprogram, they also have a higher percentage of cells that are SSEA-4+/TRA-1-60+. Successful cells change their morphology to resemble an ESCs and acquire low SSC/FSC values, while still under reprogramming stress and keeping their HSPA5-GFP levels high. This is when the correlation between high HSP5-GFP levels and high FSC/SSC values, true on the population level, is lost for these few cells. This happens for a very small subset of cells while most of the other cells still remain with high SSC/FSC values, high HSPA5-GFP and are SSEA-4+/TRA-1-60+.

An interesting experiment to do would be to sort high and low SSC/FSC in the high and low HSPA5-GFP; this could help to further enrich in reprogrammed cells. It would be

exciting to compare this method to the SSEA-4/TRA-1-60 enrichment strategy in term of reprogramming efficiency.

II. How does the UPR^{ER} activation increase cellular reprogramming efficiency?

a. Cytoprotective role of the UPR^{ER} during reprogramming and its interplay with other cytoprotective pathways

Modulation of the UPR^{ER} can be seen as a cytoprotective response to protect the cells undergoing reprogramming. It has been shown that reprogramming can result in apoptosis, cell-cycle arrest and senescence (Banito et al., 2009; Marión et al., 2009; Utikal et al., 2009), oxidative burst (Ji et al., 2014), and DNA damage (Ruiz et al., 2015). All these reprogramming-associated consequences are known in other contexts to disrupt the ER homeostasis. Therefore, the beneficial role of the UPR^{ER} activation during reprogramming can be explained by a better capacity to integrate and respond to these cues and alleviate more efficiently the ER stress during reprogramming.

Cellular reprogramming requires a dramatic remodeling of the cell structure and in particular of its organelles. A very powerful remodeling process in the cell is autophagy. It is a self-catabolic mechanism through which dysfunctional and unnecessary components of the cell are degraded such as organelles and proteins (Bento et al., 2016). It has been recently reported that robust induction of autophagy happens during reprogramming in mouse fibroblasts (Wu et al., 2015). The authors limit the role of autophagy to the degradation of p62 whose accumulation in autophagy-deficient cells facilitates reprogramming. The cell reshaping, such as the cell size and the mitochondrial remodeling, is achieved by the inhibition of mTORC1. Remarkably, ER stress is capable at the same time to activate mTORC1 (Kato et al., 2012) and autophagy (Ogata et al., 2006) suggesting it could be an early step in the process. It is noteworthy that p62 is activated by TRIM-13, an ER resident ubiquitin E3 ligase, during tunicamycin-induced ER stress (Tomar et al., 2013). The role of TRIM-13 during reprogramming would be interesting to investigate since another E3 ligase, FBXW7, was shown to regulate cellular

reprogramming and stemness in mice (Buckley et al., 2012b). Interestingly, knockdown of FBXW7 increased the reprogramming efficiency. Conversely, knockdown of the deubiquinating enzyme PSMD14 failed to reprogram and generate IPSCs from mouse embryonic fibroblasts (Buckley et al., 2012a).

Previous work in our lab has already linked protein quality control with stem cell maintenance. A high level of proteasome activity is observed in hESCs and is required for their pluripotency. PSMD11 levels, a 19S proteasome subunit, was shown to play an important role in increasing the proteasome activity in hESCs (Vilchez et al., 2012). We anticipate that increased levels of proteasome activity through the overexpression of PSMD11 would increase the reprogramming efficiency.

Besides the induction of ER chaperones, the UPR^{ER} activates key players of the ER-associated protein degradation (ERAD) pathway (Travers et al., 2000). This process mediates the delivery of unfolded proteins from the ER to the cytosol for proteasomal degradation. When the proteasome machinery is unable to degrade the unfolded proteins either because of their size of because of their aggregation status, another more potent mechanism is activated: autophagy. Not only are proteins and aggregates degraded, but entire organelles are recycled. Key members of the autophagy pathway are UPR^{ER} target genes (Bernales et al., 2006).

Interestingly, in some cases UPR^{ER} activation can induce the expression of *c-MYC* (Shi et al., 2016) and *KLF4* (Sugiura et al., 2009). This activates the expression of the endogenous *c-MYC* and *KLF4* possibly speeding up the process of reprogramming.

The role of other regulatory elements of protein quality control such as the mitochondrial UPR (UPR^{mt}), and molecular chaperones involved in the heat shock response remain largely unexplored in the regulation of stem cell differentiation or reprogramming. How these processes are involved in reprogramming, as well as their potential cross-play with the UPR^{ER} will need to be explored.

Mitochondria have been shown to go through remodeling during reprogramming (Folmes et al., 2011), thus, it is tempting to speculate that the UPR^{mt} might be turned on during the early stages of cellular reprogramming. Links between regulatory components of the

UPR^{ER} with mitochondrial regulation and function exist. For example, ATF4 can control the expression of Parkin, a ubiquitin ligase crucial for mitochondria function and dynamics (Bouman et al., 2011). Parkin, in turn, is able to enhance branches of the UPR^{ER} through the activation of XBP1s (Duplan et al., 2013). The activity of PGC1α, a master regulator of mitochondrial biogenesis, was associated with ATF6 (Arensdorf et al., 2013).

Evidence tends to support the presence of cross talk between UPR, autophagy and mitochondria underlying the UPR^{ER} activation (Senft and Ronai, 2015) offering new avenues to study and understand cellular reprogramming through the prism of protein control quality.

b. Resetting the ER towards pluripotency

Acquisition of pluripotency implies a major remodeling of the organelles. ER morphology, for instance, changes drastically. The ER size correlates with the UPR^{ER} activation in order to respond to physiological demand. The UPR^{ER} can modulate the secretory capacity of the ER. During reprogramming, it is important to erase the somatic proteome and establish one of an embryonic stem cell. The UPR^{ER} activation could reset the ER associated proteome and contribute to reprogramming through two major pathways: translation and translocation.

The phosphorylation of eIF2α by PERK reduces translation initiation. This not only reduces the load of potentially misfolded proteins, which increases the quality of the ER proteome, but also stops the expression of the somatic genes. In parallel, the activation of IRE1 leads to the degradation of ER-bound mRNA through the RIDD pathway (Hollien and Weissman, 2006). Thus, a global reset of the somatic ER associated proteome occurs. The GADD34 restoration of translation initiation through eIF2α dephosphorylation could enable the translation of the newly activated genes by the reprogramming factors. Indeed, it is very likely that the reprogramming factors induce a high expression of genes that are

ensuring stemness and therefore their mRNA would outcompete the ones that ensure the somatic cell identity. This could lead to the reprogramming of the ER proteome.

A complementary mechanism occurs at the translocons. Translocons are channels through which nascent peptides enter the ER lumen. ER chaperones can assist during translocation of the newly synthesized peptide into the lumen (Brodsky et al., 1995). When the UPR^{ER} is activated, the chaperones are titrated away from this task and as a result the translocation efficiency is reduced. Thus, fewer proteins are loaded into the ER reducing the global load. This could also contribute to reset the previous somatic ER proteome. Interestingly, Kang and colleagues (Kang et al., 2006) observed a preferential translocation of proteins such as HSPA5 into the ER under stressful conditions. This mechanism is based on the "strength" of the signal peptide harbored by the secreted proteins. Besides increasing the quality of the ER proteome, it would be interesting to investigate if stem cell specific secreted proteins present a "strong" signal peptide that could play a role in the establishment of pluripotency. Conversely, some secreted proteins or receptors reminiscent of the somatic state could be negative regulators of stemness. A more comprehensive analysis of the secretome could give very interesting hints into this hypothesis. Consistent with this hypothesis, the mesenchymal-to-epithelial transition relies on signaling pathways and is an essential step during cellular reprogramming of mouse embryonic fibroblasts (Li et al., 2010). Li and colleagues proposed that SOX2, OCT4 and c-MYC inhibit the TGF-β (transforming growth factor β) signaling pathway while KLF4 induced E-cadherin, an epithelial gene. While there might be species-specific differences, this observation highlights the role of signaling molecules during cellular reprogramming and potentially a connection with the modulation of ER secretion capacity by the activation of the UPR^{ER}.

c. Between life and death, a second chance for reprogramming

The different UPR^{ER} branches play important roles in the decision whether the cell has to activate apoptosis or not. Apoptosis is a major barrier for cellular reprogramming

(Marión et al., 2009). A notable gene involved in pro-apoptotic signal is CHOP. As mentioned in the introduction, *CHOP* is induced by ATF4 (Marciniak et al., 2004) and ATF6 (Yoshida et al., 2000). Sustained and/or strong activation of the UPR^{ER} leads to the expression of CHOP and initiates apoptosis. Interestingly, sustained activation of the IRE1 pathway via the splicing of *XBP1* promotes cell survival (Lin et al., 2009). Therefore overexpression of XBP1s or addition of APY29 (promoting the splicing of XBP1) during reprogramming could protect the cells from the stress imposed by reprogramming. This could offer a wider range of possibilities for the cell to explore different cell states and maybe find a path towards pluripotency. The protection conferred by higher levels of UPR^{ER} activity increases the cell state plasticity.

d. Reprogramming as a reversal of development: lessons from the role of the UPR^{ER} during normal development and differentiation

Reprogramming can be comprehended as a reversal of development. Using a mouse secondary reprogramming system, Cacchiarelli and colleagues (Cacchiarelli et al., 2015) observed distinct waves of gene network activation corresponding to developmental genes characteristic of early embryonic patterning genes and followed by a pre-implantation gene signature. We reported in the introduction that numerous UPR^{ER} effectors are required during development. For example the homozygous deletion of either *Hspa5* (Luo et al., 2006), *Grp94* (Wanderling et al., 2007), *Grp58* (Garbi et al., 2006), *Ire1a* (Iwawaki et al., 2009), *Xbp1* (Reimold et al., 2000), *Calreticulin* (Mesaeli et al., 1999), or deletion of both *Atf6a* and *Atf6b* (Yamamoto et al., 2007) leads to embryonic lethality in mice. Furthermore, several components of the UPR^{ER} have an important role during differentiation. IRE1 increases lymphopoiesis of B cells (Zhang et al., 2005), XBP1 induces osteogenic and plasma differentiations (Iwakoshi et al., 2003), and CHOP plays an important role in the differentiation of B cells, erythrocytes, osteocytes and chondrocytes (Cui et al., 2000; Pereira et al., 2004; Skalet et al., 2005; Yang et al., 2005). These observations demonstrate the pleiotropic mode of action of the UPR^{ER} in different differentiation contexts and during normal development. It is

therefore not surprising that the UPR^{ER} plays such an important role during cellular reprogramming.

The role of the UPR^{ER} during normal development can be comprehended as a need to deal with the newly synthesized and the remodeling of the ER. Pieces of evidence suggest a more physiological role where the UPR^{ER} is activated even when the protein-processing capacity of the ER is not exceeded. During development, some cells require a drastic expansion of their ER. The UPR^{ER} has an important proactive role in this context. For instance, in the context of B cells differentiation into antibody-producing plasma cells the UPR^{ER} is activated even before any Ig synthesis occurs, suggesting a possible proactive role of the UPR^{ER} (van Anken et al., 2003). Consistently, B cells lacking the ability to produce Ig still activate XBP1 and differentiate normally (Hu et al., 2009). These observations suggest that the UPR^{ER} can be activated in preparation for the upcoming load of proteins. This proactive role suggests that the UPR^{ER} is a driving force for cellular state changes and not just a consequence. We believe that the proactive function of the UPR^{ER} could be at play during cellular reprogramming. By further activating the UPR^{ER}, genetically or pharmacologically, the cells are better primed for cellular reprogramming. The ER could better cope with the load of proteins generated by the addition of the Yamanaka factors and also with the results of the morphological changes. This is line with our data suggesting a transient role of the UPR^{ER}. Activation of the UPR^{ER} by XBP1s overexpression or addition of APY29 for only 3 days during the early step of reprogramming, when most of transcriptional changes happen, was able to prime the cells to reprogram with a higher efficiency. Conversely, inhibiting the UPR^{ER} with GSK2656157 for only 3 days during the early step of reprogramming had potent effect in reducing the efficiency of reprogramming. We predict that ectopic activation of the UPR^{ER} later during cellular reprogramming will have less effect on the efficiency of cellular reprogramming.

III. Extrapolation of the results to other paradigms

a. Extending the findings to other cell state switch paradigms

We believe that the transient UPR^{ER} activation is a more general process that enables cells to transit between two different states by insuring the integrity of the ER proteome but also other biological pathways in the cell, thus helping cells overcome this barrier of changing cellular states. We predict that this process should operate in a very similar fashion during cases of transdifferentiation happening naturally or induced experimentally; during this process cells revert to a point where they are able to change lineages. Cells can then differentiate into another cell type. This processes involves the reprogramming of the cell's fate.

Transdifferentiation occurs naturally. The newt, a type of salamander, is able to regenerate its lens after lentectomy. Pigmented epithelial cells change their morphology and lose their pigments and after a proliferation phase, cells switch to the new lineage and differentiate into mature lens cells (Tsonis et al., 2004). Experimental transdifferentiation, also called direct conversion, can be achieved by the forced expression of different transcription factors. For example, fibroblast can be transdifferentiated into functional neurons by the overexpression of ASCL1 (achaete–scute homologue 1), BRN2 (brain-specific homeobox and POU domain 2) and MYT1L (myelin transcription factor 1-like) (Vierbuchen et al., 2010). Likewise, fibroblasts can be converted to functional cardiomyocytes with MEF2C (myocyte-specific enhancer factor 2C) and TBX5 (T-box 5) (Ieda et al., 2010).

Together with cellular reprogramming, these mechanisms can help uncover cellular and molecular pathways leading to the development of regenerative strategies. Transdifferentitaiton involves the reprogramming of a cell's fate making it similar to what happens during cellular reprogramming with the Yamanaka factors. It would be fascinating to study the contribution of the UPR^{ER} during these processes.

b. A platform to study aging and rejuvenation

In our review, Vilchez and colleagues (Vilchez et al., 2014), we highlighted the crucial role of protein quality control in the control of stemness maintenance. We also draw a parallel with cellular pathways required for organismal lifespan and health extension or "healthspan". It appears that the same cellular mechanisms at play in stem cell maintenance and lifespan extension operate. Extrapolating this hypothesis, the study of mechanisms involved in either stem cell maintenance or lifespan extension could benefit from each other. In a very striking publication, Chen and colleagues (Chen et al., 2011) showed that pro-longevity compounds such as rapamycin (an mTOR inhibitor), resveratrol, fisetin (two sirtuin activators), curcumin (an antioxidant) or spermidine (an autophagy inducer) were able to increase the reprogramming efficiency. Consistent with this observation, activation of the UPR^{ER} is a potent pro-longevity pathway as published by our laboratory (Taylor and Dillin, 2013). We therefore hypothesize that we could use the knowledge from studies that identified barriers to cellular reprogramming and test these pathways for their ability to extend lifespan and healthspan and vice versa.

IV. General conclusion: Key points

- The UPR^{ER} is transiently activated during cellular reprogramming
- Ectopic activation of the UPR^{ER} increases cellular reprogramming
- Levels of the UPR^{ER} activity, as determined by HSPA5-GFP intensity, predict the efficiency of cellular reprogramming

Common abbreviations

4F	4 factors (OCT4, SOX2, KLF4 and c-MYC)
ATF4	activating transcription factor 4
ATF6	activating transcription factor 6
bFGF	fibroblast growth factor
DAPI	4',6-diamidino-2-phenylindole
DBD	DNA binding domain
DMEM	Dulbecco's Modified Eagle Medium
DNA	deoxyribonucleic acid
ECAT	ES cell-associated transcripts
EMT	epithelial-to-mesenchymal transition
ER	endoplasmic reticulum
ESC	embryonic stem cell
FBS	fetal bovine serum
FSC	Forward Scatter
GFP	green fluorescent protein
GFP94	glucose-regulated protein 94
HDF	human dermal fibroblasts
HSP	heat-shock protein
IPSC	induced pluripotent stem cell
IRE1	inositol-requiring protein-1
KLF4	Krüppel-like factor 4
MET	mesenchymal-to-epithelial transition
mRNA	messenger ribonucleic acid
MYOD	myoblast determination protein
OCT-3/4 or OCT4	octamer-binding protein 3/4
OSKM	OCT4, SOX2, KLF4 and c-MYC
PBS	phosphate buffered saline
PERK	protein kinase RNA (PRK)-like ER kinase
POUF5F1	refer to OCT4
PSC	Pluripotent stem cell
qRT-PCR	quantitative reverse transcription real-time polymerase chain reaction
SCNT	somatic cell nuclear transfer
SOX2	SRY box-containing factor 2
SSC	Side SCatter
TBS-T	Tris-Buffered Saline and Tween 20
TRIS	tris(hydroxymethyl)aminomethane
UPR^{ER}	endoplasmic reticulum unfolded protein response
UPR^{mt}	mitochondrial unfolded protein response
UPS	ubiquitin-proteasome system

References

Adler-Wailes, D.C., Alberobello, A.T., Ma, X., Hugendubler, L., Stern, E.A., Mou, Z., Han, J.C., Kim, P.W., Sumner, A.E., Yanovski, J.A., et al. (2015). Analysis of variants and mutations in the human winged helix FOXA3 gene and associations with metabolic traits. Int. J. Obes. 2005 *39*, 888–892.

Ang, Y.-S., Tsai, S.-Y., Lee, D.-F., Monk, J., Su, J., Ratnakumar, K., Ding, J., Ge, Y., Darr, H., Chang, B., et al. (2011). Wdr5 Mediates Self-Renewal and Reprogramming via the Embryonic Stem Cell Core Transcriptional Network. Cell *145*, 183–197.

van Anken, E., Romijn, E.P., Maggioni, C., Mezghrani, A., Sitia, R., Braakman, I., and Heck, A.J.R. (2003). Sequential Waves of Functionally Related Proteins Are Expressed When B Cells Prepare for Antibody Secretion. Immunity *18*, 243–253.

Arensdorf, A.M., DeZwaan McCabe, D., Kaufman, R.J., and Rutkowski, D.T. (2013). Temporal clustering of gene expression links the metabolic transcription factor HNF4α to the ER stress-dependent gene regulatory network. Genomic Endocrinol. *4*, 188.

Atkins, C., Liu, Q., Minthorn, E., Zhang, S.-Y., Figueroa, D.J., Moss, K., Stanley, T.B., Sanders, B., Goetz, A., Gaul, N., et al. (2013). Characterization of a Novel PERK Kinase Inhibitor with Antitumor and Antiangiogenic Activity. Cancer Res. *73*, 1993–2002.

Badr, C.E., Hewett, J.W., Breakefield, X.O., and Tannous, B.A. (2007). A Highly Sensitive Assay for Monitoring the Secretory Pathway and ER Stress. PLoS ONE *2*, e571.

Banito, A., Rashid, S.T., Acosta, J.C., Li, S., Pereira, C.F., Geti, I., Pinho, S., Silva, J.C., Azuara, V., Walsh, M., et al. (2009). Senescence impairs successful reprogramming to pluripotent stem cells. Genes Dev. *23*, 2134–2139.

Benosman, S., Ravanan, P., Correa, R.G., Hou, Y.-C., Yu, M., Gulen, M.F., Li, X., Thomas, J., Cuddy, M., Matsuzawa, Y., et al. (2013). Interleukin-1 Receptor-Associated Kinase-2 (IRAK2) Is a Critical Mediator of Endoplasmic Reticulum (ER) Stress Signaling. PLOS ONE *8*, e64256.

Bento, C.F., Renna, M., Ghislat, G., Puri, C., Ashkenazi, A., Vicinanza, M., Menzies, F.M., and Rubinsztein, D.C. (2016). Mammalian Autophagy: How Does It Work? Annu. Rev. Biochem. *85*, null.

Bernales, S., McDonald, K.L., and Walter, P. (2006). Autophagy Counterbalances Endoplasmic Reticulum Expansion during the Unfolded Protein Response. PLOS Biol *4*, e423.

Blau, H.M., Chiu, C.-P., and Webster, C. (1983). Cytoplasmic activation of human nuclear genes in stable heterocaryons. Cell *32*, 1171–1180.

Bock, C., Kiskinis, E., Verstappen, G., Gu, H., Boulting, G., Smith, Z.D., Ziller, M., Croft, G.F., Amoroso, M.W., Oakley, D.H., et al. (2011). Reference Maps of Human ES and iPS Cell Variation Enable High-Throughput Characterization of Pluripotent Cell Lines. Cell *144*, 439–452.

Boden, G., Duan, X., Homko, C., Molina, E.J., Song, W., Perez, O., Cheung, P., and Merali, S. (2008). Increase in Endoplasmic Reticulum Stress–Related Proteins and Genes in Adipose Tissue of Obese, Insulin-Resistant Individuals. Diabetes *57*, 2438–2444.

Bouman, L., Schlierf, A., Lutz, A.K., Shan, J., Deinlein, A., Kast, J., Galehdar, Z., Palmisano, V., Patenge, N., Berg, D., et al. (2011). Parkin is transcriptionally regulated by ATF4: evidence for an interconnection between mitochondrial stress and ER stress. Cell Death Differ. *18*, 769–782.

Boyer, L.A., Lee, T.I., Cole, M.F., Johnstone, S.E., Levine, S.S., Zucker, J.P., Guenther, M.G., Kumar, R.M., Murray, H.L., Jenner, R.G., et al. (2005). Core Transcriptional Regulatory Circuitry in Human Embryonic Stem Cells. Cell *122*, 947–956.

Brodsky, J.L., Goeckeler, J., and Schekman, R. (1995). BiP and Sec63p are required for both co- and posttranslational protein translocation into the yeast endoplasmic reticulum. Proc. Natl. Acad. Sci. *92*, 9643–9646.

Buckley, S.M., Aranda-Orgilles, B., Strikoudis, A., Apostolou, E., Loizou, E., Moran-Crusio, K., Farnsworth, C.L., Koller, A.A., Dasgupta, R., Silva, J.C., et al. (2012a). Regulation of Pluripotency and Cellular Reprogramming by the Ubiquitin-Proteasome System. Cell Stem Cell *11*, 783–798.

Buganim, Y., Faddah, D.A., Cheng, A.W., Itskovich, E., Markoulaki, S., Ganz, K., Klemm, S.L., van Oudenaarden, A., and Jaenisch, R. (2012). Single-Cell Expression Analyses during Cellular Reprogramming Reveal an Early Stochastic and a Late Hierarchic Phase. Cell *150*, 1209–1222.

Buganim, Y., Faddah, D.A., and Jaenisch, R. (2013). Mechanisms and models of somatic cell reprogramming. Nat. Rev. Genet. *14*, 427–439.

Burdon, T., Stracey, C., Chambers, I., Nichols, J., and Smith, A. (1999a). Suppression of SHP-2 and ERK Signalling Promotes Self-Renewal of Mouse Embryonic Stem Cells. Dev. Biol. *210*, 30–43.

Burdon, T., Chambers, I., Stracey, C., Niwa, H., and Smith, A. (1999b). Signaling Mechanisms Regulating Self-Renewal and Differentiation of Pluripotent Embryonic Stem Cells. Cells Tissues Organs *165*, 131–143.

Cacchiarelli, D., Trapnell, C., Ziller, M.J., Soumillon, M., Cesana, M., Karnik, R., Donaghey, J., Smith, Z.D., Ratanasirintrawoot, S., Zhang, X., et al. (2015). Integrative Analyses of Human Reprogramming Reveal Dynamic Nature of Induced Pluripotency. Cell *162*, 412–424.

Calfon, M., Zeng, H., Urano, F., Till, J.H., Hubbard, S.R., Harding, H.P., Clark, S.G., and Ron, D. (2002). IRE1 couples endoplasmic reticulum load to secretory capacity by processing the XBP-1 mRNA. Nature *415*, 92–96.

Cartwright, P., McLean, C., Sheppard, A., Rivett, D., Jones, K., and Dalton, S. (2005). LIF/STAT3 controls ES cell self-renewal and pluripotency by a Myc-dependent mechanism. Development *132*, 885–896.

Chan, E.M., Ratanasirintrawoot, S., Park, I.-H., Manos, P.D., Loh, Y.-H., Huo, H., Miller, J.D., Hartung, O., Rho, J., Ince, T.A., et al. (2009). Live cell imaging distinguishes bona fide human iPS cells from partially reprogrammed cells. Nat. Biotechnol. *27*, 1033–1037.

Chen, J., Zhang, Z., Li, L., Chen, B.-C., Revyakin, A., Hajj, B., Legant, W., Dahan, M., Lionnet, T., Betzig, E., et al. (2014). Single-Molecule Dynamics of Enhanceosome Assembly in Embryonic Stem Cells. Cell *156*, 1274–1285.

Chen, T., Shen, L., Yu, J., Wan, H., Guo, A., Chen, J., Long, Y., Zhao, J., and Pei, G. (2011). Rapamycin and other longevity-promoting compounds enhance the generation of mouse induced pluripotent stem cells. Aging Cell *10*, 908–911.

Cheng, A.M., Saxton, T.M., Sakai, R., Kulkarni, S., Mbamalu, G., Vogel, W., Tortorice, C.G., Cardiff, R.D., Cross, J.C., Muller, W.J., et al. (1998). Mammalian Grb2 Regulates Multiple Steps in Embryonic Development and Malignant Transformation. Cell *95*, 793–803.

Cheng, L., Hansen, N.F., Zhao, L., Du, Y., Zou, C., Donovan, F.X., Chou, B.-K., Zhou, G., Li, S., Dowey, S.N., et al. (2012). Low Incidence of DNA Sequence Variation in Human Induced Pluripotent Stem Cells Generated by Nonintegrating Plasmid Expression. Cell Stem Cell *10*, 337–344.

Cowan, C.A., Atienza, J., Melton, D.A., and Eggan, K. (2005). Nuclear reprogramming of somatic cells after fusion with human embryonic stem cells. Science *309*, 1369–1373.

Cox, J.S., and Walter, P. (1996). A Novel Mechanism for Regulating Activity of a Transcription Factor That Controls the Unfolded Protein Response. Cell *87*, 391–404.

Cox, J.S., Shamu, C.E., and Walter, P. (1993). Transcriptional induction of genes encoding endoplasmic reticulum resident proteins requires a transmembrane protein kinase. Cell *73*, 1197–1206.

Credle, J.J., Finer-Moore, J.S., Papa, F.R., Stroud, R.M., and Walter, P. (2005). On the mechanism of sensing unfolded protein in the endoplasmic reticulum. Proc. Natl. Acad. Sci. U. S. A. *102*, 18773–18784.

Cui, K., Coutts, M., Stahl, J., and Sytkowski, A.J. (2000). Novel Interaction between the Transcription Factor CHOP (GADD153) and the Ribosomal Protein FTE/S3a Modulates Erythropoiesis. J. Biol. Chem. *275*, 7591–7596.

Davis, R.L., Weintraub, H., and Lassar, A.B. (1987). Expression of a single transfected cDNA converts fibroblasts to myoblasts. Cell *51*, 987–1000.

Dorner, A.J., Wasley, L.C., Raney, P., Haugejorden, S., Green, M., and Kaufman, R.J. (1990). The stress response in Chinese hamster ovary cells. Regulation of ERp72 and protein disulfide isomerase expression and secretion. J. Biol. Chem. *265*, 22029–22034.

Duplan, E., Giaime, E., Viotti, J., Sévalle, J., Corti, O., Brice, A., Ariga, H., Qi, L., Checler, F., and Costa, C.A. da (2013). ER-stress-associated functional link between Parkin and DJ-1 via a transcriptional cascade involving the tumor suppressor p53 and the spliced X-box binding protein XBP-1. J Cell Sci *126*, 2124–2133.

Edel, M.J., Menchon, C., Menendez, S., Consiglio, A., Raya, A., and Belmonte, J.C.I. (2010). Rem2 GTPase maintains survival of human embryonic stem cells as well as enhancing reprogramming by regulating p53 and cyclin D1. Genes Dev. *24*, 561–573.

Evans, M.J., and Kaufman, M.H. (1981). Establishment in culture of pluripotential cells from mouse embryos. Nature *292*, 154–156.

Feng, B., Jiang, J., Kraus, P., Ng, J.-H., Heng, J.-C.D., Chan, Y.-S., Yaw, L.-P., Zhang, W., Loh, Y.-H., Han, J., et al. (2009). Reprogramming of fibroblasts into induced pluripotent stem cells with orphan nuclear receptor Esrrb. Nat. Cell Biol. *11*, 197–203.

Festuccia, N., Osorno, R., Halbritter, F., Karwacki-Neisius, V., Navarro, P., Colby, D., Wong, F., Yates, A., Tomlinson, S.R., and Chambers, I. (2012). Esrrb Is a Direct Nanog Target Gene that Can Substitute for Nanog Function in Pluripotent Cells. Cell Stem Cell *11*, 477–490.

Folmes, C.D.L., Nelson, T.J., Martinez-Fernandez, A., Arrell, D.K., Lindor, J.Z., Dzeja, P.P., Ikeda, Y., Perez-Terzic, C., and Terzic, A. (2011). Somatic Oxidative Bioenergetics Transitions into Pluripotency-Dependent Glycolysis to Facilitate Nuclear Reprogramming. Cell Metab. *14*, 264–271.

Fornace, A.J., Alamo, I., and Hollander, M.C. (1988). DNA damage-inducible transcripts in mammalian cells. Proc. Natl. Acad. Sci. *85*, 8800–8804.

Friedman, J.R., and Voeltz, G.K. (2011). The ER in 3D: a multifunctional dynamic membrane network. Trends Cell Biol. *21*, 709–717.

Fusaki, N., Ban, H., Nishiyama, A., Saeki, K., and Hasegawa, M. (2009). Efficient induction of transgene-free human pluripotent stem cells using a vector based on Sendai virus, an RNA virus that does not integrate into the host genome. Proc. Jpn. Acad. Ser. B *85*, 348–362.

Garbi, N., Tanaka, S., Momburg, F., and Hämmerling, G.J. (2006). Impaired assembly of the major histocompatibility complex class I peptide-loading complex in mice deficient in the oxidoreductase ERp57. Nat. Immunol. *7*, 93–102.

González, F., Boué, S., and Belmonte, J.C.I. (2011). Methods for making induced pluripotent stem cells: reprogramming à la carte. Nat. Rev. Genet. *12*, 231–242.

González, F., Georgieva, D., Vanoli, F., Shi, Z.-D., Stadtfeld, M., Ludwig, T., Jasin, M., and Huangfu, D. (2013). Homologous Recombination DNA Repair Genes Play a Critical Role in Reprogramming to a Pluripotent State. Cell Rep. *3*, 651–660.

Gore, A., Li, Z., Fung, H.-L., Young, J.E., Agarwal, S., Antosiewicz-Bourget, J., Canto, I., Giorgetti, A., Israel, M.A., Kiskinis, E., et al. (2011). Somatic coding mutations in human induced pluripotent stem cells. Nature *471*, 63–67.

Gorman, A.M., Healy, S.J.M., Jäger, R., and Samali, A. (2012). Stress management at the ER: Regulators of ER stress-induced apoptosis. Pharmacol. Ther. *134*, 306–316.

Guenther, M.G., Frampton, G.M., Soldner, F., Hockemeyer, D., Mitalipova, M., Jaenisch, R., and Young, R.A. (2010). Chromatin Structure and Gene Expression Programs of Human Embryonic and Induced Pluripotent Stem Cells. Cell Stem Cell *7*, 249–257.

Gurdon, J.B. (1962). The developmental capacity of nuclei taken from intestinal epithelium cells of feeding tadpoles. J. Embryol. Exp. Morphol. *10*, 622–640.

Hackler, L., Ózsvári, B., Gyuris, M., Sipos, P., Fábián, G., Molnár, E., Marton, A., Faragó, N., Mihály, J., Nagy, L.I., et al. (2016). The Curcumin Analog C-150, Influencing NF-κB, UPR and Akt/Notch Pathways Has Potent Anticancer Activity In Vitro and In Vivo. PloS One *11*, e0149832.

Han, J., Yuan, P., Yang, H., Zhang, J., Soh, B.S., Li, P., Lim, S.L., Cao, S., Tay, J., Orlov, Y.L., et al. (2010). Tbx3 improves the germ-line competency of induced pluripotent stem cells. Nature *463*, 1096–1100.

Hansson, J., Rafiee, M.R., Reiland, S., Polo, J.M., Gehring, J., Okawa, S., Huber, W., Hochedlinger, K., and Krijgsveld, J. (2012). Highly Coordinated Proteome Dynamics during Reprogramming of Somatic Cells to Pluripotency. Cell Rep. *2*, 1579–1592.

Harding, H.P., Zhang, Y., and Ron, D. (1999). Protein translation and folding are coupled by an endoplasmic-reticulum-resident kinase. Nature *397*, 271–274.

Harding, H.P., Zhang, Y., Zeng, H., Novoa, I., Lu, P.D., Calfon, M., Sadri, N., Yun, C., Popko, B., Paules, R., et al. (2003). An Integrated Stress Response Regulates Amino Acid Metabolism and Resistance to Oxidative Stress. Mol. Cell *11*, 619–633.

Haze, K., Yoshida, H., Yanagi, H., Yura, T., and Mori, K. (1999). Mammalian transcription factor ATF6 is synthesized as a transmembrane protein and activated by proteolysis in response to endoplasmic reticulum stress. Mol. Biol. Cell *10*, 3787–3799.

Heijmans, J., van Lidth de Jeude, J.F., Koo, B.-K., Rosekrans, S.L., Wielenga, M.C.B., van de Wetering, M., Ferrante, M., Lee, A.S., Onderwater, J.J.M., Paton, J.C., et al.

(2013). ER Stress Causes Rapid Loss of Intestinal Epithelial Stemness through Activation of the Unfolded Protein Response. Cell Rep. *3*, 1128–1139.

Heng, J.-C.D., Feng, B., Han, J., Jiang, J., Kraus, P., Ng, J.-H., Orlov, Y.L., Huss, M., Yang, L., Lufkin, T., et al. (2010). The Nuclear Receptor Nr5a2 Can Replace Oct4 in the Reprogramming of Murine Somatic Cells to Pluripotent Cells. Cell Stem Cell *6*, 167–174.

Hetz, C., Chevet, E., and Harding, H.P. (2013). Targeting the unfolded protein response in disease. Nat. Rev. Drug Discov. *12*, 703–719.

Hetzer, M.W., Walther, T.C., and Mattaj, I.W. (2005). PUSHING THE ENVELOPE: Structure, Function, and Dynamics of the Nuclear Periphery. Annu. Rev. Cell Dev. Biol. *21*, 347–380.

Hochedlinger, K., and Jaenisch, R. (2002). Monoclonal mice generated by nuclear transfer from mature B and T donor cells. Nature *415*, 1035–1038.

Hockemeyer, D., and Jaenisch, R. (2016). Induced Pluripotent Stem Cells Meet Genome Editing. Cell Stem Cell *18*, 573–586.

Hockemeyer, D., Wang, H., Kiani, S., Lai, C.S., Gao, Q., Cassady, J.P., Cost, G.J., Zhang, L., Santiago, Y., Miller, J.C., et al. (2011). Genetic engineering of human pluripotent cells using TALE nucleases. Nat. Biotechnol. *29*, 731–734.

Hollien, J., and Weissman, J.S. (2006). Decay of Endoplasmic Reticulum-Localized mRNAs During the Unfolded Protein Response. Science *313*, 104–107.

Hong, H., Takahashi, K., Ichisaka, T., Aoi, T., Kanagawa, O., Nakagawa, M., Okita, K., and Yamanaka, S. (2009). Suppression of induced pluripotent stem cell generation by the p53–p21 pathway. Nature *460*, 1132–1135.

Hu, C.-C.A., Dougan, S.K., McGehee, A.M., Love, J.C., and Ploegh, H.L. (2009). XBP-1 regulates signal transduction, transcription factors and bone marrow colonization in B cells. EMBO J. *28*, 1624–1636.

Hussein, S.M., Batada, N.N., Vuoristo, S., Ching, R.W., Autio, R., Närvä, E., Ng, S., Sourour, M., Hämäläinen, R., Olsson, C., et al. (2011). Copy number variation and selection during reprogramming to pluripotency. Nature *471*, 58–62.

Ieda, M., Fu, J.-D., Delgado-Olguin, P., Vedantham, V., Hayashi, Y., Bruneau, B.G., and Srivastava, D. (2010). Direct Reprogramming of Fibroblasts into Functional Cardiomyocytes by Defined Factors. Cell *142*, 375–386.

Iwakoshi, N.N., Lee, A.-H., and Glimcher, L.H. (2003). The X-box binding protein-1 transcription factor is required for plasma cell differentiation and the unfolded protein response. Immunol. Rev. *194*, 29–38.

Iwawaki, T., Akai, R., Yamanaka, S., and Kohno, K. (2009). Function of IRE1 alpha in the placenta is essential for placental development and embryonic viability. Proc. Natl. Acad. Sci. *106*, 16657–16662.

Jagannathan, S., Hsu, J.C.-C., Reid, D.W., Chen, Q., Thompson, W.J., Moseley, A.M., and Nicchitta, C.V. (2014). Multifunctional Roles for the Protein Translocation Machinery in RNA Anchoring to the Endoplasmic Reticulum. J. Biol. Chem. *289*, 25907–25924.

Jeanne, M., Labelle-Dumais, C., Jorgensen, J., Kauffman, W.B., Mancini, G.M., Favor, J., Valant, V., Greenberg, S.M., Rosand, J., and Gould, D.B. (2012). COL4A2 mutations impair COL4A1 and COL4A2 secretion and cause hemorrhagic stroke. Am. J. Hum. Genet. *90*, 91–101.

Ji, J., Sharma, V., Qi, S., Guarch, M.E., Zhao, P., Luo, Z., Fan, W., Wang, Y., Mbabaali, F., Neculai, D., et al. (2014). Antioxidant Supplementation Reduces Genomic Aberrations in Human Induced Pluripotent Stem Cells. Stem Cell Rep. *2*, 44–51.

Kahler, D.J., Ahmad, F.S., Ritz, A., Hua, H., Moroziewicz, D.N., Sproul, A.A., Dusenberry, C.R., Shang, L., Paull, D., Zimmer, M., et al. (2013). Improved Methods for Reprogramming Human Dermal Fibroblasts Using Fluorescence Activated Cell Sorting. PLoS ONE *8*, e59867.

Kaji, K., Norrby, K., Paca, A., Mileikovsky, M., Mohseni, P., and Woltjen, K. (2009). Virus-free induction of pluripotency and subsequent excision of reprogramming factors. Nature *458*, 771–775.

Kang, S.-W., Rane, N.S., Kim, S.J., Garrison, J.L., Taunton, J., and Hegde, R.S. (2006). Substrate-Specific Translocational Attenuation during ER Stress Defines a Pre-Emptive Quality Control Pathway. Cell *127*, 999–1013.

Kato, H., Nakajima, S., Saito, Y., Takahashi, S., Katoh, R., and Kitamura, M. (2012). mTORC1 serves ER stress-triggered apoptosis via selective activation of the IRE1–JNK pathway. Cell Death Differ. *19*, 310–320.

Kawamura, T., Suzuki, J., Wang, Y.V., Menendez, S., Morera, L.B., Raya, A., Wahl, G.M., and Belmonte, J.C.I. (2009). Linking the p53 tumour suppressor pathway to somatic cell reprogramming. Nature *460*, 1140–1144.

Kim, D., Kim, C.-H., Moon, J.-I., Chung, Y.-G., Chang, M.-Y., Han, B.-S., Ko, S., Yang, E., Cha, K.Y., Lanza, R., et al. (2009). Generation of Human Induced Pluripotent Stem Cells by Direct Delivery of Reprogramming Proteins. Cell Stem Cell *4*, 472–476.

Kleizen, B., and Braakman, I. (2004). Protein folding and quality control in the endoplasmic reticulum. Curr. Opin. Cell Biol. *16*, 343–349.

Koche, R.P., Smith, Z.D., Adli, M., Gu, H., Ku, M., Gnirke, A., Bernstein, B.E., and Meissner, A. (2011). Reprogramming Factor Expression Initiates Widespread Targeted Chromatin Remodeling. Cell Stem Cell *8*, 96–105.

Kozutsumi, Y., Segal, M., Normington, K., Gething, M.-J., and Sambrook, J. (1988). The presence of malfolded proteins in the endoplasmic reticulum signals the induction of glucose-regulated proteins. Nature *332*, 462–464.

Kuwabara, W.M.T., Zhang, L., Schuiki, I., Curi, R., Volchuk, A., and Alba-Loureiro, T.C. (2015). NADPH oxidase-dependent production of reactive oxygen species induces endoplasmatic reticulum stress in neutrophil-like HL60 cells. PloS One *10*, e0116410.

Laurent, L.C., Ulitsky, I., Slavin, I., Tran, H., Schork, A., Morey, R., Lynch, C., Harness, J.V., Lee, S., Barrero, M.J., et al. (2011). Dynamic Changes in the Copy Number of Pluripotency and Cell Proliferation Genes in Human ESCs and iPSCs during Reprogramming and Time in Culture. Cell Stem Cell *8*, 106–118.

Lee, A.-H., Iwakoshi, N.N., and Glimcher, L.H. (2003). XBP-1 Regulates a Subset of Endoplasmic Reticulum Resident Chaperone Genes in the Unfolded Protein Response. Mol. Cell. Biol. *23*, 7448–7459.

Li, H., Collado, M., Villasante, A., Strati, K., Ortega, S., Cañamero, M., Blasco, M.A., and Serrano, M. (2009). The Ink4/Arf locus is a barrier for iPS cell reprogramming. Nature *460*, 1136–1139.

Li, R., Liang, J., Ni, S., Zhou, T., Qing, X., Li, H., He, W., Chen, J., Li, F., Zhuang, Q., et al. (2010). A Mesenchymal-to-Epithelial Transition Initiates and Is Required for the Nuclear Reprogramming of Mouse Fibroblasts. Cell Stem Cell *7*, 51–63.

Lin, J.H., Li, H., Zhang, Y., Ron, D., and Walter, P. (2009). Divergent Effects of PERK and IRE1 Signaling on Cell Viability. PLOS ONE *4*, e4170.

Lowry, W.E., Richter, L., Yachechko, R., Pyle, A.D., Tchieu, J., Sridharan, R., Clark, A.T., and Plath, K. (2008). Generation of human induced pluripotent stem cells from dermal fibroblasts. Proc. Natl. Acad. Sci. *105*, 2883–2888.

Lu, P.D., Jousse, C., Marciniak, S.J., Zhang, Y., Novoa, I., Scheuner, D., Kaufman, R.J., Ron, D., and Harding, H.P. (2004). Cytoprotection by pre-emptive conditional phosphorylation of translation initiation factor 2. EMBO J. *23*, 169–179.

Luo, S., Mao, C., Lee, B., and Lee, A.S. (2006). GRP78/BiP Is Required for Cell Proliferation and Protecting the Inner Cell Mass from Apoptosis during Early Mouse Embryonic Development. Mol. Cell. Biol. *26*, 5688–5697.

MacArthur, B.D., Ma'ayan, A., and Lemischka, I.R. (2009). Systems biology of stem cell fate and cellular reprogramming. Nat. Rev. Mol. Cell Biol. *10*, 672–681.

Maherali, N., Ahfeldt, T., Rigamonti, A., Utikal, J., Cowan, C., and Hochedlinger, K. (2008). A High-Efficiency System for the Generation and Study of Human Induced Pluripotent Stem Cells. Cell Stem Cell *3*, 340–345.

Marciniak, S.J., Yun, C.Y., Oyadomari, S., Novoa, I., Zhang, Y., Jungreis, R., Nagata, K., Harding, H.P., and Ron, D. (2004). CHOP induces death by promoting protein synthesis and oxidation in the stressed endoplasmic reticulum. Genes Dev. *18*, 3066–3077.

Marión, R.M., Strati, K., Li, H., Murga, M., Blanco, R., Ortega, S., Fernandez-Capetillo, O., Serrano, M., and Blasco, M.A. (2009). A p53-mediated DNA damage response limits reprogramming to ensure iPS cell genomic integrity. Nature *460*, 1149–1153.

Martin, G.R. (1981). Isolation of a pluripotent cell line from early mouse embryos cultured in medium conditioned by teratocarcinoma stem cells. Proc. Natl. Acad. Sci. *78*, 7634–7638.

Matsuda, T. (1999). STAT3 activation is sufficient to maintain an undifferentiated state of mouse embryonic stem cells. EMBO J. *18*, 4261–4269.

Merksamer, P.I., Trusina, A., and Papa, F.R. (2008). Real-Time Redox Measurements during Endoplasmic Reticulum Stress Reveal Interlinked Protein Folding Functions. Cell *135*, 933–947.

Mesaeli, N., Nakamura, K., Zvaritch, E., Dickie, P., Dziak, E., Krause, K.-H., Opas, M., MacLennan, D.H., and Michalak, M. (1999). Calreticulin Is Essential for Cardiac Development. J. Cell Biol. *144*, 857–868.

Mikkelsen, T.S., Hanna, J., Zhang, X., Ku, M., Wernig, M., Schorderet, P., Bernstein, B.E., Jaenisch, R., Lander, E.S., and Meissner, A. (2008). Dissecting direct reprogramming through integrative genomic analysis. Nature *454*, 49–55.

Ming, J., Ruan, S., Wang, M., Ye, D., Fan, N., Meng, Q., Tian, B., and Huang, T. (2015). A novel chemical, STF-083010, reverses tamoxifen-related drug resistance in breast cancer by inhibiting IRE1/XBP1. Oncotarget *6*, 40692–40703.

Mitsui, K., Tokuzawa, Y., Itoh, H., Segawa, K., Murakami, M., Takahashi, K., Maruyama, M., Maeda, M., and Yamanaka, S. (2003). The Homeoprotein Nanog Is Required for Maintenance of Pluripotency in Mouse Epiblast and ES Cells. Cell *113*, 631–642.

Mori, K., Kawahara, T., Yoshida, H., Yanagi, H., and Yura, T. (1996). Signalling from endoplasmic reticulum to nucleus: transcription factor with a basic-leucine zipper motif is required for the unfolded protein-response pathway. Genes Cells *1*, 803–817.

Morl, K., Ma, W., Gething, M.-J., and Sambrook, J. (1993). A transmembrane protein with a cdc2+CDC28-related kinase activity is required for signaling from the ER to the nucleus. Cell *74*, 743–756.

Newman, A.M., and Cooper, J.B. (2010). Lab-Specific Gene Expression Signatures in Pluripotent Stem Cells. Cell Stem Cell *7*, 258–262.

Nichols, J., and Smith, A. (2009). Naive and Primed Pluripotent States. Cell Stem Cell *4*, 487–492.

Niwa, H., Burdon, T., Chambers, I., and Smith, A. (1998). Self-renewal of pluripotent embryonic stem cells is mediated via activation of STAT3. Genes Dev. *12*, 2048–2060.

Niwa, H., Ogawa, K., Shimosato, D., and Adachi, K. (2009). A parallel circuit of LIF signalling pathways maintains pluripotency of mouse ES cells. Nature *460*, 118–122.

Ogata, M., Hino, S., Saito, A., Morikawa, K., Kondo, S., Kanemoto, S., Murakami, T., Taniguchi, M., Tanii, I., Yoshinaga, K., et al. (2006). Autophagy Is Activated for Cell Survival after Endoplasmic Reticulum Stress. Mol. Cell. Biol. *26*, 9220–9231.

Okamura, K., Kimata, Y., Higashio, H., Tsuru, A., and Kohno, K. (2000). Dissociation of Kar2p/BiP from an ER Sensory Molecule, Ire1p, Triggers the Unfolded Protein Response in Yeast. Biochem. Biophys. Res. Commun. *279*, 445–450.

Okita, K., Matsumura, Y., Sato, Y., Okada, A., Morizane, A., Okamoto, S., Hong, H., Nakagawa, M., Tanabe, K., Tezuka, K., et al. (2011). A more efficient method to generate integration-free human iPS cells. Nat. Methods *8*, 409–412.

Onder, T.T., Kara, N., Cherry, A., Sinha, A.U., Zhu, N., Bernt, K.M., Cahan, P., Mancarci, B.O., Unternaehrer, J., Gupta, P.B., et al. (2012). Chromatin-modifying enzymes as modulators of reprogramming. Nature *483*, 598–602.

Panopoulos, A.D., Yanes, O., Ruiz, S., Kida, Y.S., Diep, D., Tautenhahn, R., Herrerías, A., Batchelder, E.M., Plongthongkum, N., Lutz, M., et al. (2012). The metabolome of induced pluripotent stem cells reveals metabolic changes occurring in somatic cell reprogramming. Cell Res. *22*, 168–177.

Pereira, R.C., Delany, A.M., and Canalis, E. (2004). CCAAT/Enhancer Binding Protein Homologous Protein (DDIT3) Induces Osteoblastic Cell Differentiation. Endocrinology *145*, 1952–1960.

Picanço-Castro, V., Russo-Carbolante, E., Reis, L.C.J., Fraga, A.M., de Magalhães, D.A.R., Orellana, M.D., Panepucci, R.A., Pereira, L.V., and Covas, D.T. (2010). Pluripotent Reprogramming of Fibroblasts by Lentiviralmediated Insertion of SOX2, C-MYC, and TCL-1A. Stem Cells Dev. *20*, 169–180.

Pluquet, O., Pourtier, A., and Abbadie, C. (2015). The unfolded protein response and cellular senescence. A Review in the Theme: Cellular Mechanisms of Endoplasmic Reticulum Stress Signaling in Health and Disease. Am. J. Physiol. - Cell Physiol. *308*, C415–C425.

Polo, J.M., Anderssen, E., Walsh, R.M., Schwarz, B.A., Nefzger, C.M., Lim, S.M., Borkent, M., Apostolou, E., Alaei, S., Cloutier, J., et al. (2012a). A Molecular Roadmap of Reprogramming Somatic Cells into iPS Cells. Cell *151*, 1617–1632.

Qin, H., Diaz, A., Blouin, L., Lebbink, R.J., Patena, W., Tanbun, P., LeProust, E.M., McManus, M.T., Song, J.S., and Ramalho-Santos, M. (2014). Systematic Identification of Barriers to Human iPSC Generation. Cell *158*, 449–461.

Reimold, A.M., Etkin, A., Clauss, I., Perkins, A., Friend, D.S., Zhang, J., Horton, H.F., Scott, A., Orkin, S.H., Byrne, M.C., et al. (2000). An essential role in liver development for transcription factor XBP-1. Genes Dev. *14*, 152–157.

Robinton, D.A., and Daley, G.Q. (2012). The promise of induced pluripotent stem cells in research and therapy. Nature *481*, 295–305.

Ron, D., and Walter, P. (2007). Signal integration in the endoplasmic reticulum unfolded protein response. Nat. Rev. Mol. Cell Biol. *8*, 519–529.

Ruberti, C., and Brandizzi, F. (2014). Conserved and plant-unique strategies for overcoming endoplasmic reticulum stress. Plant Cell Biol. *5*, 69.

Ruiz, S., Panopoulos, A.D., Montserrat, N., Multon, M.-C., Daury, A., Rocher, C., Spanakis, E., Batchelder, E.M., Orsini, C., Deleuze, J.-F., et al. (2012). Generation of a Drug-inducible Reporter System to Study Cell Reprogramming in Human Cells. J. Biol. Chem. *287*, 40767–40778.

Ruiz, S., Lopez-Contreras, A.J., Gabut, M., Marion, R.M., Gutierrez-Martinez, P., Bua, S., Ramirez, O., Olalde, I., Rodrigo-Perez, S., Li, H., et al. (2015). Limiting replication stress during somatic cell reprogramming reduces genomic instability in induced pluripotent stem cells. Nat. Commun. *6*.

Rutkowski, D.T., and Hegde, R.S. (2010). Regulation of basal cellular physiology by the homeostatic unfolded protein response. J. Cell Biol. *189*, 783–794.

Samavarchi-Tehrani, P., Golipour, A., David, L., Sung, H., Beyer, T.A., Datti, A., Woltjen, K., Nagy, A., and Wrana, J.L. (2010). Functional Genomics Reveals a BMP-Driven Mesenchymal-to-Epithelial Transition in the Initiation of Somatic Cell Reprogramming. Cell Stem Cell *7*, 64–77.

Sathananthan, H., Pera, M., and Trounson, A. (2002). The fine structure of human embryonic stem cells. Reprod. Biomed. Online *4*, 56–61.

Sato, N., Meijer, L., Skaltsounis, L., Greengard, P., and Brivanlou, A.H. (2004). Maintenance of pluripotency in human and mouse embryonic stem cells through activation of Wnt signaling by a pharmacological GSK-3-specific inhibitor. Nat. Med. *10*, 55–63.

Schuck, S., Prinz, W.A., Thorn, K.S., Voss, C., and Walter, P. (2009). Membrane expansion alleviates endoplasmic reticulum stress independently of the unfolded protein response. J. Cell Biol. *187*, 525–536.

Senft, D., and Ronai, Z.A. (2015). UPR, autophagy, and mitochondria crosstalk underlies the ER stress response. Trends Biochem. Sci. *40*, 141–148.

Shamu, C.E., and Walter, P. (1996). Oligomerization and phosphorylation of the Ire1p kinase during intracellular signaling from the endoplasmic reticulum to the nucleus. EMBO J. *15*, 3028–3039.

Shi, Y., Yang, Y., Hoang, B., Bardeleben, C., Holmes, B., Gera, J., and Lichtenstein, A. (2016). Therapeutic potential of targeting IRES-dependent c-myc translation in multiple myeloma cells during ER stress. Oncogene *35*, 1015–1024.

Shibata, Y., Voss, C., Rist, J.M., Hu, J., Rapoport, T.A., Prinz, W.A., and Voeltz, G.K. (2008). The Reticulon and Dp1/Yop1p Proteins Form Immobile Oligomers in the Tubular Endoplasmic Reticulum. J. Biol. Chem. *283*, 18892–18904.

Shibata, Y., Shemesh, T., Prinz, W.A., Palazzo, A.F., Kozlov, M.M., and Rapoport, T.A. (2010). Mechanisms Determining the Morphology of the Peripheral ER. Cell *143*, 774–788.

Sidrauski, C., and Walter, P. (1997). The Transmembrane Kinase Ire1p Is a Site-Specific Endonuclease That Initiates mRNA Splicing in the Unfolded Protein Response. Cell *90*, 1031–1039.

Sidrauski, C., Chapman, R., and Walter, P. (1998). The unfolded protein response: an intracellular signalling pathway with many surprising features. Trends Cell Biol. *8*, 245–249.

Skalet, A.H., Isler, J.A., King, L.B., Harding, H.P., Ron, D., and Monroe, J.G. (2005). Rapid B Cell Receptor-induced Unfolded Protein Response in Nonsecretory B Cells Correlates with Pro- Versus Antiapoptotic Cell Fate. J. Biol. Chem. *280*, 39762–39771.

Smith, A.G., Heath, J.K., Donaldson, D.D., Wong, G.G., Moreau, J., Stahl, M., and Rogers, D. (1988). Inhibition of pluripotential embryonic stem cell differentiation by purified polypeptides. Nature *336*, 688–690.

Soldner, F., Hockemeyer, D., Beard, C., Gao, Q., Bell, G.W., Cook, E.G., Hargus, G., Blak, A., Cooper, O., Mitalipova, M., et al. (2009). Parkinson's Disease Patient-Derived Induced Pluripotent Stem Cells Free of Viral Reprogramming Factors. Cell *136*, 964–977.

Soufi, A., Donahue, G., and Zaret, K.S. (2012). Facilitators and Impediments of the Pluripotency Reprogramming Factors' Initial Engagement with the Genome. Cell *151*, 994–1004.

Sridharan, R., Tchieu, J., Mason, M.J., Yachechko, R., Kuoy, E., Horvath, S., Zhou, Q., and Plath, K. (2009). Role of the Murine Reprogramming Factors in the Induction of Pluripotency. Cell *136*, 364–377.

Sugiura, K., Muro, Y., Futamura, K., Matsumoto, K., Hashimoto, N., Nishizawa, Y., Nagasaka, T., Saito, H., Tomita, Y., and Usukura, J. (2009). The Unfolded Protein Response Is Activated in Differentiating Epidermal Keratinocytes. J. Invest. Dermatol. *129*, 2126–2135.

Suhr, S.T., Chang, E.A., Tjong, J., Alcasid, N., Perkins, G.A., Goissis, M.D., Ellisman, M.H., Perez, G.I., and Cibelli, J.B. (2010). Mitochondrial Rejuvenation After Induced Pluripotency. PLoS ONE *5*, e14095.

Tada, M., Takahama, Y., Abe, K., Nakatsuji, N., and Tada, T. (2001). Nuclear reprogramming of somatic cells by in vitro hybridization with ES cells. Curr. Biol. *11*, 1553–1558.

Takagi, N., Yoshida, M.A., Sugawara, O., and Sasaki, M. (1983). Reversal of X-inactivation in female mouse somatic cells hybridized with murine teratocarcinoma stem cells in vitro. Cell *34*, 1053–1062.

Takahashi, K., and Yamanaka, S. (2006). Induction of Pluripotent Stem Cells from Mouse Embryonic and Adult Fibroblast Cultures by Defined Factors. Cell *126*, 663–676.

Takahashi, K., and Yamanaka, S. (2016). A decade of transcription factor-mediated reprogramming to pluripotency. Nat. Rev. Mol. Cell Biol. *advance online publication*.

Takahashi, K., Tanabe, K., Ohnuki, M., Narita, M., Ichisaka, T., Tomoda, K., and Yamanaka, S. (2007). Induction of Pluripotent Stem Cells from Adult Human Fibroblasts by Defined Factors. Cell *131*, 861–872.

Taylor, R.C., and Dillin, A. (2013). XBP-1 Is a Cell-Nonautonomous Regulator of Stress Resistance and Longevity. Cell *153*, 1435–1447.

Thomson, J.A., Itskovitz-Eldor, J., Shapiro, S.S., Waknitz, M.A., Swiergiel, J.J., Marshall, V.S., and Jones, J.M. (1998). Embryonic Stem Cell Lines Derived from Human Blastocysts. Science *282*, 1145–1147.

Tokuzawa, Y., Kaiho, E., Maruyama, M., Takahashi, K., Mitsui, K., Maeda, M., Niwa, H., and Yamanaka, S. (2003). Fbx15 Is a Novel Target of Oct3/4 but Is Dispensable for Embryonic Stem Cell Self-Renewal and Mouse Development. Mol. Cell. Biol. *23*, 2699–2708.

Tomar, D., Prajapati, P., Sripada, L., Singh, K., Singh, R., Singh, A.K., and Singh, R. (2013). TRIM13 regulates caspase-8 ubiquitination, translocation to autophagosomes and activation during ER stress induced cell death. Biochim. Biophys. Acta BBA - Mol. Cell Res. *1833*, 3134–3144.

Tomioka, M., Nishimoto, M., Miyagi, S., Katayanagi, T., Fukui, N., Niwa, H., Muramatsu, M., and Okuda, A. (2002). Identification of Sox-2 regulatory region which is under the control of Oct-3/4–Sox-2 complex. Nucleic Acids Res. *30*, 3202–3213.

Travers, K.J., Patil, C.K., Wodicka, L., Lockhart, D.J., Weissman, J.S., and Walter, P. (2000). Functional and Genomic Analyses Reveal an Essential Coordination between the Unfolded Protein Response and ER-Associated Degradation. Cell *101*, 249–258.

Tsonis, P.A., Madhavan, M., Tancous, E.E., and Del Rio-Tsonis, K. (2004). A newt's eye view of lens regeneration. Int. J. Dev. Biol. *48*, 975–980.

Tsubooka, N., Ichisaka, T., Okita, K., Takahashi, K., Nakagawa, M., and Yamanaka, S. (2009). Roles of Sall4 in the generation of pluripotent stem cells from blastocysts and fibroblasts. Genes Cells *14*, 683–694.

Utikal, J., Polo, J.M., Stadtfeld, M., Maherali, N., Kulalert, W., Walsh, R.M., Khalil, A., Rheinwald, J.G., and Hochedlinger, K. (2009). Immortalization eliminates a roadblock during cellular reprogramming into iPS cells. Nature *460*, 1145–1148.

Van Haute, L., Spits, C., Geens, M., Seneca, S., and Sermon, K. (2013). Human embryonic stem cells commonly display large mitochondrial DNA deletions. Nat. Biotechnol. *31*, 20–23.

Vattem, K.M., and Wek, R.C. (2004). Reinitiation involving upstream ORFs regulates ATF4 mRNA translation in mammalian cells. Proc. Natl. Acad. Sci. U. S. A. *101*, 11269–11274.

Vierbuchen, T., and Wernig, M. (2012). Molecular Roadblocks for Cellular Reprogramming. Mol. Cell *47*, 827–838.

Vierbuchen, T., Ostermeier, A., Pang, Z.P., Kokubu, Y., Südhof, T.C., and Wernig, M. (2010). Direct conversion of fibroblasts to functional neurons by defined factors. Nature *463*, 1035–1041.

Vilchez, D., Boyer, L., Morantte, I., Lutz, M., Merkwirth, C., Joyce, D., Spencer, B., Page, L., Masliah, E., Berggren, W.T., et al. (2012). Increased proteasome activity in human embryonic stem cells is regulated by PSMD11. Nature *489*, 304–308.

Vilchez, D., Simic, M.S., and Dillin, A. (2014). Proteostasis and aging of stem cells. Trends Cell Biol. *24*, 161–170.

Vitale, A.M., Matigian, N.A., Ravishankar, S., Bellette, B., Wood, S.A., Wolvetang, E.J., and Mackay-Sim, A. (2012). Variability in the Generation of Induced Pluripotent Stem Cells: Importance for Disease Modeling. Stem Cells Transl. Med. *1*, 641–650.

Waddington, C.H. (1957). The strategy of the genes: a discussion of some aspects of theoretical biology (Allen & Unwin).

Walter, P., and Ron, D. (2011). The Unfolded Protein Response: From Stress Pathway to Homeostatic Regulation. Science *334*, 1081–1086.

Wanderling, S., Simen, B.B., Ostrovsky, O., Ahmed, N.T., Vogen, S.M., Gidalevitz, T., and Argon, Y. (2007). GRP94 Is Essential for Mesoderm Induction and Muscle Development Because It Regulates Insulin-like Growth Factor Secretion. Mol. Biol. Cell *18*, 3764–3775.

Wang, S., Xia, P., Ye, B., Huang, G., Liu, J., and Fan, Z. (2013). Transient Activation of Autophagy via Sox2-Mediated Suppression of mTOR Is an Important Early Step in Reprogramming to Pluripotency. Cell Stem Cell *13*, 617–625.

Wang, T., Chen, K., Zeng, X., Yang, J., Wu, Y., Shi, X., Qin, B., Zeng, L., Esteban, M.A., Pan, G., et al. (2011). The Histone Demethylases Jhdm1a/1b Enhance Somatic Cell Reprogramming in a Vitamin-C-Dependent Manner. Cell Stem Cell *9*, 575–587.

Warren, L., Manos, P.D., Ahfeldt, T., Loh, Y.-H., Li, H., Lau, F., Ebina, W., Mandal, P.K., Smith, Z.D., Meissner, A., et al. (2010). Highly Efficient Reprogramming to Pluripotency and Directed Differentiation of Human Cells with Synthetic Modified mRNA. Cell Stem Cell *7*, 618–630.

Weismann, A., Parker, W.N. (William N., and Rönnfeldt, H. (1893). The germ-plasm; a theory of heredity (New York, Scribner's).

Wilmut, I., Schnieke, A.E., McWhir, J., Kind, A.J., and Campbell, K.H.S. (1997). Viable offspring derived from fetal and adult mammalian cells. Nature *385*, 810–813.

Wu, Y., Li, Y., Zhang, H., Huang, Y., Zhao, P., Tang, Y., Qiu, X., Ying, Y., Li, W., Ni, S., et al. (2015). Autophagy and mTORC1 regulate the stochastic phase of somatic cell reprogramming. Nat. Cell Biol. *17*, 715–725.

Xia, X., Zhang, Y., Zieth, C.R., and Zhang, S.-C. (2007). Transgenes Delivered by Lentiviral Vector are Suppressed in Human Embryonic Stem Cells in A Promoter-Dependent Manner. Stem Cells Dev. *16*, 167–176.

Yamamoto, K., Sato, T., Matsui, T., Sato, M., Okada, T., Yoshida, H., Harada, A., and Mori, K. (2007). Transcriptional Induction of Mammalian ER Quality Control Proteins Is Mediated by Single or Combined Action of ATF6α and XBP1. Dev. Cell *13*, 365–376.

Yan, W., Frank, C.L., Korth, M.J., Sopher, B.L., Novoa, I., Ron, D., and Katze, M.G. (2002). Control of PERK eIF2α kinase activity by the endoplasmic reticulum stress-induced molecular chaperone P58IPK. Proc. Natl. Acad. Sci. *99*, 15920–15925.

Yang, L., Carlson, S.G., McBurney, D., and Horton, W.E. (2005). Multiple Signals Induce Endoplasmic Reticulum Stress in Both Primary and Immortalized Chondrocytes Resulting in Loss of Differentiation, Impaired Cell Growth, and Apoptosis. J. Biol. Chem. *280*, 31156–31165.

Yoshida, H., Okada, T., Haze, K., Yanagi, H., Yura, T., Negishi, M., and Mori, K. (2000). ATF6 Activated by Proteolysis Binds in the Presence of NF-Y (CBF) Directly to the cis-Acting Element Responsible for the Mammalian Unfolded Protein Response. Mol. Cell. Biol. *20*, 6755–6767.

Yoshida, H., Matsui, T., Yamamoto, A., Okada, T., and Mori, K. (2001). XBP1 mRNA Is Induced by ATF6 and Spliced by IRE1 in Response to ER Stress to Produce a Highly Active Transcription Factor. Cell *107*, 881–891.

Yoshida, H., Oku, M., Suzuki, M., and Mori, K. (2006). pXBP1(U) encoded in XBP1 pre-mRNA negatively regulates unfolded protein response activator pXBP1(S) in mammalian ER stress response. J. Cell Biol. *172*, 565–575.

Yu, J., Vodyanik, M.A., Smuga-Otto, K., Antosiewicz-Bourget, J., Frane, J.L., Tian, S., Nie, J., Jonsdottir, G.A., Ruotti, V., Stewart, R., et al. (2007). Induced Pluripotent Stem Cell Lines Derived from Human Somatic Cells. Science *318*, 1917–1920.

Yu, J., Hu, K., Smuga-Otto, K., Tian, S., Stewart, R., Slukvin, I.I., and Thomson, J.A. (2009). Human Induced Pluripotent Stem Cells Free of Vector and Transgene Sequences. Science *324*, 797–801.

Zhang, J., Nuebel, E., Daley, G.Q., Koehler, C.M., and Teitell, M.A. (2012). Metabolic Regulation in Pluripotent Stem Cells during Reprogramming and Self-Renewal. Cell Stem Cell *11*, 589–595.

Zhang, K., Wong, H.N., Song, B., Miller, C.N., Scheuner, D., and Kaufman, R.J. (2005). The unfolded protein response sensor IRE1alpha is required at 2 distinct steps in B cell lymphopoiesis. J. Clin. Invest. *115*, 268–281.

Zhao, Y., Yin, X., Qin, H., Zhu, F., Liu, H., Yang, W., Zhang, Q., Xiang, C., Hou, P., Song, Z., et al. (2008). Two Supporting Factors Greatly Improve the Efficiency of Human iPSC Generation. Cell Stem Cell *3*, 475–479.

Appendix

Proteostasis and aging of stem cells

Vilchez, D.*, Simic, M.S.*, and Dillin, A. (2014). Proteostasis and aging of stem cells. **Trends Cell Biol.** *24*, 161–170.

* equal contributions

Review

Cell PRESS

Proteostasis and aging of stem cells

David Vilchez[1,2*], Milos S. Simic[1,3*], and Andrew Dillin[1,4]

[1] Molecular and Cell Biology Department, The University of California, Berkeley, Li Ka Shing Center For Biomedical and Health Sciences, Berkeley, CA 94720, USA
[2] Cologne Excellence Cluster for Cellular Stress Responses in Aging-Associated Diseases (CECAD), Institute for Genetics, University of Cologne, Zülpicher Strasse 47a, 50674 Cologne, Germany
[3] Université Pierre and Marie Curie, Paris, France
[4] Howard Hughes Medical Institute, The University of California, Berkeley, CA 94720, USA

The accumulation of misfolded or damaged proteins is an important determinant of the aging process. Mechanisms that promote the homeostasis of the proteome, or proteostasis, can slow aging and decrease the incidence of age-related diseases. Adult stem cell function declines during the aging process of an organism. This demise of somatic stem cell function could contribute to tissue degeneration and organismal aging. Accumulation of damaged proteins in embryonic stem cells (ESCs) may also have an impact on the aging process, because the passage of these proteins to progenitor cells during asymmetric division could compromise development and aging. Therefore, proteostasis maintenance in stem cells might have an important role in organismal aging. In this review, we discuss exciting new insights into stem cell aging and proteostasis and the questions raised by these findings.

Proteostasis maintenance during aging

The understanding of stem cell biology, differentiation and, cell reprogramming is currently one of the most intense and attractive fields in biology and medicine. Despite the insights gained into stem cell biology, the mechanisms that regulate stem cell identity and differentiation remain largely unknown. Pluripotent ESCs do not undergo replicative senescence and are considered to be immortal in culture [1,2]. Adult organisms have two types of stem cell: (i) adult somatic stem cells, which are found in several tissues and regenerate them; and (ii) germline stem cells (GSCs), which can generate gametes for reproduction [3]. GSCs are designed to maintain an unlimited proliferative capacity to fulfill their biological purpose: to be passed from one generation to the next. Adult somatic stem cells are critical for rejuvenating tissues and persist throughout the lifespan of the organism. However, adult somatic stem cell function declines during the aging process and this failure may contribute to age-related diseases [4,5] (Box 1).

Corresponding author: Dillin, A. (dillin@berkeley.edu).
Keywords: stem cells; proteostasis; aging; stress responses.
[*] These authors contributed equally to this work.

0962-8924/$ – see front matter
 http://dx.doi.org/10.1016/j.tcb.2013.09.002

While genome stability is central for the survival of stem cells, proteome stability may play an equally important role in stem cell identity. Proteostasis is critical for organismal development and cell function [6,7]. The quality of the proteome is regulated by a complex network of cellular mechanisms that monitors the concentration, folding, cellular localization, and interactions of proteins from their synthesis through their degradation (Figure 1) [6–8]. Protein synthesis is controlled by translational rates, which are regulated by ribosome biogenesis, recruitment, and loading [9]. The binding of chaperones to nascent proteins assists their folding into the correct structure. Thermal or oxidative stress, aging, and misfolding-prone mutations challenge the structure of proteins. Chaperones assure the proper cellular localization and folding of proteins throughout their life cycle [10,11]. Misfolded, damaged, aggregated, or unnecessary proteins are degraded by the proteasome or through autophagy [12–15]. The accumulation of misfolded or damaged proteins has a deleterious effect on cell function and viability [6,16]. Damaged proteins can disrupt cellular membranes and form toxic aggregates, overwhelming the cellular machinery required for their degradation [17,18] and causing cell malfunction and death [19]. When the stability of the proteome is challenged, a series of cellular responses is activated to maintain the quality of the proteome [7,16] (Box 2).

Defects in proteostasis lead to many metabolic, oncological, cardiovascular, and neurodegenerative disorders [6,20]. The ability to maintain a functional proteome declines during the aging process [6,11,21,22]. In cells undergoing division, mother cells retain damaged proteins while generating daughter cells with pristine proteomes [23,24]. However, postmitotic cells hold a special distinction for their susceptibility to age-onset protein-aggregation diseases [20]. A decline in the capacity of the cell to protect its proteome has been correlated with multiple age-related diseases such as Alzheimer's [25], Parkinson's [26], and Huntington's [27] disease. Several signaling pathways, such as reduced insulin/insulin-like growth factor 1 (IGF-1) signaling (IIS) or dietary restriction (DR), can extend longevity [8]. Furthermore, longevity-promoting pathways modulate the proteostasis network, providing increased stability of the proteome and delaying aging and the onset of age-related diseases [8,28,29].

The immortality and biological purpose of ESCs and GSCs and the ability of adult somatic stem cells to persist throughout life and rejuvenate tissues suggest that these

Box 1. Adult somatic stem cell exhaustion: a hallmark of aging

Adult somatic stem cells are necessary for rejuvenating tissues and persist throughout the lifespan of the organism. However, adult somatic stem cell function declines during the aging process in tissues such as the brain, skin, blood, bone, and skeletal muscle [4,5]. Adult stem cell exhaustion is considered one of the tentative hallmarks of aging in organisms [4]. Stem cell decline with age may contribute to tissue dysfunction and age-associated diseases [4,5,118]. For instance, adult somatic stem cell failure may contribute to diseases such as frailty, atherosclerosis, and type 2 diabetes by reducing the regenerative potential of tissues [118]. Decreased hematopoiesis with age results in diminished generation of adaptive cells and in increased anemia and myeloid malignancies [119]. A decline in the proliferation of NSCs and neurogenesis produced by these cells with age [120–123] has been associated with progressive Parkinsonian disease and impairment of olfactory discrimination in mouse [123]. Besides adult somatic stem cells, specific progenitor and differentiated cells can persist throughout life in regenerative tissues and their decline with age may also contribute to age-related diseases such as type 2 diabetes and reduced immune function [5].

cells could have increased mechanisms to protect their proteome. Recently, new insights into proteostasis in stem cells have supported this hypothesis. Specifically, a role of protein degradation systems and proteotoxic stress responses has been shown. In addition, longevity mechanisms are important determinants of stem cell maintenance and function. Here we review these insights into proteostasis regulation and the role of longevity-promoting pathways in stem cells.

Response to proteostasis stress in stem cells

A series of cellular responses are activated to maintain the integrity of the proteome when damaged proteins accumulate (Box 2). The heat shock response (HSR) is an essential mechanism to assure proper cytosolic protein folding and ameliorate chronic and acute proteotoxic stress [16,22]. The endoplasmic reticulum (ER) also has a critical role in protein folding [30,31]. The ER uses complex surveillance mechanisms to promote proper protein folding and activates the unfolded protein response (UPR^{ER}) to prevent the accumulation of misfolded proteins that are targeted for degradation by ER-associated degradation (ERAD) or autophagy [30–32]. If protein misfolding overwhelms the cellular ability to maintain the quality of the proteome, the ER coordinates with mitochondria to activate apoptosis [32]. Mitochondrial activity is associated with cellular dysfunction and aging [33]. A surveillance mechanism formed by chaperones and proteases, known as the mitochondrial UPR (UPR^{mt}), maintains the quality of the proteome in mitochondria [34]. Activation of these pathways or increased levels of chaperones are associated with enhanced protection against proteotoxic stress [35].

Reactive oxygen species (ROS) generated by the mitochondrial respiration process are frequently responsible for DNA and protein damage. Both mouse ESCs (mESCs)

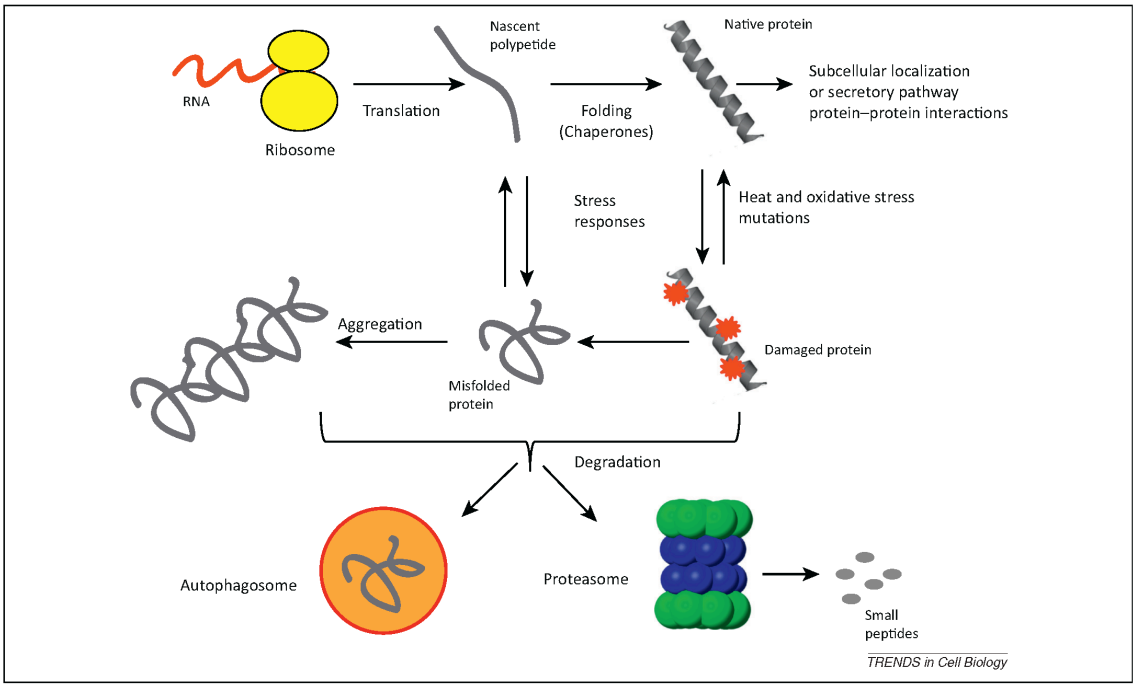

Figure 1. The proteostasis network. Protein synthesis is regulated by translational rates. Translation is controlled by ribosome biogenesis, recruitment, and loading. Chaperones assist the folding of nascent polypeptides into their correct structure. To achieve their function, native proteins are localized to their specific cellular compartment and the correct protein–protein interactions are established. Thermal or oxidative stress and misfolding-prone mutations damage and challenge the structure of proteins. When the stability of the proteome is challenged, a series of cellular stress responses are activated to maintain the quality of the proteome such as the heat-shock response or the unfolded-protein response. Misfolded, damaged, aggregated, or unnecessary proteins are degraded by the proteasome or through autophagy.

Review

Trends in Cell Biology March 2014, Vol. 24, No. 3

Box 2. Cellular stress responses

Regulation of protein synthesis represents a major component of cellular stress responses. Proteotoxic stress induces global attenuation of protein synthesis by inhibiting translation initiation [124] or pausing translation elongation [73–75]. Ribosome-associated chaperones such as HSP70 or nascent polypeptide-associated complex (NAC) play a critical role in promoting polypeptide elongation [73–75]. Under proteotoxic stress, these chaperones relocalize from ribosomes to protein aggregates resulting in diminished translational capacity and pausing of polypeptide elongation [73–75].

In addition, when the stability of the proteome is challenged a series of cellular responses such as the HSR or the UPR is activated to maintain the quality of the proteome, increasing the levels of chaperones and the degradation of misfolded proteins [6,16]. Three branches operate in parallel in the UPR^{ER}: activating transcription factor 6 (ATF6); double-stranded RNA-activated protein kinase (PRK)-like ER kinase (PERK); and inositol-requiring enzyme 1 (IRE1) [31]. On accumulation of unfolded proteins, ATF6 is delivered to the Golgi where proteases liberate its N-terminal cytosolic fragment enabling it to activate UPR genes in the nucleus. After sensing a stress, PERK oligomerizes and phosphorylates itself and eIF2α. This inhibits eIF2α and mRNA translation, thus reducing the flux of proteins in the ER. Yet, ATF4 mRNA, which has a short open reading frame in the 5′ untranslated region, is particularly translated when eIF2α is limiting. ATF4 is a transcription factor that induces CHOP, chaperones, GADD34, and various genes implicated in the antioxidant response, redox enzymes, and cell-death pathways. IRE1 transmits the UPR via unconventional XBP1 mRNA splicing. When spliced, XBP1 is translated and induces the expression of chaperones and ERAD proteins.

Under normal conditions, heat shock factor 1 (HSF-1) is negatively regulated by HSP-70/90 in eukaryotes. On non-permissive heat, HSPs such as HSP-70 restore proper folding of destabilized proteins. Inhibitory binding of HSF-1 by HSPs is released in times of protein misfolding stress, which enables HSF-1 trimerization, translocation to the nucleus, and the activation of genes required to maintain proteostasis, especially HSPs. When proteostasis is restored, HSPs negatively regulate HSF-1 and abolish the transcriptional stress response [35].

Likewise, in mammalian cells when unfolded proteins accumulate in the mitochondrial matrix, CHOP is transcriptionally upregulated via JNK2 and c-Jun. CHOP induces the transcription of the protease ClpP and the chaperonin HSP60. When unfolded proteins accumulate in the intermembrane space, AKT kinase is activated and the estrogen receptor is alpha phosphorylated, resulting in the induction of Htra2, an IMS protease, and the transcription of NRF1 [125].

and human ESCs (hESCs) generate fewer ROS than their differentiated counterparts [36,37]. In parallel, ESCs exhibit higher antioxidant defense potential that diminishes during differentiation. For instance, the glutathione/thioredoxin system enzymes (Tgr, Gpx2/3/4, Gsta3, Prdx2, Pdh2) are highly expressed in ESCs compared with their differentiated counterparts. These enzymes prevent ROS accumulation and promote a redox environment compatible with proper tertiary conformation of proteins [38]. An increase in the levels of ROS limits the lifespan of adult somatic stem cells such as hematopoietic stem cells (HSCs) and neural stem cells (NSCs) [39–42]. Notably, ROS levels serve as signals for differentiation or self-renewal in mouse adult somatic stem cells. HSCs retain self-renewal capacity under reduced conditions [43], whereas increased oxidative status promotes the stem cell activity of neuroepithelial stem cells in the central nervous system [44].

Notably, ESCs have increased levels of heat-shock proteins (HSPs). For instance, mESCs exhibit increased levels of HSPA1a, HSPA1b, HSPA9 (also known as mortalin), and HSPB1 [36] compared with their differentiated counterparts. Likewise, hESCs also have increased levels of HSPA1b [37]. However, hESCs do not show increased levels of HSPB1 [37]. Both HSP27 and HSPA9 levels decrease during mESC differentiation into neurogenic embryoid bodies [45]. Taken together, these data suggest that ESCs might have a greater ability to respond to protein misfolding. However, these increased levels of HSPs might not be conserved in all adult somatic stem cell types. Consistent with findings in ESCs, the HSR is attenuated on differentiation of neural progenitor cells [46]. HSP25 is excluded from neural precursors and other differentiating cells. However, the levels of HSPB1, HSPB5, HSPB6, and HSP60 decrease when human adipose-derived adult stem cells differentiate [47].

Supporting evidence suggests that HSPs may play a role in stemness and differentiation. Inhibition of HSP90 leads to mESC differentiation whereas overexpression of HSP90β partially rescues this phenotype [48]. HSP90 associates with Oct-4 and Nanog, protecting them from degradation by the ubiquitin–proteasome system (UPS) [48]. HSPs might also be significant determinants for the genesis of several tissues. HSPB5 overexpression modulates the activity of MyoD, the master regulator of myogenesis, by reducing its synthesis and increasing its degradation, therefore retarding differentiation [49]. HSPA8 (a non-inducible HSP) negatively influences the stability of proapoptotic Bim mRNA, increasing HSC survival and preventing their differentiation [50]. Bim mRNA is required for apoptosis during hematopoiesis and leukemogenesis. HSP70 indirectly triggers erythropoiesis by preventing caspase-3-mediated cleavage of GATA-1 [51], an essential transcriptional factor for maturation and differentiation within the erythroid lineage. Several components of the UPR^{ER} have an important role during differentiation. For example, IRE1 increases lymphopoiesis of B cells [52], XBP1 induces osteogenic and plasma differentiations [53], and CHOP promotes differentiation of B cells, erythrocytes, osteocytes, and chondrocytes [54–57]. Furthermore, the UPR^{ER}, as a stress-coordinated pathway, has an important role in the regulation of differentiation of the mouse intestinal epithelial stem cell [58]. The transition from stem cell to transit-amplifying cells of the intestine is accompanied by induced ER stress and activity of the UPR^{ER}. ER stress induction by Perk–eIF2α can promote loss of stemness. In organoid cultures of primary intestinal epithelium, when Perk–eIF2α is inhibited, stem cells accumulate. Taken together, these observations make it difficult clearly to correlate high levels of HSPs or cytotoxic protection with adult somatic stem cell differentiation and further insights into the impact of these mechanisms on stem cell function are needed. In addition, it will be fascinating to define whether the UPR^{mt} is enhanced in stem cells or whether it has a role in stem cell function.

Protein degradation systems as a determinant of stem cell function

When damaged or misfolded proteins cannot be 'rescued' by chaperones and the UPRs, they are degraded through the proteasome or autophagy. The proteasome is a complex

proteolytic machine formed by the assembly of several subunits that mostly degrades proteins that have been modified by the attachment of ubiquitin [12]. The UPS is critical for maintaining the proper concentration of many regulatory proteins involved in the cell cycle, apoptosis, inflammation, signal transduction, and other biological processes [12,59]. In addition, the UPS is a key component of the protein quality-control system to terminate damaged proteins [14]. The proteasome exists in several forms but its major assembly is formed by the core particle (20S), which contains the proteolytic active sites, and the regulatory particle (19S), which regulates the activity of the holocomplex (26S, single capped, and 30S, double capped) [12]. Although 20S particles can exist in a free form, they are inactive and unable to degrade proteins [60]. 19S recognizes polyubiquitylated proteins and unfolds and translocates these proteins to 20S for degradation [12,59].

The UPS has been shown to regulate ESC pluripotency and cellular reprogramming [61–63]. hESCs exhibit high proteasome activity compared with their differentiated counterparts such as neurons, fibroblasts, or trophoblasts [63]. This increased proteasome activity is correlated with increased levels of the 19S proteasome subunit PSMD11/RPN-6 [61,63,64], which is an essential subunit for the activity of the 26S/30S proteasome that stabilizes the otherwise weak interaction between the 20S core and the 19S cap [63,65]. GSCs can acquire *in vitro* properties similar to those of ESCs such as pluripotency [66]. GSCs generate the gametes that will produce embryos after reproduction. ESCs and oocytes share a common transcriptome signature [64] and hESCs provide an *in vitro* system to study oocyte development [67]. Similar to hESCs, human oocytes have increased expression levels of PSMD11 [64]. Notably, oocytes and gonads of *Drosophila melanogaster* have increased 26S proteasome activity and accumulate fewer damaged proteins than aging somatic tissues [68,69]. Although proteasome activity declines in somatic tissues during the aging process, maturating oocytes maintain their high activity [68]. Whether adult somatic stem cells also have enhanced proteasome activity remains to be elucidated, but the maintenance of this activity may critically impact organismal aging. Increased proteasome activity was found to be necessary for maintaining hESC pluripotency [63]. Additionally, other components of the UPS regulate pluripotency in mESCs such as the deubiquitinating enzyme Psmd14 and the E3 ligase Fbxw7 [61]. Psmd14 is part of the 19S proteasome subunit and its deubiquitinating activity is essential for mESC pluripotency [61]. These findings raise the intriguing question of why these cells need enhanced activity of the proteasome. ESCs show a remarkable capacity to replicate continuously in the absence of senescence. Therefore, increased proteostasis ability in ESCs could be required to avoid senescence and maintain an intact proteome either for self-renewal or for the generation of an intact cell lineage. Notably, degradation of damaged proteins is triggered on the first signs of mESC differentiation [70,71]. Induction of the proteasome activator PA28, normally associated with the immunoproteasome, is required for degradation of these damaged proteins during the first signs of cell fate specification [71]. Increased proteasome activity could also be critical for maintaining the proper concentration of many regulatory proteins at specific times, such as transcription factors involved in either pluripotency maintenance or the differentiation process. Interestingly, proteolytic degradation by the proteasome has a role in controlling transcription factor and Pol II binding to regulatory regions of cell type-specific gene domains in ESCs, thereby restricting permissive transcriptional activity and keeping genes in a potentiated state, ready for activation at specific stages [72]. Another possibility is that increased proteasome activity may be coupled to an intrinsic challenge to hESCs such as increased translation, which could be associated with translation errors. However, protein expression has not been examined in ESCs. In this context, it will be fascinating to analyze the role of ribosome-associated chaperones (Box 2) [73–75] in translational rates in ESCs.

Macroautophagy (hereafter referred to as autophagy) is a self-catabolic mechanism through which dysfunctional and unnecessary components of the cell such as organelles and proteins are degraded. In addition, autophagy provides a means to keep energy and nutrients to levels compatible with survival under starvation and stress. These components are engulfed in a double membrane, the autophagosome, which is subsequently fused with lysosomes. Lysosomal enzymes degrade the contents of autophagosomes, producing amino acids and fatty acids that are recycled in the cytoplasm [13]. A multitude of stressors such as ROS, starvation, DNA damage and ER stress activates autophagy in terminally differentiated cells [13].

Both mESCs and hESCs exhibit higher autophagy activity on early differentiation [76]. Induced pluripotent stem cells generated from patients with Parkinson's disease show more autophagic vacuoles when differentiated into dopaminergic neurons [77], suggesting an active rejuvenation step to generate a pool of 'healthy' cells. Experiments with adult somatic stem cells cultured *in vitro* such as human mesenchymal stem cells (hMSCs) [78], HSCs, dermal stem cells (DSCs), and epidermal stem cells [79] suggest that autophagy activity is increased in these cells compared with their differentiated counterparts. It is noteworthy that experimental conditions might be unfavorable and lead to higher autophagy levels in adult somatic stem cells. Developing conditions that would mimic the stem cell niche are necessary for a better understanding of autophagy regulation in these cells. In fetal and postnatal mHSCs, a deficiency in essential autophagy genes such as FIP200 or Atg7 deregulates proliferation, suggesting that autophagy is required for stemness in fetal and postnatal mHSCs [80–83]. FoxO3, a forkhead transcription factor linked to stem cell maintenance and longevity [84], maintains the expression of proautophagy genes in adult mHSCs to allow a quick autophagic response on stress [85]. Notably, old mHSCs have higher basal levels of autophagy activity, a characteristic required for their cloning efficiency, and are able to induce autophagy much like young HSCs. However, autophagy activity in young HSCs is not required for their cloning efficiency [85]. This observation is controversial because previous data showed the opposite effect [81–83,86]. The difference might be that one study [85] used a drug to block autophagy in normally

developed adult mHSCs whereas the latter study used a genetic model to block autophagy that causes severe defects early in life leading to death and thus looked at fetal and early stages. The higher levels of autophagy activity in old adult mHSCs were due to attenuated nutrient (2-NBD glucose) uptake [85]. That old adult mHSCs maintain an autophagy potential similar to young mHSCs and exhibit higher levels of autophagy for their survival confronts the prevailing, traditional view where compromised autophagy is seen as a determinant of aging [13].

In NSCs or cardiac stem cells (CSCs), autophagy activity increases on their differentiation [87–89]. This enhanced autophagy might be due to a specific increase in the requirements of their differentiated counterparts, such as neurons, to recycle their cellular components. During the initial period of neuronal differentiation (E15.5 mouse embryos), expression of the autophagy genes *Atg7*, *Becn1*, *Ambra1*, and *LC3* are increased *in vivo* in the mouse embryonic olfactory bulb (OB) [87]. *In vitro* neuronal differentiation of OB-derived stem cells is accompanied by increased autophagy flux and LC3 lipidation in Tuj1-positive cells [87]. Blocking autophagy chemically or genetically can impair NSC and CSC differentiation [87–89]. Inhibition of autophagy by 3-MA or wortmannin decreases neurogenesis of OB-derived stem cells. In addition, *Ambra1* loss-of-function mice show decreased neural markers in the E13.5 OB [87]. However, FIP200 is required for NSC proliferation [90]. Knock down of *Becn1* or *Atg7* suppresses the expression of cardiomyocyte markers such as α-actin and smooth muscle α-actin in embryoid bodies of mESCs [88,89]. Moreover, treatment of embryoid bodies with the autophagy inhibitor NH_4Cl or bafilomycin A1 decreases the number of beating foci whereas activation with rapamycin increases their number [88,89]. Similarly, *ex vivo* treatment of E8.5 mouse embryos with rapamycin increases the expression of cardiomyocyte markers in the second heart field.

Overall, these observations suggest a higher degree of protection, at least, to cytotoxic stresses in adult somatic stem cells. Consistent with this idea, impairment of autophagy in epidermal stem cells, DSCs, and HSCs leads to increased susceptibility to cytotoxic stress such as etoposide, doxorubicid, or UV [79]. In addition, autophagy might be an efficient mechanism to replace transcription factors and associated proteins of stemness and initiate more rapid differentiation, especially in ESCs.

Longevity-promoting pathways regulate stem cell function

A series of signaling pathways promote longevity and provide increased stability to the proteome, delaying the onset of age-related diseases [8,28,91]. Reduced IIS extends lifespan in both invertebrates and vertebrates [84,92,93] and correlates with increased longevity of humans [92,94]. The insulin/IGF-1 receptor activates a conserved phosphatidylinositol (PI) 3-kinase/PDK/AKT signaling cascade that phosphorylates FOXO transcription factors, thereby preventing their nuclear localization. When IIS signaling is reduced, FOXO accumulates in the nucleus and regulates downstream genes that extend lifespan and increase stress resistance in worms, flies, and mice [84,93]. Delayed aging by IIS reduction protects worms and mice from protein-aggregation toxicity [8,28]. Notably, FOXO transcription factors are important regulators of the proliferation and self-renewal of NSCs and HSCs in mice. A combined deficiency of FoxO1, FoxO3, and FoxO4 depletes the NSC and HSC pools in mice [41,42]. FOXO transcription factors protect from oxidative stress and promote the expression of antioxidant enzymes [95]. Combined deficiency of FoxO1, FoxO3, and FoxO4 increases ROS levels in NSCs and HSCs [41,42], which may increase protein misfolding. FoxO3 is essential for regulating this process in mice, because FoxO3 deficiency alone increases ROS levels and depletes the pool of NSCs and HSCs [96,97].

Among invertebrates, birds, and mammals, experimental paradigms that limit reproductive investment also cause lifespan extension [98]. Hypothetically, the need for repairing and preventing damage to the germline dominates resource allocation strategies, while the somatic tissues age and deteriorate [99]. In support of such theories, modulations of reproduction that eliminate germ cells in *Caenorhabditis elegans* and *D. melanogaster* provide effective mechanisms for extending lifespan [98,100]: phenotypes that may be caused by heightened resource availability and proteome stability within the postmitotic soma [29,101]. Similar to hESCs, proteasome activity and RPN-6 levels are increased in these germline-lacking worms [29]. Furthermore, increased proteasome activity, *rpn-6* expression, and longevity are modulated by DAF-16, the worm FOXO transcription factor [29]. Notably, FOXO4 is necessary for increased proteasome activity in hESCs and reduces the potential of these cells to differentiate into neural lineages [63,102]. In addition, hESC pluripotency requires FOXO1 [103]. Therefore, FOXOs cross evolutionary boundaries and link hESC function to invertebrate longevity modulation. FOXO4 is specifically critical for the differentiation of hESCs into neural cells and it will be fascinating to understand how this regulation is achieved. However, the loss of FOXO3 in mouse causes increased neurogenesis during development followed by NSC depletion in adulthood [96]. Interestingly, it was recently found that FOXO3-bound genes thoroughly overlap with those bound by the proneuronal bHLH transcription factor ASCL/MASH1 in cultured neural progenitor cells [104]. FOXO3 represses the expression of specific ASCL1 neurogenic targets and restrains neurogenesis. Therefore, FOXO3 may help maintain the NSC pool by negatively regulating neurogenesis. These results suggest that FOXO4 and FOXO3 might have opposing effects in hESCs versus mouse NSCs. Different hypotheses could explain these opposing effects: different cell-type requirements (hESCs versus NSCs); the different models and species used for these assays (*in vitro* cultured hESCs versus mouse models); the differentiation stage at the time point chosen; and that different FOXO isoforms may act in different pathways during cellular commitment. It is intriguing to speculate that FOXO4 may be required for the differentiation of hESCs into neural cells and that FOXO3 is later required for maintaining the pool of adult NSCs and avoiding a premature burst of neurogenesis. Accordingly, FOXO4 levels decrease during neural differentiation of hESCs whereas FOXO3 levels increase [63,102].

Review

Trends in Cell Biology March 2014, Vol. 24, No. 3

Reduced food intake without malnutrition, or DR, also extends lifespan in multiple species and delays the onset of diverse pathologies related to age [8,105]. DR decreases protein synthesis by modulating translational rates [106,107], which can improve proteostasis maintenance. The decrease in the load of nascent polypeptides to the proteostasis machinery may allow more efficient protein folding and degradation and, therefore, decrease the accumulation of misfolded and damaged proteins. The protein mammalian target of rapamycin (mTOR) plays a pivotal role in the modulation of translational rates induced by DR [106,107]. mTOR associates with other proteins to form two different complexes: mTORC1 and mTORC2. mTORC1 activity is inhibited by DR, resulting in lifespan extension and delayed onset of protein aggregation [108]. Recent studies suggest a role of DR in stem cell proliferation. Stem cell function of mouse intestinal stem cells (ISCs) was found to be increased by DR via a non-cell-autonomous mechanism acting through adjacent Paneth cells present in the ISC niche. DR downregulated mTORC1 activity in Paneth cells but not in the ISCs, creating an environment where ISC function is enhanced [109]. Decreased activity of mTORC1 in Paneth cells upregulates levels of bst1, a protein that promotes cell proliferation in bone marrow. Regulation of bst1 levels by mTORC1 is essential for the improved ISC function on DR. Similarly, the regenerative potential of muscle satellite cells increased on DR in young and old mice [110]. The number of satellite cells per fibers is increased after 3 months of DR. DR also increases neurogenesis [111], but the effects are incompatible with *in vivo* application because a high deprivation of intake is required. These data suggest a beneficial role in various tissues mediated by DR that can help us understand its pro-longevity role by enhanced stem cell function.

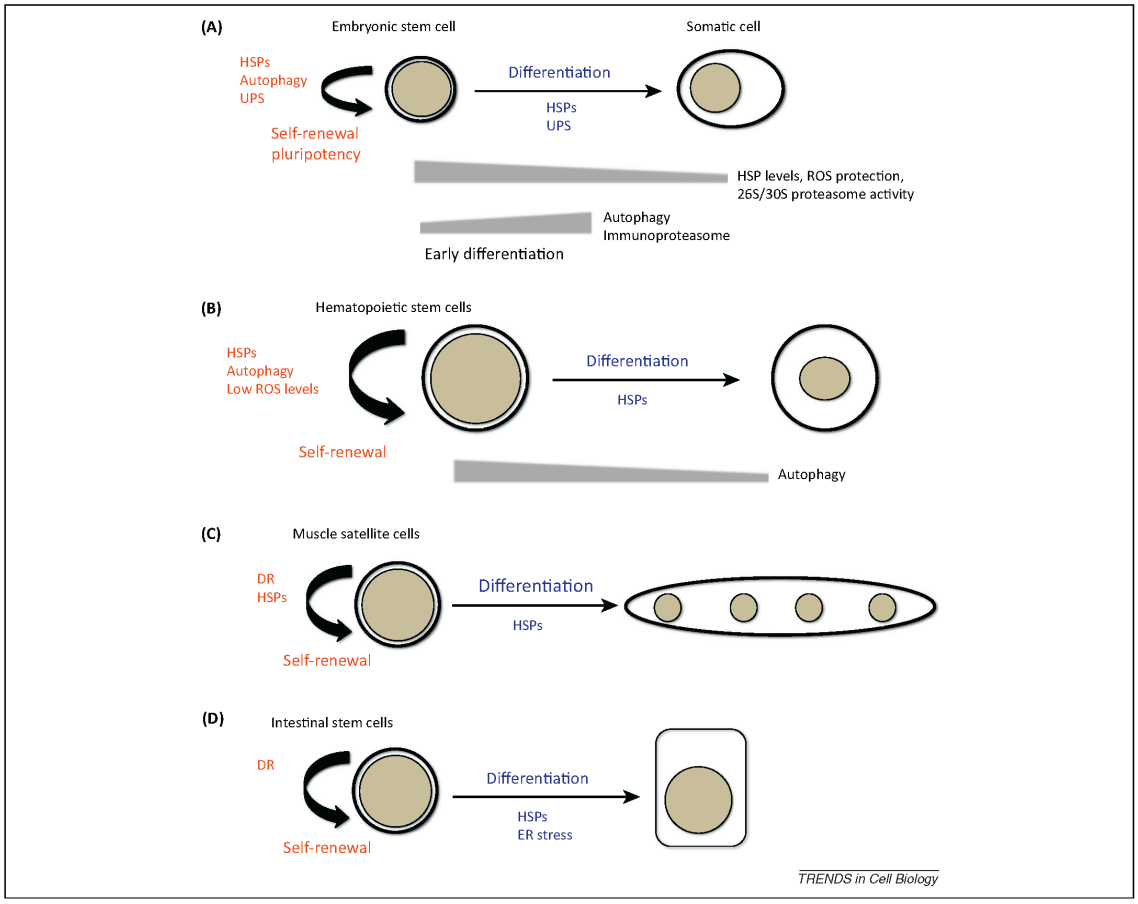

Figure 2. Proteostasis in stem cells. **(A)** Embryonic stem cells (ESCs) exhibit increased levels of heat-shock protein (HSPs) and 26S/30S proteasome activity and are more protected from reactive oxygen species (ROS) than their differentiated counterparts. In an active rejuvenation step, both autophagy and the immunoproteasome activities increase during the first days of differentiation. HSPs, autophagy, and the ubiquitin–proteasome system (UPS) are required to maintain ESC features such as self-renewal and pluripotency. HSPs and the UPS are required for differentiation of ESCs into specific cellular lineages. **(B)** Hematopoietic stem cells (HSCs) exhibit increased levels of autophagy activity compared with their differentiated counterparts. Low levels of ROS and increased levels of HSPs and autophagy activity are required to maintain HSC self-renewal. HSPs are required for differentiation of HSCs. **(C)** Dietary restriction (DR) improves muscle satellite cell self-renewal. HSPs are required for differentiation of muscle satellite cells. **(D)** DR and increased levels of HSPs improve intestinal stem cell (ISC) self-renewal. Endoplasmic reticulum (ER) stress and HSPs affect differentiation of ISCs.

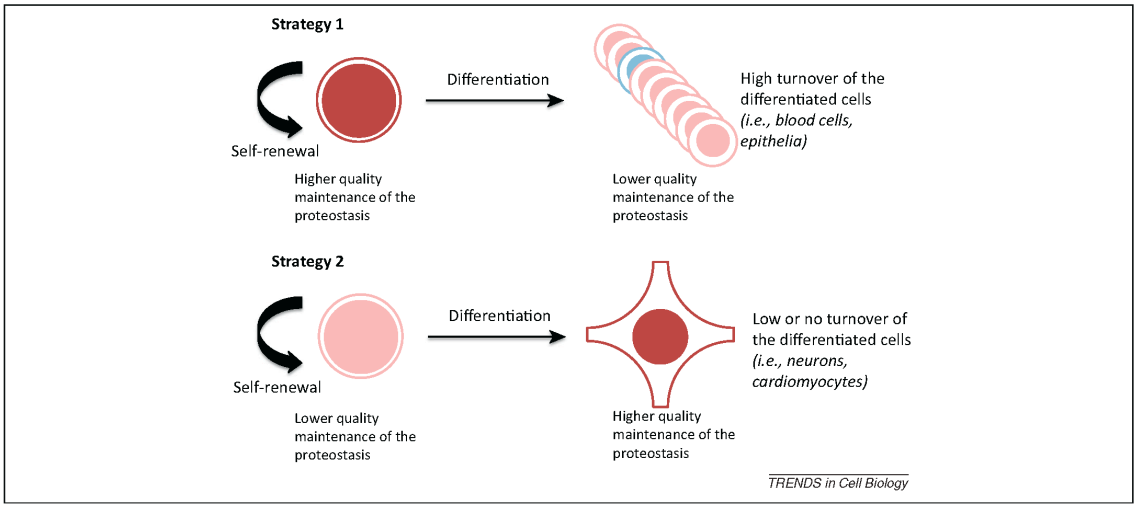

Figure 3. Proteostasis quality-maintenance strategies in stem cells. The model proposes two strategies: stem cells maintain high-quality proteostasis (darker red) and differentiated counterparts acquire higher-quality proteostasis (darker red) compared with the stem cell they are derived from (lighter red). We hypothesize that this might be important in the long-term versus short-term life of differentiated cells and the proliferation rate of stem cells. A compromised short-term differentiated cell (blue) will be diluted and turned over rapidly with limited consequences, whereas this might be more damaging with long-term and slowly regenerated differentiated cells.

Concluding remarks

Insights into the epigenome and transcriptome of stem cells have helped to define the mechanisms that regulate pluripotency or multipotency, differentiation, and cell reprogramming. Likewise, a better understanding of how stem cells regulate their proteostasis network will shed new light on stem cell biology and identity. In addition, it could have a great impact on cell therapy and organism health during the aging process.

ESCs exhibit higher levels of chaperones and higher antioxidant defense potential that could prevent the accumulation of misfolded proteins. ESCs also have increased proteasome activity. Whether this enhanced activity is necessary to potentiate the termination of damaged proteins or specific regulatory proteins remains unknown. Activation of the immunoproteasome and autophagy occurs during the early stages of ESC differentiation, providing a means to degrade damaged proteins and avoid passage to their differentiated counterparts. In adult somatic stem cells, the level of chaperones and autophagy activity depends on the stem cell type. Regardless of these differences, the proteostasis network critically impacts adult somatic stem cell function (Figure 2).

The differences in proteostasis pattern observed between stem cell types suggest distinctive mechanisms to ensure the functionality of their differentiated pools (Figure 2). Two strategies can be proposed (Figure 3): first, the stem cell maintains high-quality proteostasis; and second, differentiated counterparts acquire increased proteome surveillance compared with the stem cell they are derived from. This can be relevant regarding the number of divisions that stem cells undergo. Indeed, long-term stem cells that give rise to differentiated cells with a high turnover, such as blood cells and epithelia, seem to follow the first strategy. Having a high-quality pool of long-term and highly proliferative stem cells might be beneficial; if there is any impairment in the differentiated cells, it will be diluted and disappear rapidly, going unnoticed. The second strategy might be advantageous for differentiated cells such as neurons or cardiomyocytes that persist longer in the organism. Here, defects would have more severe consequences for the tissue and the organism.

Furthermore, a better knowledge of how stem cells maintain proteostasis may help us to understand how cancer stem cells are generated in an organism and to find specific treatments against these cells. The autophagy rate in breast cancer stem cells is higher than in parental cells [112]. When the autophagy gene Atg7 or Beclin1 is knocked down, self-renewal is impaired and its tumorigenicity reduced. By modulating ATP levels and the organization of subcellular structures, autophagy was shown to be important for glioblastoma stem cell migration and invasion [113]. Likewise, higher HSP levels have been reported in cancer stem cells [114]. HSP27 contributes to the maintenance of breast cancer stem cells [115,116] and DNAJB8 controls the early phase of renal cancer stem cell onset [117]. Because both stem cells and cancer stem cells rely on similar protective mechanisms, specifically targeting these pathways in cancer cells may be difficult. Therefore, deciphering the differences in proteostasis regulation between stem cells and cancer stem cells will be needed for efficient treatment implementation.

Acknowledgments

This work was supported by the Howard Hughes Medical Institute. David Vilchez is funded by the Deutsche Forschungsgemeinschaft (DFG) (CECAD).

References

1 Evans, M.J. and Kaufman, M.H. (1981) Establishment in culture of pluripotential cells from mouse embryos. *Nature* 292, 154–156
2 Thomson, J.A. *et al.* (1998) Embryonic stem cell lines derived from human blastocysts. *Science* 282, 1145–1147

3 Li, L. and Xie, T. (2005) Stem cell niche: structure and function. *Annu. Rev. Cell Dev. Biol.* 21, 605–631
4 Lopez-Otin, C. *et al.* (2013) The hallmarks of aging. *Cell* 153, 1194–1217
5 Signer, R.A. and Morrison, S.J. (2013) Mechanisms that regulate stem cell aging and life span. *Cell Stem Cell* 12, 152–165
6 Balch, W.E. *et al.* (2008) Adapting proteostasis for disease intervention. *Science* 319, 916–919
7 Powers, E.T. *et al.* (2009) Biological and chemical approaches to diseases of proteostasis deficiency. *Annu. Rev. Biochem.* 78, 959–991
8 Taylor, R.C. and Dillin, A. (2011) Aging as an event of proteostasis collapse. *Cold Spring Harb. Perspect. Biol.* 3, a004440
9 Gebauer, F. and Hentze, M.W. (2004) Molecular mechanisms of translational control. *Nat. Rev. Mol. Cell Biol.* 5, 827–835
10 Hartl, F.U. *et al.* (2011) Molecular chaperones in protein folding and proteostasis. *Nature* 475, 324–332
11 Morimoto, R.I. (2008) Proteotoxic stress and inducible chaperone networks in neurodegenerative disease and aging. *Genes Dev.* 22, 1427–1438
12 Finley, D. (2009) Recognition and processing of ubiquitin-protein conjugates by the proteasome. *Annu. Rev. Biochem.* 78, 477–513
13 Rubinsztein, D.C. *et al.* (2011) Autophagy and aging. *Cell* 146, 682–695
14 Tanaka, K. and Matsuda, N. (2013) Proteostasis and neurodegeneration: the roles of proteasomal degradation and autophagy. *Biochim. Biophys. Acta* http://dx.doi.org/10.1016/j.bbamcr.2013.03.012
15 Wong, E. and Cuervo, A.M. (2010) Integration of clearance mechanisms: the proteasome and autophagy. *Cold Spring Harb. Perspect. Biol.* 2, a006734
16 Gidalevitz, T. *et al.* (2011) The stress of protein misfolding: from single cells to multicellular organisms. *Cold Spring Harb. Perspect. Biol.* 3, a009704
17 Bence, N.F. *et al.* (2001) Impairment of the ubiquitin–proteasome system by protein aggregation. *Science* 292, 1552–1555
18 Bennett, E.J. *et al.* (2005) Global impairment of the ubiquitin–proteasome system by nuclear or cytoplasmic protein aggregates precedes inclusion body formation. *Mol. Cell* 17, 351–365
19 Bucciantini, M. *et al.* (2002) Inherent toxicity of aggregates implies a common mechanism for protein misfolding diseases. *Nature* 416, 507–511
20 Lindquist, S.L. and Kelly, J.W. (2011) Chemical and biological approaches for adapting proteostasis to ameliorate protein misfolding and aggregation diseases: progress and prognosis. *Cold Spring Harb. Perspect. Biol.* 3, a004507
21 Morimoto, R.I. and Cuervo, A.M. (2009) Protein homeostasis and aging: taking care of proteins from the cradle to the grave. *J. Gerontol. A: Biol. Sci. Med. Sci.* 64, 167–170
22 Vabulas, R.M. *et al.* (2010) Protein folding in the cytoplasm and the heat shock response. *Cold Spring Harb. Perspect. Biol.* 2, a004390
23 Aguilaniu, H. *et al.* (2003) Asymmetric inheritance of oxidatively damaged proteins during cytokinesis. *Science* 299, 1751–1753
24 Lindner, A.B. *et al.* (2008) Asymmetric segregation of protein aggregates is associated with cellular aging and rejuvenation. *Proc. Natl. Acad. Sci. U.S.A.* 105, 3076–3081
25 Selkoe, D.J. (2011) Alzheimer's disease. *Cold Spring Harb. Perspect. Biol.* 3, a004457
26 Bosco, D.A. *et al.* (2011) Proteostasis and movement disorders: Parkinson's disease and amyotrophic lateral sclerosis. *Cold Spring Harb. Perspect. Biol.* 3, a007500
27 Finkbeiner, S. (2011) Huntington's disease. *Cold Spring Harb. Perspect. Biol.* 3, a007476
28 Cohen, E. *et al.* (2009) Reduced IGF-1 signaling delays age-associated proteotoxicity in mice. *Cell* 139, 1157–1169
29 Vilchez, D. *et al.* (2012) RPN-6 determines C. elegans longevity under proteotoxic stress conditions. *Nature* 489, 263–268
30 Araki, K. and Nagata, K. (2011) Protein folding and quality control in the ER. *Cold Spring Harb. Perspect. Biol.* 3, a007526
31 Walter, P. and Ron, D. (2011) The unfolded protein response: from stress pathway to homeostatic regulation. *Science* 334, 1081–1086
32 Malhotra, J.D. and Kaufman, R.J. (2011) ER stress and its functional link to mitochondria: role in cell survival and death. *Cold Spring Harb. Perspect. Biol.* 3, a004424
33 Seo, A.Y. *et al.* (2010) New insights into the role of mitochondria in aging: mitochondrial dynamics and more. *J. Cell Sci.* 123, 2533–2542
34 Baker, M.J. *et al.* (2011) Quality control of mitochondrial proteostasis. *Cold Spring Harb. Perspect. Biol.* 3, a007559
35 Morimoto, R.I. (2011) The heat shock response: systems biology of proteotoxic stress in aging and disease. *Cold Spring Harb. Symp. Quant. Biol.* 76, 91–99
36 Saretzki, G. *et al.* (2004) Stress defense in murine embryonic stem cells is superior to that of various differentiated murine cells. *Stem Cells* 22, 962–971
37 Saretzki, G. *et al.* (2008) Downregulation of multiple stress defense mechanisms during differentiation of human embryonic stem cells. *Stem Cells* 26, 455–464
38 Schafer, F.Q. and Buettner, G.R. (2001) Redox environment of the cell as viewed through the redox state of the glutathione disulfide/glutathione couple. *Free Radic. Biol. Med.* 30, 1191–1212
39 Chuikov, S. *et al.* (2010) Prdm16 promotes stem cell maintenance in multiple tissues, partly by regulating oxidative stress. *Nat. Cell Biol.* 12, 999–1006
40 Liu, J. *et al.* (2009) Bmi1 regulates mitochondrial function and the DNA damage response pathway. *Nature* 459, 387–392
41 Paik, J.H. *et al.* (2009) FoxOs cooperatively regulate diverse pathways governing neural stem cell homeostasis. *Cell Stem Cell* 5, 540–553
42 Tothova, Z. *et al.* (2007) FoxOs are critical mediators of hematopoietic stem cell resistance to physiologic oxidative stress. *Cell* 128, 325–339
43 Juntilla, M.M. *et al.* (2010) AKT1 and AKT2 maintain hematopoietic stem cell function by regulating reactive oxygen species. *Blood* 115, 4030–4038
44 Le Belle, J.E. *et al.* (2011) Proliferative neural stem cells have high endogenous ROS levels that regulate self-renewal and neurogenesis in a PI3K/Akt-dependant manner. *Cell Stem Cell* 8, 59–71
45 Battersby, A. *et al.* (2007) Comparative proteomic analysis reveals differential expression of Hsp25 following the directed differentiation of mouse embryonic stem cells. *Biochim. Biophys. Acta* 1773, 147–156
46 Yang, J. *et al.* (2008) Neural differentiation and the attenuated heat shock response. *Brain Res.* 1203, 39–50
47 DeLany, J.P. *et al.* (2005) Proteomic analysis of primary cultures of human adipose-derived stem cells: modulation by adipogenesis. *Mol. Cell. Proteomics* 4, 731–740
48 Bradley, E. *et al.* (2012) Regulation of embryonic stem cell pluripotency by heat shock protein 90. *Stem Cells* 30, 1624–1633
49 Singh, B.N. *et al.* (2010) Ubiquitin–proteasome-mediated degradation and synthesis of MyoD is modulated by alphaB-crystallin, a small heat shock protein, during muscle differentiation. *Biochim. Biophys. Acta* 1803, 288–299
50 Matsui, H. *et al.* (2007) Cytokines direct the regulation of Bim mRNA stability by heat-shock cognate protein 70. *Mol. Cell* 25, 99–112
51 Ribeil, J.A. *et al.* (2007) Hsp70 regulates erythropoiesis by preventing caspase-3-mediated cleavage of GATA-1. *Nature* 445, 102–105
52 Zhang, K. *et al.* (2005) The unfolded protein response sensor IRE1alpha is required at 2 distinct steps in B cell lymphopoiesis. *J. Clin. Invest.* 115, 268–281
53 Iwakoshi, N.N. *et al.* (2003) The X-box binding protein-1 transcription factor is required for plasma cell differentiation and the unfolded protein response. *Immunol. Rev.* 194, 29–38
54 Cui, K. *et al.* (2000) Novel interaction between the transcription factor CHOP (GADD153) and the ribosomal protein FTE/S3a modulates erythropoiesis. *J. Biol. Chem.* 275, 7591–7596
55 Pereira, R.C. *et al.* (2004) CCAAT/enhancer binding protein homologous protein (DDIT3) induces osteoblastic cell differentiation. *Endocrinology* 145, 1952–1960
56 Skalet, A.H. *et al.* (2005) Rapid B cell receptor-induced unfolded protein response in nonsecretory B cells correlates with pro- versus antiapoptotic cell fate. *J. Biol. Chem.* 280, 39762–39771
57 Yang, L. *et al.* (2005) Multiple signals induce endoplasmic reticulum stress in both primary and immortalized chondrocytes resulting in loss of differentiation, impaired cell growth, and apoptosis. *J. Biol. Chem.* 280, 31156–31165
58 Heijmans, J. *et al.* (2013) ER stress causes rapid loss of intestinal epithelial stemness through activation of the unfolded protein response. *Cell Rep.* 3, 1128–1139
59 Tanaka, K. (2013) The proteasome: from basic mechanisms to emerging roles. *Keio J. Med.* 62, 1–12

60 Kisselev, A.F. and Goldberg, A.L. (2005) Monitoring activity and inhibition of 26S proteasomes with fluorogenic peptide substrates. *Methods Enzymol.* 398, 364–378
61 Buckley, S.M. *et al.* (2012) Regulation of pluripotency and cellular reprogramming by the ubiquitin–proteasome system. *Cell Stem Cell* 11, 783–798
62 Okita, Y. and Nakayama, K.I. (2012) UPS delivers pluripotency. *Cell Stem Cell* 11, 728–730
63 Vilchez, D. *et al.* (2012) Increased proteasome activity in human embryonic stem cells is regulated by PSMD11. *Nature* 489, 304–308
64 Assou, S. *et al.* (2009) A gene expression signature shared by human mature oocytes and embryonic stem cells. *BMC Genomics* 10, 10
65 Pathare, G.R. *et al.* (2012) The proteasomal subunit Rpn6 is a molecular clamp holding the core and regulatory subcomplexes together. *Proc. Natl. Acad. Sci. U.S.A.* 109, 149–154
66 Guan, K. *et al.* (2006) Pluripotency of spermatogonial stem cells from adult mouse testis. *Nature* 440, 1199–1203
67 Nicholas, C.R. *et al.* (2009) Transplantation directs oocyte maturation from embryonic stem cells and provides a therapeutic strategy for female infertility. *Hum. Mol. Genet.* 18, 4376–4389
68 Fredriksson, A. *et al.* (2012) Effects of aging and reproduction on protein quality control in soma and gametes of *Drosophila melanogaster*. *Aging Cell* 11, 634–643
69 Tsakiri, E.N. *et al.* (2013) Differential regulation of proteasome functionality in reproductive vs. somatic tissues of *Drosophila* during aging or oxidative stress. *FASEB J.* 27, 2407–2420
70 Hernebring, M. *et al.* (2006) Elimination of damaged proteins during differentiation of embryonic stem cells. *Proc. Natl. Acad. Sci. U.S.A.* 103, 7700–7705
71 Hernebring, M. *et al.* (2013) Removal of damaged proteins during ES cell fate specification requires the proteasome activator PA28. *Sci. Rep.* 3, 1381
72 Szutorisz, H. *et al.* (2006) The proteasome restricts permissive transcription at tissue-specific gene loci in embryonic stem cells. *Cell* 127, 1375–1388
73 Kirstein-Miles, J. *et al.* (2013) The nascent polypeptide-associated complex is a key regulator of proteostasis. *EMBO J.* 32, 1451–1468
74 Liu, B. *et al.* (2013) Cotranslational response to proteotoxic stress by elongation pausing of ribosomes. *Mol. Cell* 49, 453–463
75 Shalgi, R. *et al.* (2013) Widespread regulation of translation by elongation pausing in heat shock. *Mol. Cell* 49, 439–452
76 Tra, T. *et al.* (2011) Autophagy in human embryonic stem cells. *PLoS ONE* 6, e27485
77 Sanchez-Danes, A. *et al.* (2012) Disease-specific phenotypes in dopamine neurons from human iPS-based models of genetic and sporadic Parkinson's disease. *EMBO Mol. Med.* 4, 380–395
78 Oliver, L. *et al.* (2012) Basal autophagy decreased during the differentiation of human adult mesenchymal stem cells. *Stem Cells Dev.* 21, 2779–2788
79 Salemi, S. *et al.* (2012) Autophagy is required for self-renewal and differentiation of adult human stem cells. *Cell Res.* 22, 432–435
80 Liu, F. *et al.* (2010) FIP200 is required for the cell-autonomous maintenance of fetal hematopoietic stem cells. *Blood* 116, 4806–4814
81 Mortensen, M. *et al.* (2010) Loss of autophagy in erythroid cells leads to defective removal of mitochondria and severe anemia *in vivo*. *Proc. Natl. Acad. Sci. U.S.A.* 107, 832–837
82 Mortensen, M. *et al.* (2011) The autophagy protein Atg7 is essential for hematopoietic stem cell maintenance. *J. Exp. Med.* 208, 455–467
83 Mortensen, M. *et al.* (2011) Lack of autophagy in the hematopoietic system leads to loss of hematopoietic stem cell function and dysregulated myeloid proliferation. *Autophagy* 7, 1069–1070
84 Eijkelenboom, A. and Burgering, B.M. (2013) FOXOs: signalling integrators for homeostasis maintenance. *Nat. Rev. Mol. Cell Biol.* 14, 83–97
85 Warr, M.R. *et al.* (2013) FOXO3A directs a protective autophagy program in haematopoietic stem cells. *Nature* 494, 323–327
86 Liu, F. and Guan, J.L. (2011) FIP200, an essential component of mammalian autophagy is indispensible for fetal hematopoiesis. *Autophagy* 7, 229–230
87 Vazquez, P. *et al.* (2012) Atg5 and Ambra1 differentially modulate neurogenesis in neural stem cells. *Autophagy* 8, 187–199
88 Zhang, J. *et al.* (2012) FRS2alpha-mediated FGF signals suppress premature differentiation of cardiac stem cells through regulating autophagy activity. *Circ. Res.* 110, e29–e39
89 Zhang, J. *et al.* (2012) The fibroblast growth factor signaling axis controls cardiac stem cell differentiation through regulating autophagy. *Autophagy* 8, 690–691
90 Wang, C. *et al.* (2013) FIP200 is required for maintenance and differentiation of postnatal neural stem cells. *Nat. Neurosci.* 16, 532–542
91 Cohen, E. *et al.* (2006) Opposing activities protect against age-onset proteotoxicity. *Science* 313, 1604–1610
92 Bartke, A. (2008) Insulin and aging. *Cell Cycle* 7, 3338–3343
93 Panowski, S.H. and Dillin, A. (2009) Signals of youth: endocrine regulation of aging in *Caenorhabditis elegans*. *Trends Endocrinol. Metab.* 20, 259–264
94 Flachsbart, F. *et al.* (2009) Association of FOXO3A variation with human longevity confirmed in German centenarians. *Proc. Natl. Acad. Sci. U.S.A.* 106, 2700–2705
95 Salih, D.A. and Brunet, A. (2008) FoxO transcription factors in the maintenance of cellular homeostasis during aging. *Curr. Opin. Cell Biol.* 20, 126–136
96 Renault, V.M. *et al.* (2009) FoxO3 regulates neural stem cell homeostasis. *Cell Stem Cell* 5, 527–539
97 Yalcin, S. *et al.* (2008) Foxo3 is essential for the regulation of ataxia telangiectasia mutated and oxidative stress-mediated homeostasis of hematopoietic stem cells. *J. Biol. Chem.* 283, 25692–25705
98 Partridge, L. *et al.* (2005) Sex and death: what is the connection? *Cell* 120, 461–472
99 Kirkwood, T.B. (1977) Evolution of ageing. *Nature* 270, 301–304
100 Kenyon, C. (2010) A pathway that links reproductive status to lifespan in *Caenorhabditis elegans*. *Ann. N. Y. Acad. Sci.* 1204, 156–162
101 Shemesh, N. *et al.* (2013) Germline stem cell arrest inhibits the collapse of somatic proteostasis early in *Caenorhabditis elegans* adulthood. *Aging Cell* http://dx.doi.org/10.1111/acel.12110
102 Vilchez, D. *et al.* (2013) FOXO4 is necessary for neural differentiation of human embryonic stem cells. *Aging Cell* 12, 518–522
103 Zhang, X. *et al.* (2011) FOXO1 is an essential regulator of pluripotency in human embryonic stem cells. *Nat. Cell Biol.* http://dx.doi.org/10.1111/acel.12110
104 Webb, A.E. *et al.* (2013) FOXO3 shares common targets with ASCL1 genome-wide and inhibits ASCL1-dependent neurogenesis. *Cell Rep.* 4, 477–491
105 Fontana, L. *et al.* (2010) Extending healthy life span – from yeast to humans. *Science* 328, 321–326
106 Wullschleger, S. *et al.* (2006) TOR signaling in growth and metabolism. *Cell* 124, 471–484
107 Zid, B.M. *et al.* (2009) 4E-BP extends lifespan upon dietary restriction by enhancing mitochondrial activity in *Drosophila*. *Cell* 139, 149–160
108 Stanfel, M.N. *et al.* (2009) The TOR pathway comes of age. *Biochim. Biophys. Acta* 1790, 1067–1074
109 Yilmaz, O.H. *et al.* (2012) mTORC1 in the Paneth cell niche couples intestinal stem-cell function to calorie intake. *Nature* 486, 490–495
110 Cerletti, M. *et al.* (2012) Short-term calorie restriction enhances skeletal muscle stem cell function. *Cell Stem Cell* 10, 515–519
111 Park, H.R. and Lee, J. (2011) Neurogenic contributions made by dietary regulation to hippocampal neurogenesis. *Ann. N. Y. Acad. Sci.* 1229, 23–28
112 Gong, C. *et al.* (2013) Beclin 1 and autophagy are required for the tumorigenicity of breast cancer stem-like/progenitor cells. *Oncogene* 32, 2261–2272
113 Galavotti, S. *et al.* (2013) The autophagy-associated factors DRAM1 and p62 regulate cell migration and invasion in glioblastoma stem cells. *Oncogene* 32, 699–712
114 Bensaude, O. and Morange, M. (1983) Spontaneous high expression of heat-shock proteins in mouse embryonal carcinoma cells and ectoderm from day 8 mouse embryo. *EMBO J.* 2, 173–177
115 Lee, C.H. *et al.* (2012) Inhibition of heat shock protein (Hsp) 27 potentiates the suppressive effect of Hsp90 inhibitors in targeting breast cancer stem-like cells. *Biochimie* 94, 1382–1389

116 Wei, L. *et al.* (2011) Hsp27 participates in the maintenance of breast cancer stem cells through regulation of epithelial–mesenchymal transition and nuclear factor-kappaB. *Breast Cancer Res.* 13, R101
117 Nishizawa, S. *et al.* (2012) HSP DNAJB8 controls tumor-initiating ability in renal cancer stem-like cells. *Cancer Res.* 72, 2844–2854
118 Sharpless, N.E. and DePinho, R.A. (2007) How stem cells age and why this makes us grow old. *Nat. Rev. Mol. Cell Biol.* 8, 703–713
119 Shaw, A.C. *et al.* (2010) Aging of the innate immune system. *Curr. Opin. Immunol.* 22, 507–513
120 Kuhn, H.G. *et al.* (1996) Neurogenesis in the dentate gyrus of the adult rat: age-related decrease of neuronal progenitor proliferation. *J. Neurosci.* 16, 2027–2033
121 Maslov, A.Y. *et al.* (2004) Neural stem cell detection, characterization, and age-related changes in the subventricular zone of mice. *J. Neurosci.* 24, 1726–1733
122 Molofsky, A.V. *et al.* (2006) Increasing p16INK4a expression decreases forebrain progenitors and neurogenesis during ageing. *Nature* 443, 448–452
123 Wong, K.K. *et al.* (2003) Telomere dysfunction and Atm deficiency compromises organ homeostasis and accelerates ageing. *Nature* 421, 643–648
124 Spriggs, K.A. *et al.* (2010) Translational regulation of gene expression during conditions of cell stress. *Mol. Cell* 40, 228–237
125 Pellegrino, M.W. *et al.* (2013) Signaling the mitochondrial unfolded protein response. *Biochim. Biophys. Acta* 1833, 410–416

HSF-1–mediated cytoskeletal integrity determines thermotolerance and life span

Baird, N.A.*, Douglas, P.M.*, Simic, M.S., Grant, A.R., Moresco, J.J., Wolff, S.C., Yates, J.R., Manning, G., and Dillin, A. (2014). HSF-1–mediated cytoskeletal integrity determines thermotolerance and life span. **Science** *346*, 360–363.

* equal contributions

AGING

HSF-1–mediated cytoskeletal integrity determines thermotolerance and life span

Nathan A. Baird,[1]* Peter M. Douglas,[1]* Milos S. Simic,[1] Ana R. Grant,[2] James J. Moresco,[3] Suzanne C. Wolff,[1] John R. Yates III,[3] Gerard Manning,[4] Andrew Dillin[1]†

The conserved heat shock transcription factor–1 (HSF-1) is essential to cellular stress resistance and life-span determination. The canonical function of HSF-1 is to regulate a network of genes encoding molecular chaperones that protect proteins from damage caused by extrinsic environmental stress or intrinsic age-related deterioration. In *Caenorhabditis elegans*, we engineered a modified HSF-1 strain that increased stress resistance and longevity without enhanced chaperone induction. This health assurance acted through the regulation of the calcium-binding protein PAT-10. Loss of *pat-10* caused a collapse of the actin cytoskeleton, stress resistance, and life span. Furthermore, overexpression of *pat-10* increased actin filament stability, thermotolerance, and longevity, indicating that in addition to chaperone regulation, HSF-1 has a prominent role in cytoskeletal integrity, ensuring cellular function during stress and aging.

The survival of an organism is intricately linked to its ability to maintain cellular quality control, including organelle integrity, lipid homeostasis, proper protein folding, and cellular communication. The organismal response to unpredictable environmental changes is critical to mitigate damages caused by stress. Genes encoding the heat shock protein (HSP) family of molecular chaperones show the largest transcriptional increase in response to thermal stress, suggesting that these proteins are part of a fundamental defense against proteotoxic stress. Consistent with this hypothesis, ectopic expression of the master transcriptional regulator of HSPs, HSF-1, is sufficient to confer resistance to thermal stress and increase life span in the nematode *Caenorhabditis elegans* (*1*). Furthermore, *hsf-1* overexpression can alleviate toxicity associated with diseases caused by misfolded or aggregated proteins (*2*).

However, chaperones may be dispensable for thermotolerance and longevity. Neither a hypomorphic mutation of *hsf-1*, nor preventing the up-regulation of HSPs affects thermotolerance of *C. elegans* (*3*, *4*). However, other studies using the same *hsf-1* mutant show decreased heat resistance (*5*). The conflicting data may result from differences in experimental design, but it is clear that HSF-1 function is not fully explained by chaperones mediating stress resistance and life-span determination.

To test for protective mechanisms independent of enhancing chaperone induction, we generated

[1]Howard Hughes Medical Institute, University of California Berkeley, Berkeley, CA 94720, USA. [2]Department of Computational Medicine and Bioinformatics, University of Michigan Medical School, Ann Arbor, MI 48109, USA. [3]Scripps Research Institute, La Jolla, CA 92037, USA. [4]Genentech, South San Francisco, CA 94080, USA. *These authors contributed equally to this work. †Corresponding author. E-mail: dillin@berkeley.edu

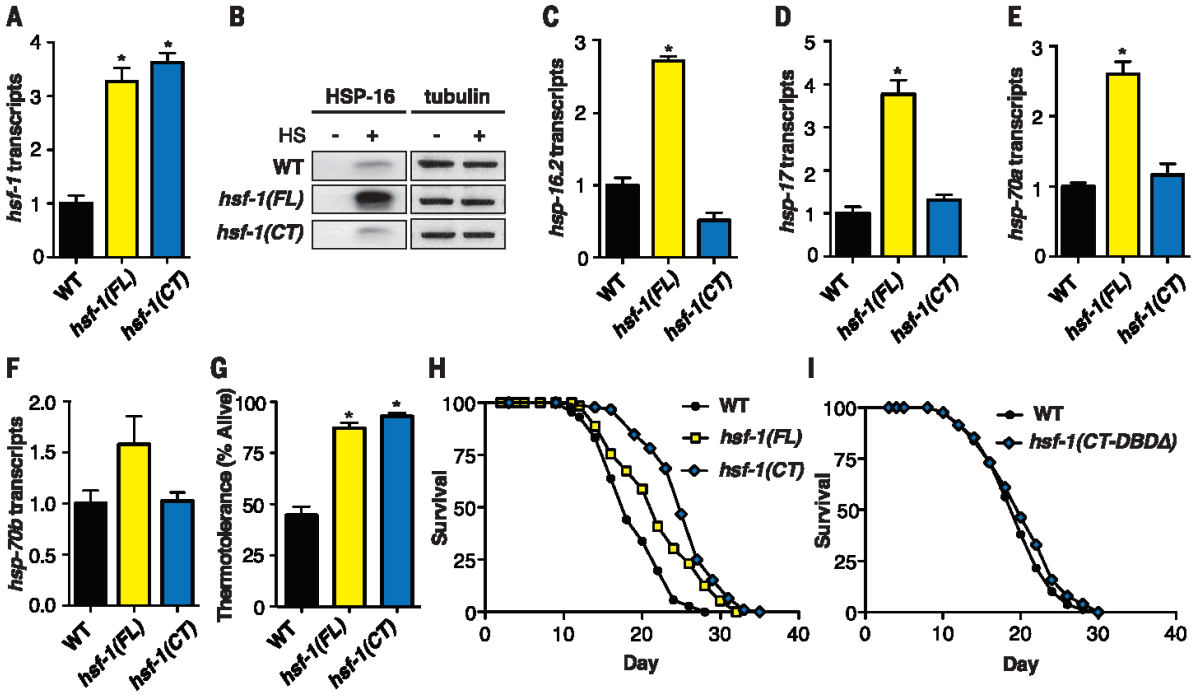

Fig. 1. *hsf-1(CT)* increases life span and thermotolerance without enhancing chaperone induction. (**A**) Equal overexpression of *hsf-1(FL)* and *hsf-1(CT)* determined by means of quantitative polymerase chain reaction (PCR). (**B**) Western blot of HSP-16 before and after heat shock (HS). (**C** to **F**) Quantitative PCR of (C) *hsp-16.2*, (D) *hsp-17*, (E) *hsp-70a* (C12C8.1), and (F) *hsp-70b* (F44E5.4) show enhanced induction in *hsf-1(FL)*. (**G**) Thermotolerance assay of WT, *hsf-1(FL)*, and *hsf-1(CT)* worms shifted from 20° to 34° for 13 hours. (**H**) Life-span survival curves of WT, *hsf-1(FL)*, and *hsf-1(CT)* strains. (**I**) Life-span survival curves of WT and *hsf-1(CT)* strains with the DNA-binding domain deleted (*CT-DBDΔ*). *$P < 0.005$; error bars indicate SEM.

Appendix- HSF-1–mediated cytoskeletal integrity determines thermotolerance and life span

transgenic nematodes overexpressing full-length *hsf-1* [*hsf-1(FL)*] or a *hsf-1* C-terminal truncation [*hsf-1(CT)*]. The *hsf-1(CT)* variant was designed to mimic the C-terminal missense mutation found in the *hsf-1(sy441)* mutant, a widely used allele that decreases stress-induced HSP transcription via the removal of a transactivation domain (*6*). *hsf-1(FL)* was overexpressed in the N2 wild-type (WT) background, and *hsf-1(CT)* was overexpressed in the *hsf-1(sy441)* mutant. Therefore, the *hsf-1(CT)* strain mirrored the overexpression of *hsf-1(FL)* but contained no endogenous copies of full-length *hsf-1* (fig. S1). Both transgenes were expressed threefold higher than endogenous *hsf-1* (Fig. 1A).

Analysis of protein and transcript abundance confirmed that overexpression of *hsf-1(FL)* enhanced heat-inducible expression of all HSPs tested, whereas *hsf-1(CT)* caused no difference from wild type (Fig. 1, B to F, and fig. S2). Yet, both *hsf-1(FL)* and *hsf-1(CT)* transgenic worms had increased thermotolerance and life span (Fig. 1, G and H). The life-span extension of *hsf-1(CT)* was unexpected, so we tested whether this phenotype was dependent on a functional DNA-binding domain. Increased longevity was abolished upon removal of the DNA binding domain (*hsf-1(CT-DBDΔ)*) (Fig. 1I). Thus, increased life span and thermotolerance did not correlate with enhanced HSP transcription.

To find other cellular networks that contribute to HSF-1–mediated stress resistance and longevity assurance, we performed quantitative transcriptomic and proteomic analyses comparing *hsf-1(FL)* and *hsf-1(CT)* strains with WT and *hsf-1(sy441)* strains. We filtered for transcripts or proteins that showed increased abundance, under basal or heat-stressed conditions, exclusively in the heat-protected strains (fig. S3). The 98 genes that met our filtering criteria were enriched for functions in development, cytoskeleton organization, complex assembly, and immune defense response (fig. S4).

Reduced expression of genes essential to thermotolerance should lower survival under heat stress. Therefore, we performed a RNA interference (RNAi)–based thermotolerance screen on the genes that passed our filtering criteria (fig. S5 and table S1). From the screen, we identified a troponin-like calcium-binding protein, PAT-10, as essential for thermotolerance (Fig. 2A). Transcription of *pat-10* was heat-inducible in all strains (Fig. 2B). Furthermore, *hsf-1* overexpression strains showed an increase in *pat-10* transcripts under basal and heat-stress conditions (Fig. 2B). After examining the upstream promoter region of *pat-10*, a putative binding site for HSF-1 (*7*, *8*) was identified within 500 base pairs of the transcription start site (fig. S6). Additionally, *hsf-1* RNAi blocked the up-regulation of *pat-10* upon heat shock (Fig. 2C). Therefore, *pat-10* appears to be a direct target of HSF-1 transcriptional regulation.

Because loss of *pat-10* expression reduced thermotolerance, we tested whether ectopic overexpression of *pat-10* could render animals more thermotolerant. Twofold overexpression of *pat-10* (Fig. 2D) significantly increased heat protection (Fig. 2E) and extended life span (Fig. 2F). Furthermore, RNAi of *pat-10* eliminated the increased thermotolerance (Fig. 2E) and life span (Fig. 2F) of the *pat-10* overexpression strain. *pat-10* RNAi also abolished the extended life spans of the *hsf-1* overexpression strains (Fig. 2G). Thus, *pat-10* appears to be necessary and sufficient for increased thermotolerance and longevity. Additionally, the beneficial effects of *pat-10* overexpression were not due to increases in basal HSP transcription (fig. S7). One function of *pat-10* is its role in the troponin complex (*9*–*11*), which is necessary for the contraction of body wall muscles.

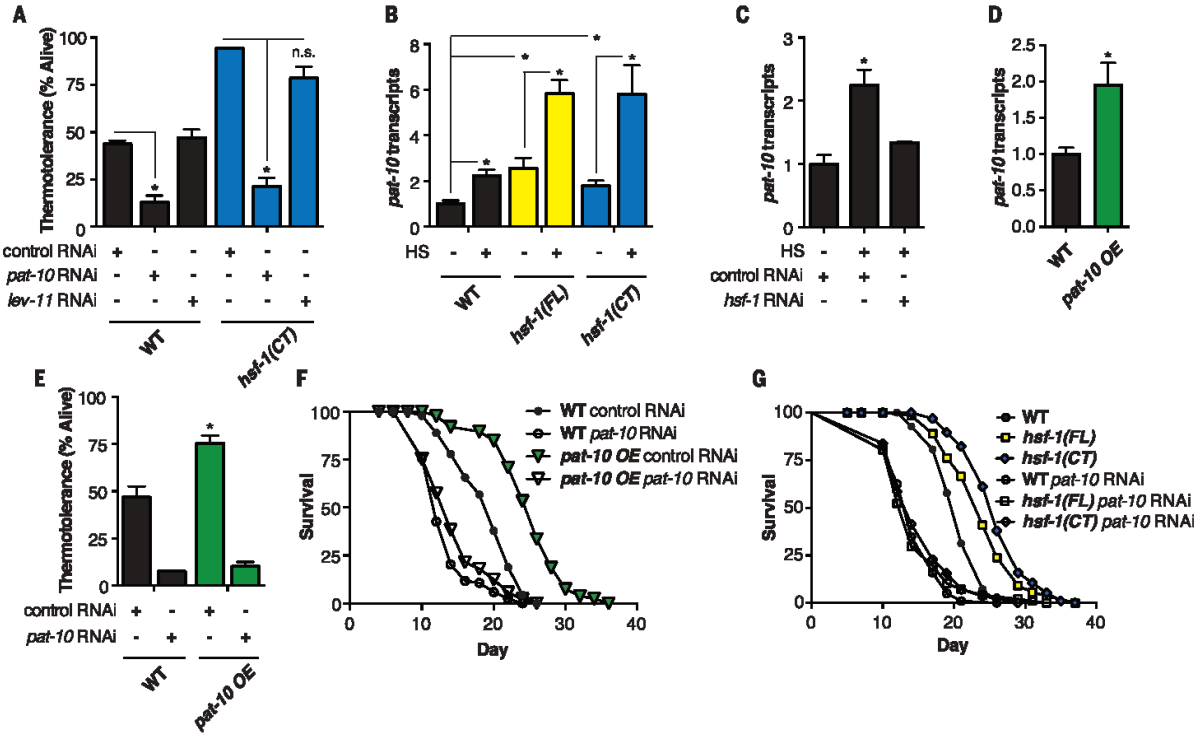

Fig. 2. *pat-10* is necessary and sufficient for thermotolerance and longevity. (**A**) Thermotolerance of WT and *hsf-1(CT)* strains treated with *pat-10* or *lev-11* RNAi. (**B**) Quantitative PCR of *pat-10* with and without heat shock (HS). (**C**) Effect of *hsf-1* RNAi on *pat-10* transcription upon heat shock. (**D**) Quantified expression of *pat-10* in the *pat-10 OE* strain. (**E**) Effect of *pat-10* overexpression or *pat-10* RNAi on thermotolerance. (**F**) Life-span survival curves for WT or *pat-10*–overexpressing strains treated with control or *pat-10* RNAi. (**G**) Life-span survival curves for WT or *hsf-1*–overexpressing strains treated with control or *pat-10* RNAi. *$P < 0.05$; error bars indicate SEM.

Appendix- HSF-1–mediated cytoskeletal integrity determines thermotolerance and life span

However, RNAi toward the worm homolog of tropomyosin—*lev-11*, a partner with *pat-10* in the troponin complex—did not affect heat resistance (Fig. 2A). This suggests that the role of *pat-10* in muscle contraction does not influence thermotolerance.

Loss of *pat-10* also disrupts actin cytoskeleton dynamics and endocytosis (*10*–*13*). To address these potential mechanisms of protection, we used green fluorescent protein (GFP)–labeled muscle filaments to assess actin organization (*14*). Upon heat shock, muscle filaments became unorganized and damaged, leading to impaired motility (Fig. 3, A and B). However, *pat-10* overexpression was sufficient to prevent heat-induced muscle and motility deterioration (Fig. 3, A and B). Furthermore, heat shock decreased the ratio of the filamentous (F) actin to globular (G) actin in WT worms, whereas the protected *pat-10* overexpression animals maintained F actin upon exposure to heat stress (Fig. 3C and fig. S8). With regard to aging, the ratio of F to G actin also decreased with age, and *pat-10* overexpression lessened this decline (Fig. 3D and fig. S8). Hence, under conditions of acute stress or gradual age-related deterioration, the integrity of the actin cytoskeleton is correlated with organismal survival, and overexpression of *pat-10* can abrogate the collapse of actin filaments.

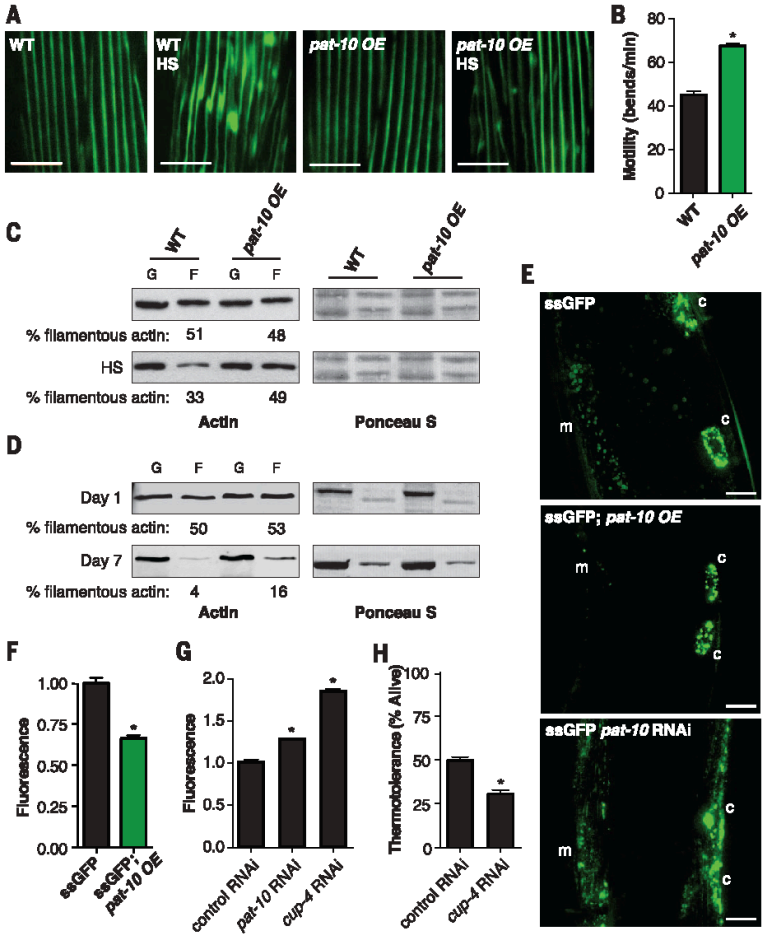

Fig. 3. *pat-10* overexpression improves actin cytoskeletal integrity and cellular trafficking. (**A**) GFP-tagged myosin heavy chain in muscle detected by means of fluorescent microscopy, before and after heat shock (HS). (**B**) Worm thrashes per minute in liquid to monitor motility after heat shock. (**C** and **D**) Abundance of filamentous (F) actin or globular (G) actin after (C) heat shock or (D) aging. Ponceau S staining shown as a loading control. (**E**) Microscopy showing ssGFP derived from muscle cells (m), endocytosed by coelomocytes (c) to be degraded. (**F**) Normalized ssGFP fluorescence quantification with and without *pat-10* overexpression. (**G**) Effect of blocking coelomocytic endocytosis on GFP fluorescence in the ssGFP reporter strain. (**H**) Thermotolerance after RNAi of *cup-4*. *$P < 0.05$; error bars indicate SEM. Scale bars, 10 μm.

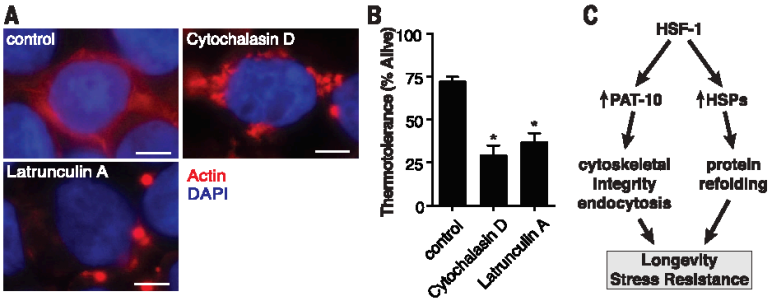

Fig. 4. Impairing actin dynamics decreases thermotolerance in mammalian cell culture. (**A**) Microscopy of HEK293T cells treated with cytochalasin D or latrunculin A [phalloidin stain of actin in red, 4′,6-diamidino-2-phenylindole (DAPI) stain of DNA in blue]. (**B**) Thermotolerance of HEK293T cells after a heat shock at 45°C for 2 hours treated with cytochalasin D or latrunculin A. (**C**) Proposed model of the dual pathways of HSF-1–mediated health assurance. *$P < 0.05$; error bars indicate SEM. Scale bars, 5 μm.

Appendix- HSF-1–mediated cytoskeletal integrity determines thermotolerance and life span

RNAi-induced loss of *pat-10* disrupts endocytosis through impairment of the actin cytoskeleton (*12*, *13*, *15*). To assay the role of *pat-10* in endocytosis, we used a secretion and endocytosis reporter designed to actively secrete GFP (ssGFP) from muscle cells into the pseudocoelomic fluid, where it is endocytosed by the coelomocyte cells and degraded (fig. S9A) (*16*). Therefore, the ssGFP reports upon effective muscular secretion and endocytosis by coelomocytes. Fitting the hypothesis that *pat-10* overexpression improves transport and cellular processing through improved subcellular scaffolding, the *pat-10 OE* strain had a decrease in overall ssGFP fluorescence (Fig. 3, E and F). The decrease in ssGFP resulted from improved secretion and uptake, as shown by the absence of fluorescence in the muscle and pseudocoelomic fluid (Fig. 3E). This decrease was not due to an overall decrease in expression of GFP (fig. S9B). Conversely, RNAi of *pat-10* increased overall fluorescence through decreased muscle secretion and coelomocytic endocytosis (Fig. 3, E and G). To fully block coelomocytic uptake and degradation of ssGFP, RNAi of *cup-4*, a ligand-gated ion channel required in endocytosis (*17*), showed an even higher increase in fluorescence (Fig. 3G) and also reduced thermotolerance in the wild type (Fig. 3H). Collectively, these data indicate *pat-10* has an active role in cytoskeletal maintenance, which is critical to cellular transport.

To test for conservation, we disrupted the actin cytoskeleton in human embryonic kidney (HEK) 293T cells using cytochalasin D, which blocks the addition of actin monomers to filaments (*18*), or latrunculin A, which binds actin monomers and prevents polymerization (Fig. 4A) (*19*). Inhibiting filamentous actin formation with either cytochalasin D or latrunculin A significantly reduced thermotolerance in human cells without causing death at permissive temperatures (Fig. 4B and fig. S10). Similar to our *C. elegans* data, these findings reiterate the importance of the actin cytoskeleton during times of cellular stress.

Elevated levels of *hsf-1* have been shown to benefit multiple organisms, yet its oncogenic properties are a major therapeutic drawback (*20*, *21*). Because the inducible chaperone network promotes survival and proliferation of metastasizing cells (*22*), the ability to harness protective, non-chaperone components within the HSF-1 signal transduction cascade appears essential for future drug development. Identification of *pat-10* as a modifier of thermotolerance and longevity may apply to mammalian systems without the typical oncogenic dangers associated with increased chaperone levels.

The *hsf-1(CT)* strain was still able to mount a transcriptional response to heat shock, albeit reduced in complexity of *hsf-1(FL)*. The molecular mechanism remains unclear by which *hsf-1(CT)* regulates transcription without the C-terminal activation domain, but possible explanations include HSF-1 containing multiple activation domains. Alternatively, the *hsf-1(CT)* modification may alter affinities to DNA-binding sites or different cofactors, which would modify the transcriptional profile.

Our findings underscore the importance of maintaining filamentous actin, as opposed to total levels of actin. We propose a model in which HSF-1 regulates chaperones and actin cytoskeletal genes in parallel to promote thermotolerance and longevity (Fig. 4C). In the absence of chaperone induction, stabilization of the actin cytoskeleton is sufficient to promote survival under conditions of cellular stress and aging.

REFERENCES AND NOTES

1. A.-L. Hsu, C. T. Murphy, C. Kenyon, *Science* **300**, 1142–1145 (2003).
2. M. Fujimoto *et al.*, *J. Biol. Chem.* **280**, 34908–34916 (2005).
3. G. McColl *et al.*, *Cell Metab.* **12**, 260–272 (2010).
4. N. Kourtis, V. Nikoletopoulou, N. Tavernarakis, *Nature* **490**, 213–218 (2012).
5. V. Prahlad, T. Cornelius, R. I. Morimoto, *Science* **320**, 811–814 (2008).
6. Y. M. Hajdu-Cronin, W. J. Chen, P. W. Sternberg, *Genetics* **168**, 1937–1949 (2004).
7. P. E. Kroeger, R. I. Morimoto, *Mol. Cell. Biol.* **14**, 7592–7603 (1994).
8. N. D. Trinklein, J. I. Murray, S. J. Hartman, D. Botstein, R. M. Myers, *Mol. Biol. Cell* **15**, 1254–1261 (2004).
9. H. Terami *et al.*, *J. Cell Biol.* **146**, 193–202 (1999).
10. K. Ono, S. Ono, *Mol. Biol. Cell* **15**, 2782–2793 (2004).
11. T. Obinata, K. Ono, S. Ono, *J. Cell Sci.* **123**, 1557–1566 (2010).
12. Z. Balklava, S. Pant, H. Fares, B. D. Grant, *Nat. Cell Biol.* **9**, 1066–1073 (2007).
13. T. Kuwahara *et al.*, *Hum. Mol. Genet.* **17**, 2997–3009 (2008).
14. L. A. Herndon *et al.*, *Nature* **419**, 808–814 (2002).
15. W. Greene, S.-J. Gao, *PLOS Pathog.* **5**, e1000512 (2009).
16. H. Fares, I. Greenwald, *Nat. Genet.* **28**, 64–68 (2001).
17. A. Patton *et al.*, *Curr. Biol.* **15**, 1045–1050 (2005).
18. J. F. Casella, M. D. Flanagan, S. Lin, *Nature* **293**, 302–305 (1981).
19. I. Spector, N. R. Shochet, Y. Kashman, A. Groweiss, *Science* **219**, 493–495 (1983).
20. L. Whitesell, S. Lindquist, *Expert Opin. Ther. Targets* **13**, 469–478 (2009).
21. C. H. Nguyen *et al.*, *Biochem. J.* **452**, 321–329 (2013).
22. D. R. Ciocca, A. P. Arrigo, S. K. Calderwood, *Arch. Toxicol.* **87**, 19–48 (2013).

ACKNOWLEDGMENTS

Bioinformatic analysis is included in the supplementary materials. The following funding sources supported this research: Howard Hughes Medical Institute, National Center for Research Resources (5P41RR011823-17), National Institute of General Medical Sciences (8 P41 GM103533-17), and National Institute on Aging (R01AG027463-04). N.A.B. was funded by a postdoctoral fellowship to the Salk Center for Nutritional Genomics from the Leona M. & Harry B. Helmsley Charitable Trust; P.M.D. was funded by George E. Hewitt Foundation for Medical Research and National Institute of Aging (1K99AG042495-01A1). We thank the laboratory of G. Lithgow for generously sharing the HSP-16 antibody and J. Durieux for helping design figure illustrations. Some of the nematode strains used in this work were provided by the *Caenorhabditis* Genetics Center (University of Minnesota), which is supported by the NIH–Office of Research Infrastructure Programs (P40 OD010440).

SUPPLEMENTARY MATERIALS

www.sciencemag.org/content/346/6207/360/suppl/DC1
Materials and Methods
Figs. S1 to S10
Tables S1
References (*23*–*40*)

10 March 2014; accepted 13 August 2014
10.1126/science.1253168

AUTOIMMUNITY

Detection of T cell responses to a ubiquitous cellular protein in autoimmune disease

Yoshinaga Ito,[1] Motomu Hashimoto,[1,2,3,4]* Keiji Hirota,[2]* Naganari Ohkura,[2,5] Hiromasa Morikawa,[2] Hiroyoshi Nishikawa,[2] Atsushi Tanaka,[2,5] Moritoshi Furu,[3,6] Hiromu Ito,[3,6] Takao Fujii,[3,4] Takashi Nomura,[1] Sayuri Yamazaki,[7] Akimichi Morita,[7] Dario A. A. Vignali,[8,9] John W. Kappler,[10,11] Shuichi Matsuda,[6] Tsuneyo Mimori,[4] Noriko Sakaguchi,[2] Shimon Sakaguchi[1,2,12]†

T cells that mediate autoimmune diseases such as rheumatoid arthritis (RA) are difficult to characterize because they are likely to be deleted or inactivated in the thymus if the self antigens they recognize are ubiquitously expressed. One way to obtain and analyze these autoimmune T cells is to alter T cell receptor (TCR) signaling in developing T cells to change their sensitivity to thymic negative selection, thereby allowing their thymic production. From mice thus engineered to generate T cells mediating autoimmune arthritis, we isolated arthritogenic TCRs and characterized the self antigens they recognized. One of them was the ubiquitously expressed 60S ribosomal protein L23a (RPL23A), with which T cells and autoantibodies from RA patients reacted. This strategy may improve our understanding of the underlying drivers of autoimmunity.

T cells mediate a variety of autoimmune diseases (*1*, *2*), likely through the recognition of self antigens. However, identification of the self antigens targeted by T cells in systemic autoimmune diseases such as rheumatoid arthritis (RA) has been technically difficult (*3*–*5*). This is because pathogenic T cells expressing high-affinity T cell receptors (TCRs) for ubiquitous self antigens may be largely deleted (i.e., negatively selected) in the thymus and

HSF-1–mediated cytoskeletal integrity determines thermotolerance and life span
Nathan A. Baird *et al.*
Science **346**, 360 (2014);
DOI: 10.1126/science.1253168

Heterotypic Signals from Neural HSF-1 Separate Thermotolerance from Longevity

Douglas, P.M.*, Baird, N.A.*, Simic, M.S., Uhlein, S., McCormick, M.A., Wolff, S.C., Kennedy, B.K., and Dillin, A. (2015). Heterotypic Signals from Neural HSF-1 Separate Thermotolerance from Longevity. **Cell Rep**. *12*, 1196–1204.

* equal contributions

Cell Reports

Article

Heterotypic Signals from Neural HSF-1 Separate Thermotolerance from Longevity

Graphical Abstract

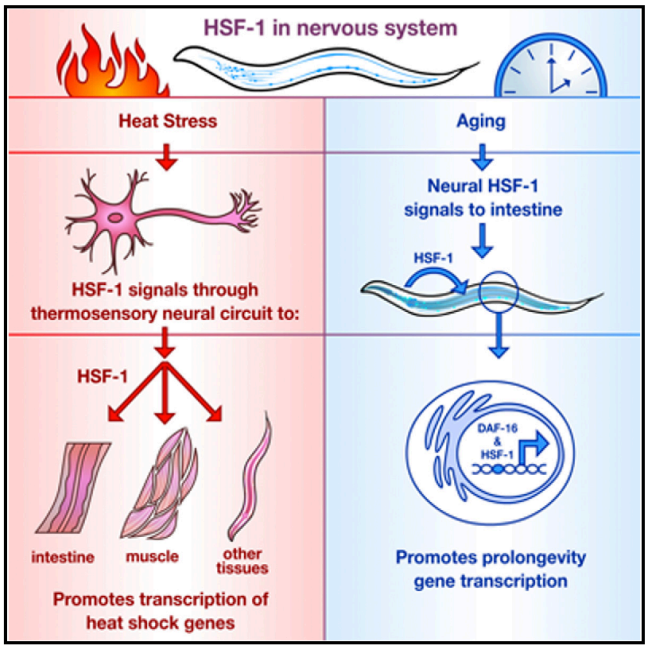

Highlights

- HSF-1 in the nervous system increases longevity and thermotolerance in *C. elegans*
- Heat protection by neural HSF-1 uses the thermosensory neural circuit, but not DAF-16
- Age determination by neural HSF-1 requires the FOXO, DAF-16, in the intestine
- Distinct signals by neural HSF-1 separate age regulation from thermal protection

Authors

Peter M. Douglas, Nathan A. Baird, Milos S. Simic, ..., Suzanne C. Wolff, Brian K. Kennedy, Andrew Dillin

Correspondence

dillin@berkeley.edu

In Brief

The heat shock transcription factor, HSF-1, regulates lifespan and stress resistance in *C. elegans*. Douglas et al. find that HSF-1 acts in neurons to emit divergent signals that independently regulate aging and thermotolerance. Thus, a single transcription factor can act within different neurons to modulate distinct protective responses in peripheral tissues.

Douglas et al., 2015, Cell Reports *12*, 1196–1204
August 18, 2015 ©2015 The Authors
http://dx.doi.org/10.1016/j.celrep.2015.07.026

OPEN ACCESS CellPress

Cell Reports
Article

Heterotypic Signals from Neural HSF-1 Separate Thermotolerance from Longevity

Peter M. Douglas,[1,4,5] Nathan A. Baird,[1,5] Milos S. Simic,[1] Sarah Uhlein,[1] Mark A. McCormick,[2] Suzanne C. Wolff,[1] Brian K. Kennedy,[2,3] and Andrew Dillin[1,*]
[1]Howard Hughes Medical Institute, University of California, Berkeley, Berkeley, CA 94720, USA
[2]The Buck Institute for Research on Aging, Novato, CA 94945, USA
[3]Department of Biochemistry, University of Washington, Seattle, WA 98195, USA
[4]Present address: Department of Molecular Biology, University of Texas Southwestern Medical Center, Dallas, TX 75390, USA
[5]Co-first author
*Correspondence: dillin@berkeley.edu
http://dx.doi.org/10.1016/j.celrep.2015.07.026

SUMMARY

Integrating stress responses across tissues is essential for the survival of multicellular organisms. The metazoan nervous system can sense protein-misfolding stress arising in different subcellular compartments and initiate cytoprotective transcriptional responses in the periphery. Several subcellular compartments possess a homotypic signal whereby the respective compartment relies on a single signaling mechanism to convey information within the affected cell to the same stress-responsive pathway in peripheral tissues. In contrast, we find that the heat shock transcription factor, HSF-1, specifies its mode of transcellular protection via two distinct signaling pathways. Upon thermal stress, neural HSF-1 primes peripheral tissues through the thermosensory neural circuit to mount a heat shock response. Independent of this thermosensory circuit, neural HSF-1 activates the FOXO transcription factor, DAF-16, in the periphery and prolongs lifespan. Thus a single transcription factor can coordinate different stress response pathways to specify its mode of protection against changing environmental conditions.

INTRODUCTION

The long-term health of an organism is linked to its ability to recognize and respond to stresses that arise in its environment. Across evolutionary spectra, organisms have developed complex and highly specialized defense pathways that become transcriptionally activated during times of stress. Often, diverse stress stimuli initiate distinct transcriptional signatures that activate protective and adaptive genes to defend against environmental challenges and restore homeostasis. In metazoa, the upregulation of stress response pathways also requires the coordinated activation of stress response machinery across multiple tissues. Consequently, a hierarchical mode of tissue regulation has evolved in which particular cell types can act as master regulators, initiating protective pathways in peripheral tissues (Wolff et al., 2014).

Organisms are frequently subjected to acute challenges that require a rapid response to potentially lethal conditions. These transient stresses elicit a dramatic cellular reaction with a rewiring of gene expression and a temporary suspension of normal cellular function. Conversely, organisms regularly encounter chronic insults that are not lethal even after long exposures. These prolonged stresses initiate distinct and more-sustained responses that allow for the continuance of most normal cellular functions. The cumulative effect of chronic stress over the lifetime of the organism is known to play a causative role in the onset and severity of many age-related diseases (Failla, 1958; Harman, 1956; Orgel, 1963). However, it is unclear how acute stress responses can alleviate the negative effects of the aging process (Lithgow et al., 1995).

Thermal adaptation in metazoans requires the perception, communication, and initiation of a response across the entire organism. The transcription factor HSF-1 is the key regulator of the cellular and organismal response to heat stress and is conserved in all eukaryotes. It is well-established that HSF-1 mediates a protective transcriptional and translational response to acute heat stress through the induced expression of molecular chaperones (Morimoto, 2008). More recently, it has been shown in the nematode worm that *hsf-1* overexpression in all tissues retards the aging process (Hsu et al., 2003). Thus, mediating stress response pathways by HSF-1 protects against both acute thermal stress and the chronic stresses associated with aging.

In nematodes, thermal adaptation is regulated by a subset of sensory neurons that activate the heat shock response in peripheral tissues (Prahlad et al., 2008). However, the role that HSF-1 plays within the nervous system is not well defined. It is also not clear whether the same sensory neural circuit that controls the heat shock response also controls processes of aging that are tightly associated with heat stress resistance.

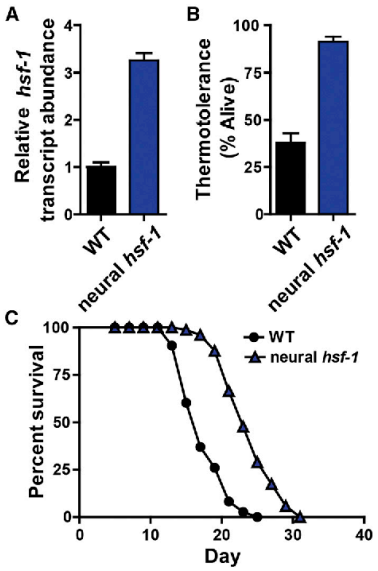

Figure 1. Neural Overexpression of *hsf-1* Protects *C. elegans* against Heat Stress and Aging

(A) Transcript abundance of *hsf-1* determined by quantitative RT-PCR analysis of wild-type (N2) and *rab-3p*::*hsf-1* transgenic animals (AGD1289). Error bars represent the SEM.

(B) Thermotolerance of wild-type and *rab-3p*::*hsf-1* transgenic worms shifted from permissive (20°) to heat shock (34°) temperatures for 14 hr. Error bars represent the SEM.

(C) Lifespan survival curves of wild-type and *rab-3p*::*hsf-1* transgenic strains at permissive temperatures (20°). Lifespan statistics are found in Table 1.

RESULTS

Neural Overexpression of *hsf-1* Promotes Heat Stress Resistance and Longevity

To explore these questions, we examined whether increasing *hsf-1* levels exclusively in the worm nervous system was sufficient to mediate protection against acute thermal stress and the aging process. Transgenic worms were generated that ectopically overexpressed *hsf-1* throughout the nervous system (Figures 1A and S1A–S1C). This level of *hsf-1* overexpression in neurons was sufficient to extend worm lifespan and protect against heat shock treatments (Figures 1B, 1C, S1D, and S1E; Table 1).

To gain insight into the neural-signaling pathways responsible for thermotolerance and longevity assurance, heat-shock-responsive transcriptional targets were examined under conditions of either acute heat stress or aging. We first utilized a transgenic reporter worm that expresses GFP under the promoter of the HSF-1 target gene, *hsp-16.2*, a member of the alpha β crystalline family of small chaperones (Link et al., 1999). Upon application of heat stress, animals robustly induced the expression of GFP driven by the *hsp-16.2* promoter compared to non-heat-treated worms (Figure 2A). Elevating neural *hsf-1* expression enhances the heat shock response throughout all worm tissues. These results strongly suggest that HSF-1 activity in neurons communicates to peripheral tissues and enables a more-robust transcriptional response to heat stress. Through large-particle flow cytometry, fluorescent quantification of individual worms reveals that heat shock induces expression of *hsp-16.2p*::*GFP* over 2-fold higher in worms that overexpressed *hsf-1* in the nervous system (Figures 2B and S2A). Similar increases of endogenous *hsp-16.2*, *hsp70a*, and *hsp-70b* transcript levels were observed upon heat shock in worms overexpressing neural *hsf-1* (Figures 2C, S2B, and S2C). Similar expression patterns of HSP-16 protein levels were also observed (Figure 2D). Genome-wide transcriptomics further confirmed that *hsf-1* overexpression in the nervous system bolsters transcription of numerous heat-responsive genes compared to wild-type animals (Figure S2D). The ability of worms overexpressing neural *hsf-1* to mount a more-robust heat shock response in peripheral tissues is consistent with the hypothesis that thermal protection is conferred by the heat shock response.

Loss of the Thermosensory Neural Circuit Disrupts Thermotolerance, but Not Longevity

We examined the role that heat-inducible chaperones might play in lifespan determination when *hsf-1* is overexpressed in the nervous system. We predicted that induction of heat-responsive genes would be correlated with neural *hsf-1* overexpression. Perplexingly, only minor differences in heat-responsive elements were observed at permissive temperatures between control animals and those overexpressing neural *hsf-1* (Figures 2B–2D and S2B–S2D). Thus, elevating *hsf-1* levels in the nervous system confers longevity without induction of the canonical heat-shock-responsive chaperones. Furthermore, RNAi knockdown of *hsp-16* expression, previously linked to age determination (Walker and Lithgow, 2003), did not alter lifespan extension by neural *hsf-1* (Figure S3A; Table 1). These data suggest that *hsf-1* overexpression elicits a divergent pathway in response to the aging process. Similar responses have been reported for HSF-1 in the context of reduced insulin/IGF-1 signaling (Hsu et al., 2003).

Because lifespan extension and thermotolerance appear divergent, we speculated that mutations might exist that abolish thermal protection but retain lifespan extension. To test this hypothesis, the thermosensory neural circuit was disrupted and the ability of neural *hsf-1* overexpression to enhance heat tolerance and extend lifespan was assessed. Genetic ablation of the AIY interneuron through a *ttx-3* mutation severs the thermosensory neural circuit and dampens the activation of heat shock responders in peripheral tissues (Prahlad et al., 2008). As expected, in the *ttx-3* mutant background, neural *hsf-1* overexpression no longer enhanced heat tolerance (Figure 2E). Surprisingly, neural *hsf-1* overexpression was still capable of prolonging lifespan in the *ttx-3* mutant (Figure 2F; Table 1). Thus, an intact thermosensory circuit is required for neural *hsf-1*-overexpressing worms to protect against heat stress but is dispensable for age regulation. More importantly, these data challenge the idea that HSF-1 regulates the aging process through the same heat shock response mechanisms and suggest that HSF-1 initiates an alternative transcriptional pathway to combat the stress of aging.

Table 1. Statistical Analysis of *C. elegans* Lifespan Data

Figure	Strain, Treatment	Mean Lifespan ± SEM (Median Lifespan in Days)	75th % (Day)	Observed/Total	% Lifespan Increase	p Value Log Rank (Mendel-Cox)
1C	N2	17.3 + 0.4 (17)	22	88/100		
1C	AGD1289 (neural *hsf-1*)	23.1 + 0.4 (24)	27	68/101	33.5	<0.0001
2F	AGD1008 non-transgenic	18.0 + 0.4 (18)	20	69/86		
2F	AGD1008 (neural *hsf-1*)	23.2 + 0.5 (24)	26	58/88	28.8	<0.0001
2F	*ttx-3*(*ks5*)	17.5 + 0.4 (18)	20	88/96	2.8	0.7231
2F	AGD1449 (neural *hsf-1 ttx-3*(*ks5*))	22.0 + 0.6 (22)	24	59/85	22.2	<0.0001
3D	N2	17.5 + 0.4 (17)	21	73/100		
3D	AGD1289 (neural *hsf-1*)	23.9 + 0.4 (23)	27	70/103	36.6	<0.0001
3D	*daf-16*(*mu86*)	15.8 + 0.4 (15)	19	61/100	−9.7	0.0022
3D	AGD1217 (neural *hsf-1*, *daf-16*(*mu86*))	16.6 + 0.3 (17)	19	72/100	−5.1	0.0578
4A	AGD1272 (neural *daf-16*)	18.7 + 0.4 (19)	22	68/108		
4A	AGD1273 (neural *daf-16*, neural *hsf-1*)	18.2 + 0.6 (17)	22	57/105	−2.6	0.6775
4B	AGD1276 (intestinal *daf-16*)	16.7 + 0.5 (17)	19	53/104		
4B	AGD1277 (intestinal *daf-16*, neural *hsf-1*)	22.7 + 0.5 (22)	26	51/110	35.9	<0.0001
4C	AGD1278 (muscle *daf-16*)	16.8 + 0.5 (17)	19	71/107		
4C	AGD1279 (muscle *daf-16*, neural *hsf-1*)	18.5 + 0.6 (19)	22	52/94	10.1	0.0429
5A	N2	18.5 + 0.2 (18)	20	90/114		
5A	AGD1289 (neural *hsf-1*)	27.6 + 0.4 (28)	31	113/123	51.9	<0.0001
5A	*hsf-1*(*sy441*)	16.8 + 0.2 (18)	18	100/114		
5A	AGD1471 (*hsf-1*(*sy441*), neural *hsf-1*)	18.4 + 0.2 (18)	20	91/120	9.5	<0.0001
S1D	N2	17.1 + 0.4 (16)	20	76/102		
S1D	AGD1053 (neural *hsf-1*)	21.2 + 0.6 (20)	25	72/100	24	<0.0001
S1D	AGD1054 (neural *hsf-1*)	21.4 + 0.4 (22)	25	76/100	25.2	<0.0001
S1E	N2	19.1 + 0.5 (20)	22	79/102		
S1E	AGD1441 (neural *hsf-1*)	22.2 + 0.7 (22)	26	62/78	16.2	0.0002
S3A	N2, vector RNAi	18.5 + 0.3 (19)	21	83/109		
S3A	AGD1289 (neural *hsf-1*), vector RNAi	23.0 + 0.3 (22)	24	94/113	24.3	<0.0001
S3A	N2, *hsp16.1* RNAi	19.6 + 0.3 (19)	22	92/105		
S3A	AGD1289 (neural *hsf-1*), *hsp-16.1* RNAi	23.5 + 0.3 (24)	26	95/106	19.9	<0.0001
S3B	N2, vector RNAi	19.3 + 0.4 (19)	22	68/103		
S3B	AGD1289 (neural *hsf-1*), vector RNAi	23.7 + 0.4 (25)	25	74/111	22.8	<0.0001
S3B	N2, *pha-4* RNAi	17.6 + 0.5 (19)	19	43/104		
S3B	AGD1289 (neural *hsf-1*), *pha-4* RNAi	22.9 + 0.4 (22)	25	77/103	30.1	<0.0001
S3C–S3E	N2, vector RNAi	17.0 + 0.4 (16)	20	90/108		
S3C–S3E	AGD1289 (neural *hsf-1*), vector RNAi	22.4 + 0.3 (22)	24	57/105	31.8	<0.0001
S3C	N2, *xbp-1* RNAi	18.6 + 0.4 (18)	22	85/98		
S3C	AGD1289 (neural *hsf-1*), *xbp-1* RNAi	23.2 + 0.4 (24)	26	63/98	24.7	<0.0001
S3D	N2, *skn-1* RNAi	15.3 + 0.2 (16)	16	89/98		
S3D	AGD1289 (neural *hsf-1*), *skn-1* RNAi	22.2 + 0.3 (22)	26	85/108	45.1	<0.0001
S3E	N2, *ubl-5* RNAi	17.1 + 0.4 (18)	20	91/100		
S3E	AGD1289 (neural *hsf-1*), *ubl-5* RNAi	21.0 + 0.4 (20)	24	67/91	22.8	<0.0001

HSF-1 Signals Heterotypically to DAF-16 in the Periphery for Increased Longevity

Intrigued by the possible separation of thermotolerance and aging, we sought to identify alternative transcriptional pathways that regulate aging independently of the heat stress response. To gain insight into alternate pathways, we analyzed genes that were significantly upregulated in multiple long-lived, *hsf-1*-overexpressing strains (Baird et al., 2014). Promoter analysis was performed on these gene data sets to identify possible transcription-factor-binding elements associated with an alternative cellular process or pathway. As expected, many of the promoters contained HSEs (heat shock elements). We also

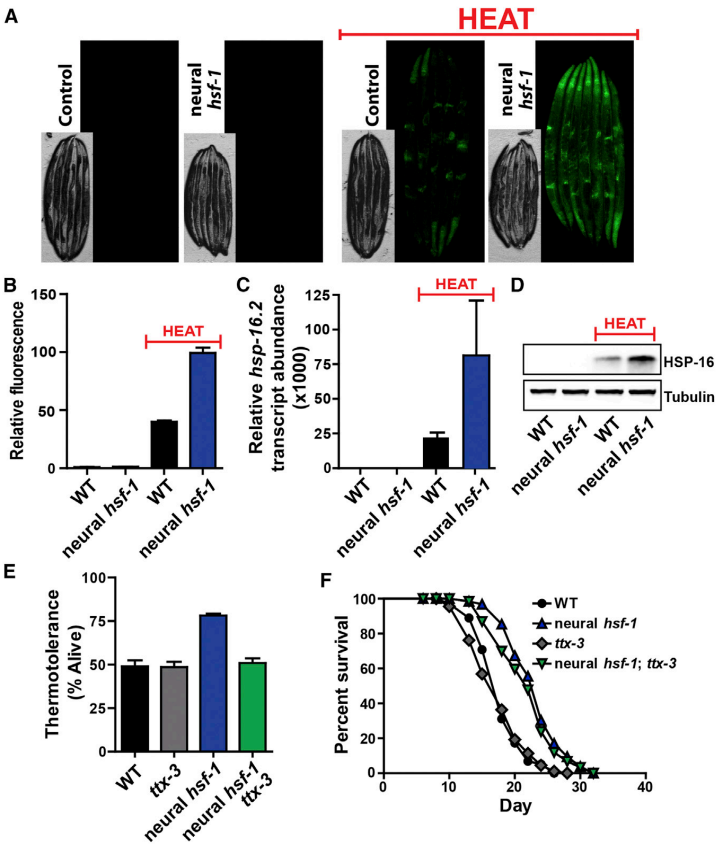

Figure 2. Neural *hsf-1* Overexpression Enhances Heat-Inducible Chaperone Expression in All Tissues and Requires an Intact Thermosensory Circuit for Heat Protection, but Not Lifespan Extension

(A) Fluorescent microscopy of *C. elegans* expressing GFP from the *hsp-16.2* promoter in control (CL2070) and *rab-3p*::*hsf-1* transgenic animals (AGD1448) at permissive (20°C) and heat shock (34°C) temperatures.

(B) Large-particle flow cytometry was used to quantify GFP fluorescence from strains used in (A). Error bars represent the SEM.

(C) Transcript levels of endogenous *hsp-16.2* determined by quantitative RT-PCR from day 1 adult wild-type and *rab-3p*::*hsf-1* transgenic animals (AGD1289). Error bars represent the SEM.

(D) Western blot analysis of endogenous HSP-16 from strains used in (C).

(E) Thermotolerance of WT, *ttx-3*(*ks5*), *rab-3p*::*hsf-1* (AGD1289), and *rab-3p*::*hsf-1*;*ttx-3*(*ks5*) (AGD1449) animals was assessed at 34°C. Error bars represent the SEM.

(F) Lifespan survival was performed at 20°C on strains used in (E). Lifespan statistics are found in Table 1.

observed a significant enrichment in DAF-16-associated elements (DAEs) (Table S1). The forkhead (FOXO) transcription factor DAF-16 is an essential component in the insulin/IGF-1-signaling cascade. This systemic process enables organisms to maintain glucose and energy homeostasis at optimal levels. HSF-1 has been linked to the insulin-signaling pathway and DAF-16 (Chiang et al., 2012; Hsu et al., 2003; Morley and Morimoto, 2004), yet it remains unclear how these essential processes function together.

Disrupting insulin signaling through various mutations in different transduction components enhances longevity (Kenyon, 2011). Moreover, this lifespan extension requires the activation of DAF-16 to drive the pro-longevity transcriptional response. The canonical DAF-16 target gene superoxide dismutase-3 (*sod-3*) exhibits expression levels highly correlative with lifespan extension (Henderson et al., 2006; Sánchez-Blanco and Kim, 2011). Because neural *hsf-1* overexpression does not activate a heat shock response at permissive temperatures, we hypothesized that *hsf-1* might be capable of activating DAF-16 target genes. Fluorescence was examined in transgenic worms that expressed GFP under the control of the *sod-3* promoter. In this manner, temporal and spatial aspects of *sod-3* transcriptional activity were analyzed in different worm tissues.

Elevated expression of *hsf-1* in the nervous system increased GFP fluorescence in all worm tissues harboring the transcriptional *sod-3* reporter (Figure 3A). We observed that overexpression of neural *hsf-1* yields twice as much GFP fluorescence (Figures 3B and S4A). GFP expression was not only elevated in the nervous system by neural *hsf-1* overexpression but also in peripheral tissues. The *daf-16*(*mu86*)-null allele prevented neural *hsf-1* overexpression from increasing GFP fluorescence of the *sod-3* reporter strain (Figures 3A, 3B, and S4A). Induction of endogenous *sod-3* transcripts by neural *hsf-1* overexpression was also *daf-16* dependent (Figure 3C). Thus, neural *hsf-1* overexpression drives FOXO-dependent activation of *sod-3* at permissive temperatures in all worm tissues.

Taken together, these results suggest that *hsf-1* combats acute heat stress through the activation of a transcellular heat shock network and *hsf-1* in the nervous system initiates an independent signal to activate DAF-16 in peripheral tissues to extend lifespan. To disprove this hypothesis, we determined the dependence of *daf-16* upon lifespan extension by neural *hsf-1*. Consistent with separation of thermotolerance and aging, *hsf-1* overexpression in the nervous system was incapable of extending worm lifespan in *daf-16* mutants (Figure 3D; Table 1). In contrast, stress-responsive transcription factors such as *pha-4*, *xbp-1*, *skn-1*, and *ubl-5* were dispensable for neural *hsf-1*-mediated lifespan extension (Figures S3B–S3E; Table 1). The ability of increased neural *hsf-1* to modulate *sod-3*

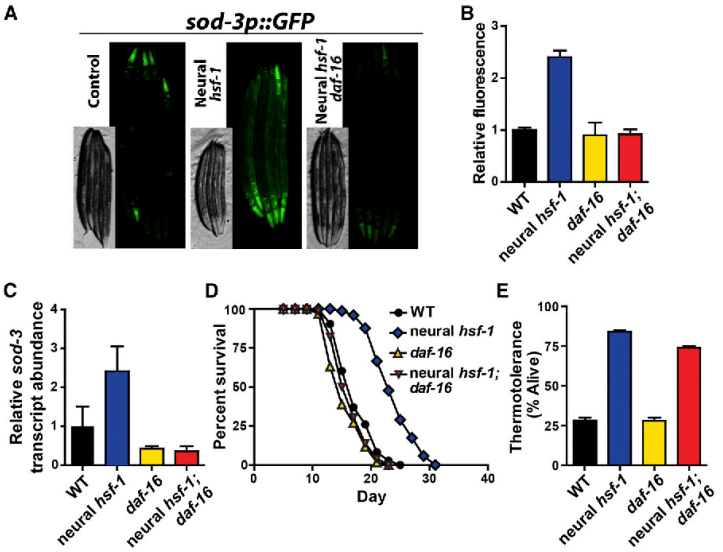

Figure 3. *daf-16* Is Required for Neural *hsf-1* to Induce *sod-3* Expression in Peripheral Tissues and Extend Lifespan but Is Dispensable for Increased Thermotolerance

(A) Fluorescent microscopy of *C. elegans* expressing GFP from the *sod-3* promoter in control (CF1553), *rab-3p::hsf-1* (AGD1198), and *rab-3p::hsf-1; daf-16(mu86)* (AGD1457) animals at 20°C.

(B) Quantification of GFP fluorescence from strains used in (A) as determined by large-particle flow cytometry. Error bars represent the SEM.

(C) Transcript levels of endogenous *sod-3* determined by quantitative RT-PCR from day 1 adult WT, *daf-16(mu86)*, *rab-3p::hsf-1* (AGD1289), and *rab-3p::hsf-1; daf-16(mu86)* (AGD1217) animals. Error bars represent the SEM.

(D) Lifespan survival was assessed at 20°C for strains used in (C). Lifespan statistics are found in Table 1.

(E) Thermotolerance was determined at 34°C for strains used in (C) and (D). Error bars represent the SEM.

levels in a *daf-16*-dependent manner correlates with its ability to extend animal lifespan. Although *daf-16* possesses thermal protective properties (Volovik et al., 2014), *daf-16* was not required for neural *hsf-1*-overexpressing worms to protect against heat stress (Figure 3E). Moreover, expression of the *sod-3* stress-responsive gene was not heat inducible and likely represents a distinct stress response pathway utilized by neural *hsf-1* during the aging process (Figures S4B–S4D).

The ability of *hsf-1* to regulate the heat shock response and aging are separable. Removal of the thermosensory circuit through a *ttx-3* mutation blocks heat resistance but has no effect on increased longevity. Conversely, eliminating *daf-16* function does not affect thermotolerance but abolishes lifespan extension by neural *hsf-1* overexpression. Therefore, distinct signaling events are communicated across an organism from *hsf-1* in the nervous system in response to acute heat stress compared to the chronic stress of aging.

Intestinal *daf-16* Is Sufficient to Extend Lifespan by Neural *hsf-1* Overexpression

Neural *hsf-1* regulates *daf-16* in peripheral tissues; however, it is not clear in what tissues *daf-16* is required for lifespan extension. By rescuing *daf-16* expression in individual worm tissues in an otherwise null *daf-16(mu86)* mutant, we tested whether restoring *daf-16* activity in a particular tissue was sufficient to drive the lifespan extension by neural *hsf-1* overexpression. Expression of *daf-16* was rescued in the nervous system, intestine, and body-wall muscle (Libina et al., 2003). Rescuing expression of *daf-16* in the nervous system was not sufficient for neural *hsf-1* overexpression to extend lifespan or enhance GFP fluorescence of the *sod-3* transcriptional reporter (Figures 4A and S4E; Table 1). This demonstrates that *daf-16* in the nervous system is not required for neural *hsf-1* to communicate to peripheral tissues. In contrast, *daf-16* expression exclusively in the intestine enabled neural *hsf-1* overexpression to both extend lifespan and modestly enhance GFP fluorescence in the *sod-3* transcriptional reporter (Figures 4B and S4E; Table 1). Additionally, neural *hsf-1* acted specifically through the intestine, as *daf-16* expression in body-wall muscles did not extend lifespan or induce the *sod-3* reporter (Figures 4C and S4E; Table 1). Therefore, neural *hsf-1* functions cell non-autonomously in lifespan regulation via a signaling mechanism that requires the activity of *daf-16* in intestinal cells. DAF-16 has previously been shown to play an important role in the worm intestine to influence lifespan (Libina et al., 2003). The communication between neural *hsf-1* and *daf-16* in the periphery does not require *daf-16* in the nervous system, indicating that *hsf-1* regulates *daf-16* in a transcellular manner (Figure 5B).

Although *daf-16* activity is required in the intestine for neural *hsf-1*-overexpressing worms to extend lifespan, it is unclear whether *hsf-1* also functions in the peripheral, non-neural tissues to mediate longevity assurance. Thus, *hsf-1* activity in peripheral tissues was reduced through a hypomorphic *hsf-1(sy441)* allele in which the carboxy-terminal transactivation domain has been removed through a premature stop codon (Hajdu-Cronin et al., 2004). Overexpressing full-length *hsf-1* in the nervous system was not able to extend the lifespan of the hypomorphic *hsf-1(sy441)* animals (Figure 5A; Table 1). These results indicate that *hsf-1* activity in the nervous system is not sufficient to increase lifespan on its own, but rather communication of neural *hsf-1* to peripheral cells expressing *hsf-1* is essential for longevity assurance.

DISCUSSION

Stress encompasses a wide spectrum of insults for which cells have evolved highly specialized responses to both combat the

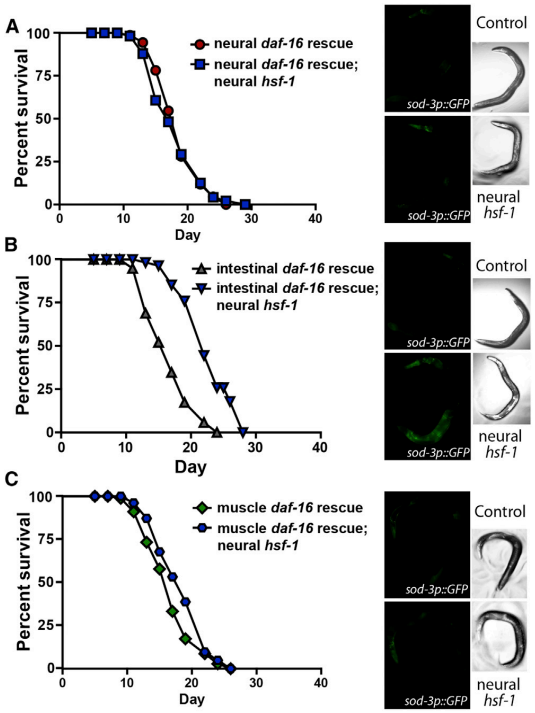

Figure 4. Neural Overexpression of *hsf-1* Requires *daf-16* in the Intestine to Activate *sod-3* and Extend Lifespan

(A–C) Lifespan survival curves and representative *sod-3p*::*GFP* fluorescent micrographs of *rab-3p*::*hsf-1* transgenic animals with different tissue-specific *daf-16* rescues in an otherwise *daf-16*(*mu86*) mutant background. Expression of *daf-16* is ectopically restored in individual tissues of *daf-16*(*mu86*)-null animals including the (A) nervous system (AGD1273), (B) intestine (AGD1277), and (C) body-wall muscle (AGD1279). Lifespan statistics are found in Table 1.

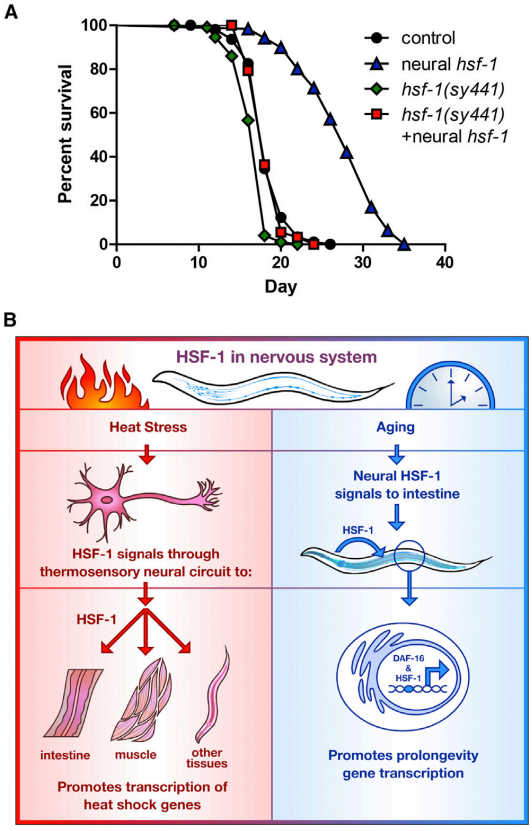

Figure 5. *hsf-1* Is Required in Peripheral Tissues for Neural *hsf-1*-Overexpressing Worms to Extend Lifespan

(A) Lifespan survival curves of WT and *rab-3p*::*hsf-1*-overexpressing nematodes (AGD1289) in the presence or absence of the hypomorphic *hsf-1*(*sy441*) mutation (AGD1471). Lifespan statistics are found in Table 1.

(B) Model depicting how heterotypic signals by neural *hsf-1* separate thermal protection from age regulation. Under thermal stress, HSF-1 in the nervous system signals to peripheral tissues through the thermosensory neural circuit and enhances the heat shock response to protect worms (left model). Conversely, neural *hsf-1* functions independently of the thermosensory circuit to generate a transcellular signal that activates DAF-16 and HSF-1 in the intestine and drives pro-longevity gene expression (right model).

immediate stress and initiate recovery mechanisms. With the evolution of multicellularity, organisms developed a hierarchical mode of stress response regulation across tissues. This normally includes a master tissue, which can both sense the particular stress and transmit the appropriate response to the pertinent peripheral tissues. Cell non-autonomous signaling of stress responses includes numerous mechanisms, such as the insulin-signaling pathway (Libina et al., 2003), germline ablation (Hsin and Kenyon, 1999), mitochondrial unfolded protein response (UPR) (Durieux et al., 2011; Owusu-Ansah et al., 2013), ER UPR (Deng et al., 2013; Taylor and Dillin, 2013), and the heat shock response (Prahlad et al., 2008). To date, each signaling mechanism arises in a particular tissue and functions in a homotypic manner whereby a single signaling cascade conveys stress responsive cues to all pertinent tissues. Consistent with these responses, neural *hsf-1* signaling directly regulates *hsf-1* targets in peripheral tissues to mount the heat shock response upon acute stress. In contrast, neural *hsf-1* initiates a distinct response under aging to coordinate *daf-16* activity in peripheral tissues in addition to *hsf-1*. Thus, *hsf-1* communicates in a heterotypic manner to regulate different stress response pathways. Given the vast array of stresses that *hsf-1* has been reported to protect against (Hsu et al., 2003; Morimoto, 2008), it is reasonable that *hsf-1* can optimally tailor stress response machinery to combat either acute or chronic insults.

Links between *hsf-1* and components of the insulin/IGF-1-signaling pathway exist in multiple experimental paradigms including aging, proteotoxicity, and thermotolerance (Hsu et al., 2003; McColl et al., 2010; Morley and Morimoto, 2004). From these reports, *hsf-1* function has been modeled to reside

downstream of, or in parallel with, the insulin-signaling pathway. Herein, we provide evidence suggesting that *hsf-1* functions upstream of *daf-16* signaling. Furthermore, mutations abolishing distinct types of neural vesicular release, *unc-13* and *unc-31*, extend worm lifespan in a *daf-16*-dependent manner (Ailion et al., 1999; Gems and Riddle, 2000). We observe that animals harboring the *unc-13* or *unc-31* mutation induce *sod-3* expression (Figure S4F), suggesting that reduced neural secretion of insulin-like peptides activates *daf-16* in distal tissues to promote longevity. Because of this functional redundancy, the signaling mechanism by which neural *hsf-1* communicates to the periphery remains unclear but could include any of the 39 insulin-like peptides found in *C. elegans*.

Within the nervous system, *hsf-1* could function at multiples steps to modulate insulin signaling: either by regulating the production, processing, trafficking, or secretion of insulin peptides during conditions of chronic stress. Future studies are needed to elucidate the molecular mechanisms by which *hsf-1* overexpression in neurons could possibly regulate insulin biogenesis. Expanding these concepts to mammalian systems, it will be interesting to understand how bolstering *hsf-1* activity in the brain influences more localized insulin secretion within the nervous system versus insulin biogenesis in pancreatic β cells. Either course of action could profoundly affect energy homeostasis and provide a novel, long-term mode of diabetes intervention.

The process of aging is due, in part, to protein misfolding events and a general deterioration in the quality of the proteome. In support of this hypothesis, metastable proteins that can fold and function in youthful cells begin to misfold upon aging, losing functionality (Ben-Zvi et al., 2009). A similar phenomenon appears in numerous age-onset neurodegenerative disorders, in which the aging brain can no longer maintain disease-linked proteins in properly folded, functional states and misfolding leads to multimerization of the disease proteins and neural death (Douglas and Dillin, 2010; Morimoto, 2008). In these studies, the levels of *hsf-1* and its chaperone target genes directly correlated with the age onset of different neurodegenerative models. Thus, by extension, it was hypothesized that *hsf-1* regulates the aging process by modulating chaperone network components to directly influence the folding state of the proteome (Morimoto, 2008). Our data suggest an alternate method by which *hsf-1* can regulate the aging process. In this model, *hsf-1* activates the FOXO transcription factor, which initiates a pro-longevity stress response that is distinct from the heat shock response. Although we cannot entirely exclude the possible involvement of the chaperone network in lifespan extension by neural *hsf-1* overexpression, we did not observe an enhancement in heat-responsive elements. Further investigation is needed to uncover stress-responsive genes within the DAF-16 activation cascade that are responsible for longevity assurance.

EXPERIMENTAL PROCEDURES

C. elegans Strains and Maintenance

All strains were maintained at 15°C on the *E. coli* strain, OP50. The following strains were used in this work: wild-type (N2), *ttx-3*(*ks5*), *daf-16*(*mu86*), *hsf-1*(*sy441*), *daf-2*(*e1370*), AM101 (rmIS110[*gref-1*p::Q40::YFP]; AGD440 (N2; uthEx457[*rab-3*p::tdTomato); *rol-6*(*su1006*)]); AGD1008 (uthEx663[*rab-3*p::*hsf-1*; *myo-2*p::tdTomato]), AGD1441 (uthEx741[*rgef-1*p::*hsf-1*; *myo-2*p::tdTomato]), AGD1289 (uthIS368[*rab-3*p::*hsf-1*; *myo-2*p::tdTomato]), AGD1053 (uthIS365[*rab-3*p::*hsf-1*; *myo-2*p::tdTomato]), AGD1054 (uthIS366 [*rab-3*p::*hsf-1*; *myo-2*p::tdTomato]), AGD1449 (*ttx-3*(*ks5*); uthEx663[*rab-3*p::*hsf-1*; *myo-2*p::tdTomato]), AGD1471 (*hsf-1*(*sy441*); uthIS368[*rab-3*p::*hsf-1*; *myo-2*p::tdTomato]), CL2070 (dvIn70[pCL25 (*hsp-16.2*p::GFP); pRF4(*rol-6*)]), AGD1448 (dvIn70[pCL25 (*hsp-16.2*p::GFP); pRF4(*rol-6*)]; uthIS368[*rab-3*p::*hsf-1*; *myo-2p*::tdTomato]), CF1553 (muIs84[pAD76(*sod-3p*::GFP)]), AGD709 (*daf-16*(*mu86*); muIs84[pAD76(*sod-3p*::GFP)]), AGD1198 (muIs84[pAD76(*sod-3p*::GFP)]; uthIS368[*rab-3*p::*hsf-1*; *myo-2*p::tdTomato]), AGD1457 (*daf-16*(*mu86*); muIs84[pAD76(*sod-3p*::GFP)]; uthIS368[*rab-3*p::*hsf-1*; *myo-2*p::tdTomato]; AGD1217 (*daf-16*(*mu86*); uthIS368[*rab-3*p::*hsf-1*; *myo-2*p::tdTomato]; AGD1272 (*daf-16*(*mu86*); muEx169[*unc-119p*::*GFP*::*daf-16*, *rol-6*(*su1006*)]); AGD1273 (*daf-16*(*mu86*); muEx169[*unc-119p*::*GFP*::*daf-16*, *rol-6*(*su1006*)]; uthIS368[*rab-3*p::*hsf-1*; *myo-2*p::tdTomato]); AGD1276 (*daf-16*(*mu86*); muEx211[pNL213(*ges-1*p::*GFP*::*daf-16*), *rol-6*(*su1006*)]); AGD1277 (*daf-16*(*mu86*); muEx211[pNL213(*ges-1*p::*GFP*::*daf-16*), *rol-6*(*su1006*)]; uthIS368[*rab-3*p::*hsf-1*; *myo-2*p::tdTomato]), AGD1278 (*daf-16*(*mu86*); muEx212[pNL212(*myo-3*p::*GFP*::*daf-16*), *rol-6*(*su1006*)]), AGD1279 (*daf-16*(*mu86*); muEx212[pNL212(*myo-3*p::*GFP*::*daf-16*), *rol-6*(*su1006*)]; uthIS368[*rab-3*p::*hsf-1*; *myo-2*p::tdTomato]), AGD1309 (*daf-16*(*mu86*); muEx169[*unc-119p*::*GFP*::*daf-16*, *rol-6*(*su1006*)]; muIs84[pAD76(*sod-3p*::GFP)]), AGD1313 (*daf-16*(*mu86*); muEx169[*unc-119p*::*GFP*::*daf-16*, *rol-6*(*su1006*)]; uthIS368[*rab-3*p::*hsf-1*; *myo-2*p::tdTomato]; muIs84[pAD76(*sod-3p*::GFP)]), AGD1311 (*daf-16*(*mu86*); muEx211[pNL213(*ges-1*p::*GFP*::*daf-16*), *rol-6*(*su1006*)]; muIs84[pAD76(*sod-3p*::GFP)]), AGD1315 (*daf-16*(*mu86*); muEx211[pNL213(*ges-1*p::*GFP*::*daf-16*), *rol-6*(*su1006*)]; uthIS368[*rab-3*p::*hsf-1*; *myo-2*p::tdTomato]; muIs84[pAD76(*sod-3p*::GFP)]), AGD1312 (*daf-16*(*mu86*); muEx212[pNL212(*myo-3*p::*GFP*::*daf-16*), *rol-6*(*su1006*)]; muIs84 [pAD76(*sod-3p*::GFP)]), AGD1316 (*daf-16*(*mu86*); muEx212[pNL212(*myo-3*p::*GFP*::*daf-16*), *rol-6*(*su1006*)]; uthIS368[*rab-3*p::*hsf-1*; *myo-2*p::tdTomato]; muIs84[pAD76(*sod-3p*::GFP)]), AGD1475 (unc-13(e450); muIs84[pAD76(sod-3p::GFP)]), and AGD1476 (unc-31(e928); muIs84[pAD76(sod-3p::GFP)]).

Wild-type (N2), *ttx-3*(*ks5*), and *daf-16*(*mu86*) CF1553 and CL2070 strains were obtained from the *Caenorhabditis* Genetics Center. For generation of transgenic overexpression strains, *hsf-1* cDNA was inserted downstream of the neural promoters *rab-3* or *gref-1* and upstream of the *unc-54* 3′ UTR. Neural *hsf-1* DNA plasmid constructs were injected at 2 ng/μl along with a co-injection marker (*myo-2p*::tdTomato) at 10 ng/μl to make transgenic overexpression worms.

Western Blot Analysis

Age-synchronized worms were cultivated on nematode growth (NG) plates containing the *E. coli* strain, OP50, at 20°C until day 1 adulthood. Worms were washed off the plate with M9 buffer pre-heated to 34°C, collected, and incubated in a 34°C water bath for 15 min. Worms were centrifuged at 1,000 × *g* for 30 s and moved back to NG plates seeded with OP50 bacteria at 20°C. Worms were allowed 1.5 hr of recovery at 20°C before worms were collected and frozen in liquid nitrogen for further processing.

Worm extracts were generated by glass bead disruption in non-denaturing lysis buffer (150 mM NaCl, 50 mM HEPES [pH 7.4], 1 mM EDTA, 1% Triton X-100, and protease inhibitor cocktail without EDTA [Roche]). Crude lysates were subject to centrifugation at 10,000 × *g* at 4°C for 5 min. The supernatant was supplemented with 2× SDS sample buffer containing 50 mM Tris-Cl (pH 6.8), 2 mM EDTA, 4% glycerol, 2% SDS, Coomassie Blue, and protease inhibitor cocktail without EDTA (Roche). Samples were boiled for 10 min and resolved by SDS-PAGE. Proteins levels were monitored by standard immuno-blotting procedures with α-Hsp-16.2 (kind gift from Lithgow Lab) and α-tubulin (Sigma T6074) antibodies.

Transcript Analysis

Total RNA was isolated from synchronized populations at day 1 of adulthood using Qiazol (QIAGEN) and then further purified with the RNeasy mini kit (QIAGEN). cDNA was synthesized using the QuantiTect kit (QIAGEN). Sybr-Green was used for quantitative PCR as described in the SsoAdvanced SYBR Green Supermix protocol (Bio-Rad). Experiments were repeated with

three biological repeats and analyzed using the comparative Ct method. Internal controls utilized a geometric mean of *cdc-42*, *pmp-3*, and *Y45F10D.4*. The Roche Universal ProbeFinder online tool was used to design primers. Primer sequences are as follows:

cdc-42 forward 5′- AGGAACGTCTTCCTTGTCTCC −3′
cdc-42 reverse 5′- GGACATAGAAAGAAAAACACAGTCAC −3′
pmp-3 forward 5′- CGGTGTTAAAACTCACTGGAGA −3′
pmp-3 reverse 5′- TCGTGAAGTTCCATAACACGA −3′
Y45F10D.4 forward 5′- AAGCGTCGGAACAGGAATC −3′
Y45F10D.4 reverse 5′- TTTTTCCGTTATCGTCGACTC −3′
hsf-1 forward 5′- TTTGCATTTTCTCGTCTCTGTC −3′
hsf-1 reverse 5′- TCTATTTCCAGCACACCTCGT −3′
hsp-16.2 forward 5′- TCCATCTGAGTCTTCTGAGATTGTTA −3′
hsp-16.2 reverse 5′- TGGTTTAAACTGTGAGACGTTGA −3′
hsp-70a (C12C8.1) forward 5′- CGGTATTTATCAAAATGGAAAGGTT −3′
hsp-70a (C12C8.1) reverse 5′- TACGAGCGGCTTGATCTTTT −3′
hsp-70b (F44E5.4) forward 5′- TGCACCAATCTGGACAATCT −3′
hsp-70b (F44E5.4) reverse 5′- TCCAGCAGTTCCAGGATTTC −3′
pat-10 forward 5′- TCGAGGAGTTCTGGGAGTTG −3′
pat-10 reverse 5′- TTGTAGATCAGCGATTTTAAAGGA −3′
sod-3 forward 5′- CACTGCTTCAAAGCTTGTTCA −3′
sod-3 reverse 5′- ATGGGAGATCTGGGAGAGTG −3′.

RNA for global sequencing analysis was prepared using Illumina TruSeq RNA Sample Prep Kit (Illumina). Paired-end sequencing was performed on an Illumina HiSeq 2000, and data were analyzed with CLC Genomics Workbench 7.0.4 software.

Promoter Analysis

We used RSAT (Thomas-Chollier et al., 2011) to ask for overrepresented sequences of length 6, 7, or 8 upstream of our ORF start sites, within 1.5 kb or until the preceding ORF, whichever was closer. e-value is a multiple testing corrected estimate of the probability of this degree of overrepresentation.

Lifespan Analysis

Lifespan experiments were conducted at 20°C as previously described (Wilkinson et al., 2012), and a minimum of three independent experiments were performed under every condition. Worms were fed different *E. coli*, OP50, or HT115 for experiments involving RNAi knockdown of gene expression. Tissue-specific *daf-16* rescue lifespans were performed on OP50. The pre-fertile period of adulthood was considered day 0. Worms were transferred to fresh plates every second day until day 12. To prevent excessive worm censorship, 5-fluoro-2′-deoxyuridine, FUDR, was supplemented into growth media of lifespan experiments involving the hypomorphic *hsf-1*(*sy441*). Lifespan analysis on Prism 6 and JMP software was used for statistical analysis to determine significance calculated using the log rank (Mantel-Cox) method.

Thermotolerance Assay

Synchronized day 1 adult worms were placed at 34°C for 12–14 hr on plates spotted with OP50 *E. coli* or HT115 for RNAi. Worms were then scored for viability. At least 80 worms were used per genotype, and experiments were repeated at least three times. Prism 6 software was used for statistical analysis.

RNAi Feeding

Worms were fed from hatch HT115 *E. coli* containing an empty vector control or expressing double-stranded RNA. RNAi strains were taken from the Vidal library if present or the Ahringer library if absent from the Vidal library. All RNAi clones were sequence verified prior to use and knockdown verified previously (Carrano et al., 2009; Durieux et al., 2011; Panowski et al., 2007; Taylor and Dillin, 2013).

Microscopy and Fluorescence Analysis

For fluorescence microscopy, worms were anesthetized with 10 mM levamisole and images were captured using a Leica DM6000 B microscope and Hamamatsu ORCA-ER camera. We also used a COPAS Biosort (Union Biometrica) to measure individual day 1 worm length, width, and GFP fluorescence. At least 500 worms were measured per genotype and pooled in three biological replicates. We normalized fluorescence by worm size to compare between genotypes.

SUPPLEMENTAL INFORMATION

Supplemental Information includes four figures and one table and can be found with this article online at http://dx.doi.org/10.1016/j.celrep.2015.07.026.

AUTHOR CONTRIBUTIONS

P.M.D., N.A.B., M.S.S., and S.U. performed the experiments and analyzed the data. M.A.M. and B.K.K. assisted P.M.D. on bioinformatics analysis. P.M.D., N.A.B., S.C.W., and A.D. wrote the manuscript. P.M.D. and N.A.B. contributed equally.

ACKNOWLEDGMENTS

We thank the laboratory of Dr. G. Lithgow for generously sharing the HSP-16 antibody and Kenyon lab for providing tissue-specific *daf-16* rescue strains. We also thank the illustrator, Lindsay Daniele, for the graphical abstract. Some of the nematode strains used in this work were provided by the *Caenorhabditis* Genetics Center (University of Minnesota), which is supported by the NIH–Office of Research Infrastructure Programs (P40 OD010440). This work was supported by NIH grants (R37AG024365, R01AG042679, and R01ES021667). P.M.D. was funded by the NIH/NIA (1K99AG042495) and the George E. Hewitt Foundation for Medical Research. N.A.B. was funded by a postdoctoral fellowship from the Salk Center for Nutritional Genomics from the Leona M. & Harry B. Helmsley Charitable Trust. S.C.W. is grateful for the generous support of the Glenn Foundation for Medical Research. M.A.M. has been supported by NIH training grant (T32AG000266). B.K.K. is supported by NIH (R01AG025549 and R01AG043080).

Received: May 5, 2015
Revised: June 5, 2015
Accepted: July 13, 2015
Published: August 6, 2015

REFERENCES

Ailion, M., Inoue, T., Weaver, C.I., Holdcraft, R.W., and Thomas, J.H. (1999). Neurosecretory control of aging in Caenorhabditis elegans. Proc. Natl. Acad. Sci. USA *96*, 7394–7397.

Baird, N.A., Douglas, P.M., Simic, M.S., Grant, A.R., Moresco, J.J., Wolff, S.C., Yates, J.R., 3rd, Manning, G., and Dillin, A. (2014). HSF-1-mediated cytoskeletal integrity determines thermotolerance and life span. Science *346*, 360–363.

Ben-Zvi, A., Miller, E.A., and Morimoto, R.I. (2009). Collapse of proteostasis represents an early molecular event in Caenorhabditis elegans aging. Proc. Natl. Acad. Sci. USA *106*, 14914–14919.

Carrano, A.C., Liu, Z., Dillin, A., and Hunter, T. (2009). A conserved ubiquitination pathway determines longevity in response to diet restriction. Nature *460*, 396–399.

Chiang, W.C., Ching, T.T., Lee, H.C., Mousigian, C., and Hsu, A.L. (2012). HSF-1 regulators DDL-1/2 link insulin-like signaling to heat-shock responses and modulation of longevity. Cell *148*, 322–334.

Deng, Y., Wang, Z.V., Tao, C., Gao, N., Holland, W.L., Ferdous, A., Repa, J.J., Liang, G., Ye, J., Lehrman, M.A., et al. (2013). The Xbp1s/GalE axis links ER stress to postprandial hepatic metabolism. J. Clin. Invest. *123*, 455–468.

Douglas, P.M., and Dillin, A. (2010). Protein homeostasis and aging in neurodegeneration. J. Cell Biol. *190*, 719–729.

Durieux, J., Wolff, S., and Dillin, A. (2011). The cell-non-autonomous nature of electron transport chain-mediated longevity. Cell *144*, 79–91.

Failla, G. (1958). The aging process and cancerogenesis. Ann. N Y Acad. Sci. *71*, 1124–1140.

Gems, D., and Riddle, D.L. (2000). Genetic, behavioral and environmental determinants of male longevity in Caenorhabditis elegans. Genetics *154*, 1597–1610.

Hajdu-Cronin, Y.M., Chen, W.J., and Sternberg, P.W. (2004). The L-type cyclin CYL-1 and the heat-shock-factor HSF-1 are required for heat-shock-induced protein expression in Caenorhabditis elegans. Genetics *168*, 1937–1949.

Harman, D. (1956). Aging: a theory based on free radical and radiation chemistry. J. Gerontol. *11*, 298–300.

Henderson, S.T., Bonafè, M., and Johnson, T.E. (2006). daf-16 protects the nematode Caenorhabditis elegans during food deprivation. J. Gerontol. A Biol. Sci. Med. Sci. *61*, 444–460.

Hsin, H., and Kenyon, C. (1999). Signals from the reproductive system regulate the lifespan of C. elegans. Nature *399*, 362–366.

Hsu, A.L., Murphy, C.T., and Kenyon, C. (2003). Regulation of aging and age-related disease by DAF-16 and heat-shock factor. Science *300*, 1142–1145.

Kenyon, C. (2011). The first long-lived mutants: discovery of the insulin/IGF-1 pathway for ageing. Philos. Trans. R. Soc. Lond. B Biol. Sci. *366*, 9–16.

Libina, N., Berman, J.R., and Kenyon, C. (2003). Tissue-specific activities of C. elegans DAF-16 in the regulation of lifespan. Cell *115*, 489–502.

Link, C.D., Cypser, J.R., Johnson, C.J., and Johnson, T.E. (1999). Direct observation of stress response in Caenorhabditis elegans using a reporter transgene. Cell Stress Chaperones *4*, 235–242.

Lithgow, G.J., White, T.M., Melov, S., and Johnson, T.E. (1995). Thermotolerance and extended life-span conferred by single-gene mutations and induced by thermal stress. Proc. Natl. Acad. Sci. USA *92*, 7540–7544.

McColl, G., Rogers, A.N., Alavez, S., Hubbard, A.E., Melov, S., Link, C.D., Bush, A.I., Kapahi, P., and Lithgow, G.J. (2010). Insulin-like signaling determines survival during stress via posttranscriptional mechanisms in C. elegans. Cell Metab. *12*, 260–272.

Morimoto, R.I. (2008). Proteotoxic stress and inducible chaperone networks in neurodegenerative disease and aging. Genes Dev. *22*, 1427–1438.

Morley, J.F., and Morimoto, R.I. (2004). Regulation of longevity in Caenorhabditis elegans by heat shock factor and molecular chaperones. Mol. Biol. Cell *15*, 657–664.

Orgel, L.E. (1963). The maintenance of the accuracy of protein synthesis and its relevance to ageing. Proc. Natl. Acad. Sci. USA *49*, 517–521.

Owusu-Ansah, E., Song, W., and Perrimon, N. (2013). Muscle mitohormesis promotes longevity via systemic repression of insulin signaling. Cell *155*, 699–712.

Panowski, S.H., Wolff, S., Aguilaniu, H., Durieux, J., and Dillin, A. (2007). PHA-4/Foxa mediates diet-restriction-induced longevity of C. elegans. Nature *447*, 550–555.

Prahlad, V., Cornelius, T., and Morimoto, R.I. (2008). Regulation of the cellular heat shock response in Caenorhabditis elegans by thermosensory neurons. Science *320*, 811–814.

Sánchez-Blanco, A., and Kim, S.K. (2011). Variable pathogenicity determines individual lifespan in Caenorhabditis elegans. PLoS Genet. *7*, e1002047.

Taylor, R.C., and Dillin, A. (2013). XBP-1 is a cell-nonautonomous regulator of stress resistance and longevity. Cell *153*, 1435–1447.

Thomas-Chollier, M., Defrance, M., Medina-Rivera, A., Sand, O., Herrmann, C., Thieffry, D., and van Helden, J. (2011). RSAT 2011: regulatory sequence analysis tools. Nucleic Acids Res. *39*, W86–W91.

Volovik, Y., Moll, L., Marques, F.C., Maman, M., Bejerano-Sagie, M., and Cohen, E. (2014). Differential regulation of the heat shock factor 1 and DAF-16 by neuronal nhl-1 in the nematode C. elegans. Cell Rep. *9*, 2192–2205.

Walker, G.A., and Lithgow, G.J. (2003). Lifespan extension in C. elegans by a molecular chaperone dependent upon insulin-like signals. Aging Cell *2*, 131–139.

Wilkinson, D.S., Taylor, R.C., and Dillin, A. (2012). Analysis of aging in Caenorhabditis elegans. Methods Cell Biol. *107*, 353–381.

Wolff, S., Weissman, J.S., and Dillin, A. (2014). Differential scales of protein quality control. Cell *157*, 52–64.